Universiteit
Leiden
The Netherlands

Determining the most appropriate dose metrics for evaluating dose-response relationships of metal-based nanoparticles to zebrafish embryos

Hua, J.

Citation

Hua, J. (2015, September 3). *Determining the most appropriate dose metrics for evaluating dose-response relationships of metal-based nanoparticles to zebrafish embryos*. Retrieved from https://hdl.handle.net/1887/34955

Version:	Corrected Publisher's Version
License:	Licence agreement concerning inclusion of doctoral thesis in the Institutional Repository of the University of Leiden
Downloaded from:	https://hdl.handle.net/1887/34955

Note: To cite this publication please use the final published version (if applicable).

Cover Page

Universiteit Leiden

The handle http://hdl.handle.net/1887/34955 holds various files of this Leiden University dissertation

Author: Jing Hua
Title: Determining the most appropriate dose metrics for evaluating dose-response relationships of metal-based nanoparticles to zebrafish embryos
Issue Date: 2015-09-03

Determining the Most Appropriate Dose Metrics for Evaluating Dose-Response Relationships of Metal-Based Nanoparticles to Zebrafish Embryos

Jing HUA

華 晶

© 2015 Jing HUA
Determining the Most Appropriate Dose Metrics for Evaluating Dose-Response Relationships of Metal-Based Nanoparticles to Zebrafish Embryos

Ph.D. thesis Leiden University, The Netherlands

Cover design: Jing HUA
Lay out: Zheng DUAN
Word cloud: http://www.tagxedo.com/app.html
Printed by: Off Page, Amsterdam
ISBN: 978-94-6182-589-6

Determining the Most Appropriate Dose Metrics for Evaluating Dose-Response Relationships of Metal-Based Nanoparticles to Zebrafish Embryos

Proefschrift

ter verkrijging van
de graad van Doctor aan de Universiteit Leiden,
op gezag van de Rector Magnificus Prof. mr. C.J.J.M. Stolker,
volgens besluit van het College van Promoties
te verdedigen op donderdag 3 september 2015
klokke 10:00 uur.

door

Jing HUA
geboren te Inner Mongolia Autonomous Region, China
in 1985

Promotiecommissie:

Promotor:	Prof. dr. W.J.G.M. Peijnenburg
Co-promotor:	Dr. M.G. Vijver
Overige Leden:	Prof. dr. A. Tukker (Leiden University) Prof. dr. ir. P.M. van Bodegom (Leiden University) Prof. dr. A.A. Koelmans (Wageningen UR) Dr. E.A.J. Bleeker (RIVM) Prof. dr. H.P. Spaink (Leiden University)

Contents

Summary ..... **v**
Samenvatting ..... **ix**
1 Introduction **1**
1.1 Nanomaterials and nanotechnology 1
1.1.1 Nanomaterials definition and classification 1
1.1.2 Nanotechnology and applications 2
1.2 Exposure, fate and risks of nanoparticles 2
1.3 Impact of physicochemical properties on nanoparticles 6
1.3.1 Size 7
1.3.2 Shape 7
1.3.3 Solubility and ion release 8
1.3.4 Other physicochemical characteristics 8
1.4 Dose metrics assessment of nanoparticles 9
1.5 Metal-based nanoparticles 10
1.5.1 Silver NPs (Ag NPs) 10
1.5.2 Copper NPs (Cu NPs) 12
1.5.3 Zinc oxide NPs (ZnO NPs) 13
1.5.4 Titanium dioxide NPs (TiO_2 NPs) 13
1.5.5 Toxicology of NPs mixtures 14
1.6 Zebrafish 16
1.7 Objectives and research questions of the thesis 17
1.8 Outline of the thesis 18
2 Toxicity of different-sized copper nano- and submicron particles and their shed copper ions to zebrafish embryos **21**
2.1 Introduction 21
2.2 Materials and methods 22
2.2.1 Preparation of Cu suspensions 22
2.2.2 Physicochemical characterization of Cu NPs 23
2.2.3 Waterborne exposure of zebrafish embryos to Cu NPs 24
2.2.4 Contribution to toxicity of Cu $NP_{(particle)}$ and Cu $NP_{(ion)}$ 24
2.2.5 Behavioral analysis and morphological assessment 25
2.2.6 Statistical analysis 25
2.3 Results 26

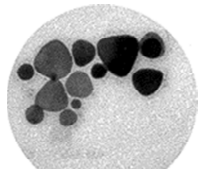

2.3.1 Physicochemical characterization of suspended copper particles 26
2.3.2 Survival and hatching rate over time 28
2.3.3 Lethal toxic effects induced by Cu NPs, submicron-sized particles, and Cu^{2+} 30
2.3.4 Relative contribution to toxicity of Cu $NP_{(particle)}$ and Cu $NP_{(ion)}$. 30
2.3.5 Behavioral analysis and morphological assessment 31
2.4 Discussion 33
2.4.1 Hatching rate over time 33
2.4.2 Lethal toxic effects induced by Cu NPs, submicron-sized particles, and Cu^{2+} 34
2.4.3 Relative contribution to toxicity of Cu $NP_{(particle)}$ and Cu $NP_{(ion)}$. 35
2.4.4 Behavioral analysis 36
2.5 Conclusions 36
Supplemental data 37
3 Particle-specific toxic effects of differently shaped zinc oxide nanoparticles to zebrafish embryos 41
3.1 Introduction 41
3.2 Materials and methods 43
3.2.1 Preparation of ZnO particle suspensions 43
3.2.2 Physicochemical characterization of ZnO NPs 43
3.2.3 Waterborne exposure of zebrafish embryos to ZnO NPs 44
3.2.4 Behavioral analysis 45
3.2.5 Mixture toxicity of ZnO $NP_{(particle)}$ and ZnO $NP_{(ion)}$ 46
3.2.6 Statistical analysis 49
3.3 Results 49
3.3.1 Physicochemical characterization of ZnO particles 49
3.3.2 Lethality of nanoparticles and zinc ions 50
3.3.3 Hatching rate 52
3.3.4 Behavioral analysis 53
3.3.5 Relative contribution to toxicity of ZnO $NP_{(particle)}$ and ZnO $NP_{(ion)}$ 56
3.4 Discussion 57
3.4.1 Lethality of ZnO $NP_{(total)}$ 57
3.4.2 Lethality of ZnO $NP_{(particle)}$ 57
3.4.3 Comparison of lethality of ZnO $NP_{(particle)}$ with different shape .. 59

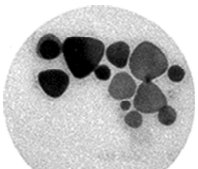

3.4.4 Sub-lethal toxicity of ZnO $NP_{(total)}$ and $NP_{(particle)}$ 60
3.5 Conclusions 61
Supplemental data 61
4 Dose metrics assessment for differently shaped and sized metal-based nanoparticles 63
4.1 Introduction 63
4.2 Materials and methods 65
4.2.1 Nanoparticles properties and toxicity to zebrafish embryos 65
4.2.2 Generic dose calculation method for differently shaped and sized NPs 65
4.2.3 Database from literature survey 68
4.3 Results 69
4.3.1 Generic dose calculation method for differently shaped and sized NPs 69
4.3.2 Database from literature survey 72
4.4 Discussion 75
4.4.1 Generic dose calculation method for differently shaped and sized NPs 75
4.4.2 The adequate dose descriptor 76
4.4.3 Impact of metal ions released from NPs 77
4.4.4 Impact of coating and experiments conditions 77
4.4.5 Impact of aggregate and agglomerates of NPs 78
4.4.6 Impact of chemical composition of NPs 79
4.4.7 Limitation of database from literature survey 80
4.5 Conclusions 80
Supplemental data 81
5 TiO_2 nanoparticles reduce the effects of ZnO nanoparticles and Zn ions on zebrafish embryos (*Danio rerio*) 95
5.1 Introduction 95
5.2 Materials and methods 97
5.2.1 Preparation of stock solutions and suspensions of nanoparticles 97
5.2.2 Physicochemical characterization of NPs 97
5.2.3 Toxicity tests 98
5.2.4 Toxic contribution of the particulate and ionic form of ZnO NPs 99
5.2.5 Statistical analysis 100

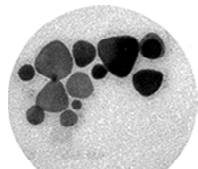

5.3 Results 100
5.3.1 Characterization of nanoparticles 100
5.3.2 Fate of nanoparticles 101
5.3.3 Lethality 103
5.3.4 Hatching rate 104
5.3.5 Effect of TiO_2 NPs on the toxicity of ZnO NP suspensions 106
5.3.6 Effect of TiO_2 NPs on the toxicity of the particulate form of ZnO NPs 107
5.3.7 Contribution of the particulate form and the ionic form of ZnO NPs to toxicity 108
5.4 Discussion 110
5.4.1 Characterization and fate of nanoparticles 110
5.4.2 Effects of TiO_2 NPs on the toxicity of ZnO NP suspensions 111
5.4.3 Effect of TiO_2 NPs on the toxicity of the particulate form of ZnO NPs 112
5.4.4 Relative contribution of ions and particles 114
5.4.5 Societal implications 114
5.5 Conclusions 114
Supplemental data 115
6 Discussion 119
6.1 Answers to research questions 120
6.2 Implications 123
6.2.1 Implications for society 123
6.2.2 Implications for environmental risk assessment 124
6.2.3 Justified alternative (non-animal) methods 127
6.2.4 Implications for mixture effects of NPs 127
6.3 Future research 128
References 131
Acknowledgements 147
Curriculum Vitae 149
List of publications 151
Journal articles 151
Conference proceeding 152

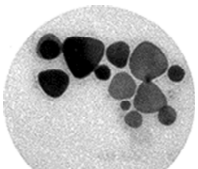

Summary

Nanoparticles (NPs) exhibit special physicochemical properties compared to bulk particles. The difference in properties could, in principle, produce different effects on organisms. It is therefore important to determine the relationship between the physicochemical characteristics of NPs and their toxicity profile, by means of experimental testing. Experimental toxicity testing data can also be used to find the best dose metric for the responses induced by NPs, which was the purpose of the research presented in this thesis. Furthermore, this thesis aims to move forward from toxicity testing primarily in animal models to computational dose metric modeling.

In Chapter 2, a general approach is proposed that allows the quantification of the relative contributions to toxicity of ions released from metal-based nanoparticles and of the particles themselves, as exemplified for the case of zebrafish embryos exposed to differently sized Cu NPs . The LC_{50} values of the particulate form of Cu particles (25 nm, 50 nm, 100 nm, and 400 nm) and $Cu(NO_3)_2$ were 0.58, 1.65, 1.90, 0.35, and 0.70 mg/L, respectively. Submicron-sized particles and copper nitrate were more toxic than Cu NPs, and smaller Cu NPs were more toxic than larger Cu NPs. In suspensions of Cu NPs and Cu submicron-sized particles (SMPs), the main contribution to the toxicity to zebrafish embryos was from the particulate form (>71%) rather than from dissolved Cu from particles. All particles tested, as well as $Cu(NO_3)_2$, inhibited hatching, altered behavioral responses, and increased the incidence of malformations.

In the study reported on in Chapter 3, we assessed the toxicity to the embryos of suspensions of ZnO NPs in the form of nanospheres, nanosticks and cuboidal SMPs, as well as $Zn(NO_3)_2$. Different addition models were used to explicitly account for the combined toxicity of the particulate form of NPs and the ions released from NPs. The LC_{50} values of the particulate form of nanospheres, nanosticks and SMPs were found to range between 7.1 and 11.9 mg Zn/L (*i.e.* to differ by a factor of 1.7). The EC_{50} values of the particles were found to range between 1.0 and 2.2 mg Zn/L. As regards mortality and hatching inhibition, the particles were responsible for 52%-72% and 38-83% of the adverse effects observed, respectively. ZnO

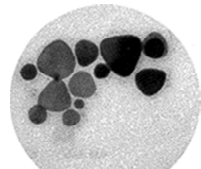

nanosticks were more toxic than any of the other NPs with regard to the endpoints of mortality and hatching inhibition.

The mean primary diameter of nanoparticles is commonly used as the best basis to assess the dose metric for expressing the toxicity of spherical NPs. However, the diameter of a particle is irrelevant for non-spherical NPs. In the study described in Chapter 4, the mean surface area to volume ratio (SA/V), which is applicable to both spherical and non-spherical NPs, was used instead of the diameter of the particle to obtain the best dose metric (volume, surface area, or number) of differently shaped metallic NPs, both *in vivo* (nine organisms) and *in vitro* (six mammalian cell lines). The slope of the curves obtained by relating the total particle number of NPs at their median effect concentrations to SA/V was subsequently used to deduce the best dose metric. For the majority of the organisms studied, the volume of NPs was found to be the most appropriate dose metric. For three organisms exposed to Ag NPs, however, surface area was found to be the best dose metric. We therefore concluded that the optimum dose metric depends on both the organism tested and the properties of the nanoparticles.

In the study discussed in Chapter 5, we investigated the toxicity of a mixture of stick-shaped ZnO NPs and spherically shaped TiO_2 NPs to zebrafish embryos. The EC_{50} value of hatching inhibition of embryos exposed to ZnO NPs was 1.3 mg/L. Addition of TiO_2 NPs to suspensions of ZnO NPs increased the EC_{50} value by up to a factor of 6.3. A similar reduction of toxicity was found for mortality of embryos, as the LC_{50} values were reduced significantly by the addition of TiO_2 NPs at higher concentrations. A $Zn(NO_3)_2$ solution was used as a positive reference to assess the toxicity of Zn^{2+}. This toxicity was reduced when TiO_2 NPs were added as compared to the effects found when embryos were exposed to $Zn(NO_3)_2$ solutions without TiO_2 NPs. The contribution to toxicity of the particulate form of ZnO NPs was found to dominate the contribution of the ions released from ZnO NPs in terms of explaining the toxicity of the suspensions of ZnO NPs in the absence and presence of TiO_2 NPs to zebrafish embryos.

To conclude, in our studies we developed a generic dose calculation method which is suitable for expressing the toxicity of different shaped and sized NPs across various biological species. The generic method can be helpful in changing

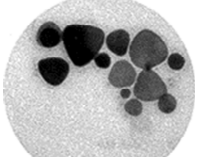

nanotoxicology and the risk assessment of engineered nanomaterials, developing it from an observational to a predictive science.

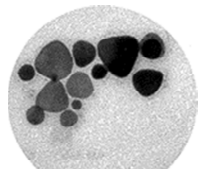

Kinderdijk, the Netherlands

Photo by Jing HUA

Samenvatting

Nanodeeltjes vertonen in vergelijking met grotere deeltjes van dezelfde samenstelling (vanaf nu bulkdeeltjes genoemd) andere fysisch-chemische eigenschappen, die in principe zouden kunnen leiden tot andere effecten op organismen. Het is daarom van belang het verband te onderzoeken tussen de fysisch-chemische eigenschappen van nanodeeltjes en hun experimenteel bepaalde toxiciteitsprofiel. Ook kunnen gegevens uit toxiciteits-proeven worden gebruikt om de beste manier waarop de dosis moet worden uitgedrukt, te bepalen voor de door nanodeeltjes geïnduceerde respons, wat het doel is van dit onderzoek. Doel van het onderzoek was tevens om de extrapolatie tussen toxiciteitsonderzoek op voornamelijk diermodellen naar computermodellen op basis van deze dosisparameter te ondersteunen.

In Hoofdstuk 2 wordt een algemene benadering geïntroduceerd waarmee de relatieve bijdrage van door metallische nanodeeltjes afgegeven ionen aan de toxiciteit kan worden gekwantificeerd, evenals de bijdrage van de nanodeeltjes zelf. Dit is onderzocht aan de hand van het voorbeeld van blootstelling van zebravis-embryo's aan Cu-nanodeeltjes van verschillende afmetingen. De LC_{50} van de deeltjesvorm van Cu (25 nm, 50 nm, 100 nm en 400 nm) en van $Cu(NO_3)_2$ was respectievelijk 0,58; 1,65; 1,90; 0,35 en 0,70 mg/L. Deeltjes van submicron-grootte en kopernitraat bleken meer toxisch dan Cu-nanodeeltjes, en kleinere Cu-nanodeeltjes waren meer toxisch dan grotere Cu-nanodeeltjes. In suspensies van Cu-nanodeeltjes en submicron Cu-deeltjes bleek de grootste bijdrage aan de toxiciteit voor zebravis-embryo's (>71%) te worden geleverd door de deeltjesvorm, en niet door het uit de deeltjes opgeloste Cu. Alle geteste deeltjes, en ook $Cu(NO_3)_2$, hadden een remmende werking op het uitkomen van de eieren, veroorzaakten gedragsveranderingen en gaven aanleiding tot een verhoogde incidentie van misvormingen.

In Hoofdstuk 3 wordt het onderzoek besproken naar de toxiciteit voor zebravis-embryo's van suspensies van ZnO-nanodeeltjes, met inbegrip van nanobolletjes, nanostaafjes, kubusvormige submicron-deeltjes en $Zn(NO_3)_2$. Met behulp van verschillende additiemodellen werd expliciet rekening gehouden met

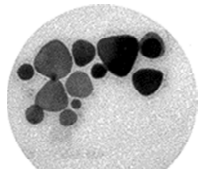

de gecombineerde toxiciteit van de deeltjesvorm en de uit nanodeeltjes vrijkomende ionen. De LC_{50} van de deeltjesvorm van de nanobolletjes, nanostaafjes en submicron-deeltjes varieerde van 7,1 tot 11,9 mg Zn/L (dus een verschil van een factor 1,7). De EC_{50} van de deeltjes varieerde van 1,0 tot 2,2 mg Zn/L. Voor wat betreft de effecten op mortaliteit en de remming van het uitkomen van de eieren bleken de deeltjes verantwoordelijk voor respectievelijk 52-72% en 38-83% van de waargenomen negatieve effecten. De ZnO-nanostaafjes bleken meer toxisch dan alle andere nanodeeltjes voor wat betreft de eindpunten mortaliteit en remming van het uitkomen van de eieren.

De gemiddelde primaire diameter van nanodeeltjes wordt vaak gebruikt als de beste basis voor het bepalen van de dosisparameter als maat voor de toxiciteit van nanobolletjes. Maar de diameter is niet relevant bij niet-bolvormige deeltjes. Het in Hoofdstuk 4 besproken onderzoek richtte zich daarom op de gemiddelde oppervlakte-volume verhouding (surface area to volume ratio, SA/V). Deze kan gebruikt worden bij zowel bolvormige als niet-bolvormige nanodeeltjes, in plaats van de diameter, voor het verkrijgen van de beste dosisparameter (volume, oppervlakte of aantal) voor metallische nanodeeltjes van uiteenlopende vorm, zowel in vivo (9 organismen) als in vitro (6 zoogdier-cellijnen). De beste beschrijving van de dosisparameter werd afgeleid uit de helling van de curve die werd verkregen door het totale aantal deeltjes te nemen van de nanodeeltjes bij de mediaan-effect concentratie en die uit te zetten tegen de SA/V ratio. Voor de meeste van de bestudeerde organismen bleek het volume van de nanodeeltjes de beste dosisparameter te zijn, maar voor drie aan Ag-nanodeeltjes blootgestelde organismen bleek de oppervlakte de beste parameter te zijn. Geconcludeerd werd daarom dat de optimale dosisparameter afhangt van het geteste organisme en van de eigenschappen van de nanodeeltjes.

Het in Hoofdstuk 5 beschreven onderzoek had betrekking op de toxiciteit van een mengsel van staafvormige ZnO-nanodeeltjes en bolvormige TiO_2-nanodeeltjes voor zebravis-embryo's. De EC_{50} voor de remming van het uitkomen van de eieren bij aan ZnO nanodeeltjes blootgestelde embryo's bedroeg 1,3 mg/L. Wanneer de TiO_2-nanodeeltjes aan de suspensie van ZnO-nanodeeltjes werden toegevoegd, steeg de EC_{50} met maximaal een factor 6,3. Een soortgelijke afname van de toxiciteit werd gevonden voor de mortaliteit van de embryo's: toevoeging van

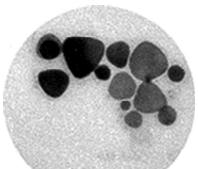

TiO_2-nanodeeltjes in hogere concentraties leidde tot een significante daling van de LC_{50}. Als positieve referentie voor het bepalen van de toxiciteit van Zn^{2+} werd een oplossing van $Zn(NO_3)_2$ gebruikt. De toxiciteit van Zn^{2+} daalde na toevoeging van TiO_2 nanodeeltjes, vergeleken met het effect van blootstelling aan een oplossing van $Zn(NO_3)_2$ zonder TiO_2-nanodeeltjes. Als het ging om het verklaren van de toxiciteit voor de embryo's van de suspensies van ZnO-nanodeeltjes met en zonder toevoeging van TiO_2-nanodeeltjes, bleek de bijdrage aan de toxiciteit van de deeltjesvorm van ZnO groter dan die van de uit de ZnO-nanodeeltjes vrijgekomen ionen.

Geconcludeerd kan worden dat het onderzoek heeft geleid tot een algemene methode voor dosisberekening die geschikt is voor het uitdrukken van de toxiciteit van nanodeeltjes van uiteenlopende vorm en grootte voor diverse soorten organismen. Deze generieke methode kan nuttig zijn voor de verdere ontwikkeling van de nanotoxicologie en het bepalen van de risico's van gesynthetiseerde nanomaterialen, wat een ontwikkeling betekent van een observationele tot een predictieve wetenschap.

Kotor, Montenegro

Photo by Jing HUA

1

Introduction

1.1 Nanomaterials and nanotechnology

Nanomaterials (NMs) and nanotechnology constitute a scientific breakthrough in industry and consumer products. Nowadays, nanotechnology is one of the key technological drivers in building an innovative European Union (EU) and the whole world based on smart, sustainable and inclusive growth (Savolainen *et al.*, 2013). Due to the small size (surface area and size distribution) of NMs, they have some specific physicochemical characteristics compared to their bulk counterpart, allowing them to perform exceptional feats of conductivity, reactivity, and optical sensitivity (Nel *et al.*, 2006). The products made by NMs are in general smaller, lighter, stronger, harder, and more stable as compared to bulk products of the same composition. However, the research about hazardous effects of NMs is still in its infancy.

1.1.1 Nanomaterials definition and classification

According to the recommendation by the European Commission (2011), a nanomaterial can be defined as follows:

"Nanomaterial" means "a natural, incidental or manufactured material containing particles, in an unbound state or as an aggregate or as an agglomerate and where, for 50 % or more of the particles in the number size distribution, one or more external dimensions is in the size range 1 nm - 100 nm. In specific cases and where warranted by concerns for the environment, health, safety or competitiveness the number size distribution threshold of 50 % may be replaced by a threshold between 1 and 50 %."

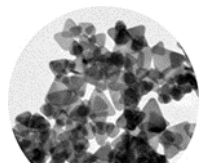

It is worth mentioning that there is still no consensus on the definition of nanomaterial. The definitions of nanomaterial are based on only the size aspect (1-100 nm) as described above. However, NMs cover a very diverse group of materials with largely varying properties. Therefore, as described in the strategy document entitled "Nanosafety in Europe 2015-2025: Towards Safe and Sustainable Nanomaterials and Nanotechnology Innovations" (Strategic Research Agenda; SRA), other key properties of materials, such as shape, composition, should be considered as well in the definitions (Savolainen *et al.*, 2013).

The SRA also mentioned that NMs can be generally classified based on the following aspects: dimensionality, shape and morphology; chemical composition; complexity and functionality; biointerface. Details on the classification system can be found in the SRA (Savolainen *et al.*, 2013).

1.1.2 Nanotechnology and applications

Nanotechnology and NMs are increasingly used in various products including antibacterial coatings, cosmetic products, constructions, food technology, high-tech, environmental technologies, drug delivery and medical applications, nano-biocide applications and energy production as well as new agriculture, water purification systems and the utilization of solar energy among others (Nel *et al.*, 2006; Maynard *et al.*, 2006). Table 1.1 briefly summarizes commonly used NMs in various products.

1.2 Exposure, fate and risks of nanoparticles

NMs promise remarkable benefits but their successful use requires resolution of potential health concerns. The increasing application of NMs will inevitably lead to a higher possibility that humans and ecosystems are exposed to NMs through different ways. For example, human exposure to NMs can arise from the life cycle of NMs (production, transport and storage, use, and disposal of NMs) (Nordberg *et al.*, 2014). Any release from the life cycle of NMs will end up in some compartments of our environment. Consequently, this may then lead to an exposure of the environment and humans through the environmental compartments.

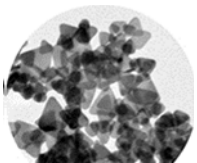

Table 1.1 Commonly used nanomaterials in various products

Nanomaterials	Typical example of the product
Ag	Bactericide, cosmetics, personal care products, clothing, wound plasters, food packaging, food supplements, water treatment, medical applications
Cu (CuO)	Catalysis, capacitor materials, catalysts, conductive coatings, conductive inks, conductive paste, high thermal conductivity materials, lubricant additive, sintering additive
TiO_2	Sunscreens, antibacterial coatings, cleaning products, paints
ZnO	Sunscreens, semiconductor, food packaging, food additives, wall coating, polymer fillers, UV absorbents, antibacterial
Si (SiO_2)	Paints, cleaning products, cosmetics, food supplements, sporting goods
Au	Cosmetics, personal care products, fuel catalysts, food supplements
C incl. C_{60}, C_{70}	Sporting goods, filtration and storage devices, OLEDs, computer RAM, cosmetics, computer hardware

(Modified from sources: http://www.eeb.org/EEB/?LinkServID=540E4DA2-D449-3BEB-90855B4AE64E8CE6)

NMs may undergo various changes during subsequent processing activities and after their release, and changes may also occur during environmental transport. Transformation processes may take place in air as well as in water, sediments and soils (Klaine *et al.*, 2008; Savolainen *et al.*, 2013). Nanoparticles (NPs) may aggregate, dissolve or attach to dust particles, aerosol, and natural organic matter (NOM) in the ambient atmosphere (Klaine *et al.*, 2008; Stahlmecke *et al.*, 2009; Schneider and Jensen, 2009; Lin *et al.*, 2010; Batley *et al.*, 2013; Garner and Keller, 2014). In aqueous environments, stability and aggregation of NPs are key elements for their transport and fate (Klaine *et al.*, 2008; Garner and Keller, 2014). Small aggregates of NPs may be transported widely and have higher chances to induce toxic effects to organisms, while large aggregated NPs may quickly precipitate onto the sediment and their transport and bioavailability will be greatly restricted (Lin *et al.*, 2010). In aqueous environments, ion release from NPs is also an important element that determines the fate of NPs. NPs submerged into

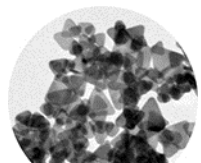

water may partially or totally convert into the ionic form, or form complexes with other ions (Gutleb *et al.*, 2015). Soils and sediments are major sinks for NMs after release into the environment and a possible source of NMs in groundwater (Lin *et al.*, 2010). NMs may attach to soil particles, clay particles, and natural organic matter (NOM). NMs and organisms also have specific interactions in ecosystems. The interactions are also related to environmental characteristics, particle properties, and ecological traits (Song *et al.*, 2011). For the fate of NMs, biological uptake, translocation, degradation and excretion are important routes of clearance. Figure 1.1 shows the fate and transport of NMs in the environment.

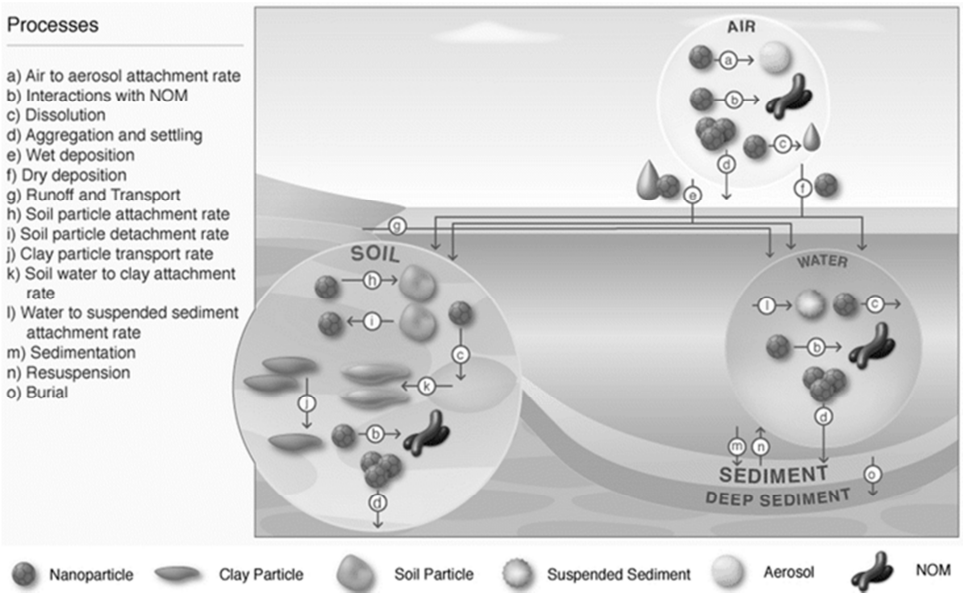

Figure 1.1 The fate and transport of NMs and interactions with various constituents in the environment (Garner and Keller, 2014).

Considering the possible increasing human and environmental exposure to NMs, it is of great importance to investigate whether NMs pose a risk to human health and the environment. (Nordberg *et al.*, 2014) Apart from exposure considerations, the risk of a given NMs depends on its toxicity, persistence and bioaccumulation (Ngô and van de Voorde, 2014). Different NMs are found to show large variation in their toxicity. For instance, TiO_2 NPs and Au NPs induce in general low toxicity (Zhu *et al.*, 2008; Bar-Ilan *et al.*, 2009; George *et al.*, 2011a), while other particles, such as

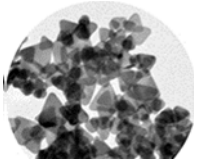

Ag NPs and Cu NPs, generally show high toxicity (George *et al.*, 2011b). A number of injury-response mechanisms in cells have emerged that can be quantitatively implemented to assess hazardous properties of NMs. The mechanisms of actions (MoAs) of the particle form of NPs ($NP_{(particle)}$) include inducing a higher level of reactive oxidative species (ROS) that cause a cellular oxidative stress response; cellular oxidative damage may also cause DNA damage and lipid peroxidation effects; membrane damage; mitochondrial damage; cationic injury to surface membrane and organelles; inflammasome activation by long-aspect-ratio NMs; photoactivation and influence of bandgap; cell membrane lysis by surface reactivity (Nel *et al.*, 2006; Nel *et al.*, 2009; Thomas *et al.*, 2011; Zhu *et al.*, 2013; Nel *et al.*, 2013; Ivask *et al.*, 2014a). Figure 1.2 shows some possible MoAs of $NP_{(particle)}$ and $NP_{(ion)}$ in cells. However, the information on the environmental fate, transport, exposure, ecotoxicity, and life cycle of NMs is quite limited; and the knowledge on the mechanisms of toxicity of NMs *in vivo* and *in vitro* is still in its infancy. It is essential to determine the environmental and health impacts of NMs for an environment-friendly nanotechnology.

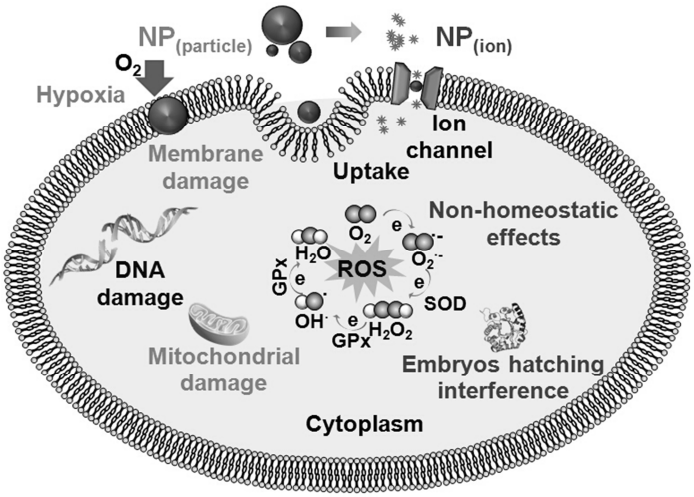

Figure 1.2 The mechanisms of actions (MoAs) of the particle form of NPs ($NP_{(particle)}$) and their released metal ions from NPs ($NP_{(ion)}$) in cells. The $NP_{(particle)}$ and $NP_{(ion)}$ both can be taken up by organisms, induce a higher level of reactive oxidative species (ROS), then cause DNA damage and lipid peroxidation effects. The MoAs of $NP_{(particle)}$ include membrane damage; mitochondrial damage, and hypoxia; the MoAs of $NP_{(ion)}$ including interfere embryos hatching, low as well as high levels of free metal ions can disrupt homeostatic mechanisms.

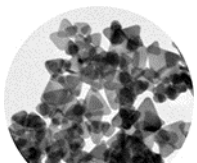

1.3 Impact of physicochemical properties on nanoparticles

Compared with the same materials in the bulk form, NPs exhibit different physicochemical and biological characteristics (Alivisatos *et al.*, 1996; Wautelet *et al.*, 2003). Figure 1.3 summarizes the major physicochemical properties of NPs impacting the fate of NPs and their biological interactions at the cellular level. The following subsections describe the impacts of size, shape, dissolution ability and ion release, and other physicochemical characteristics related to this thesis.

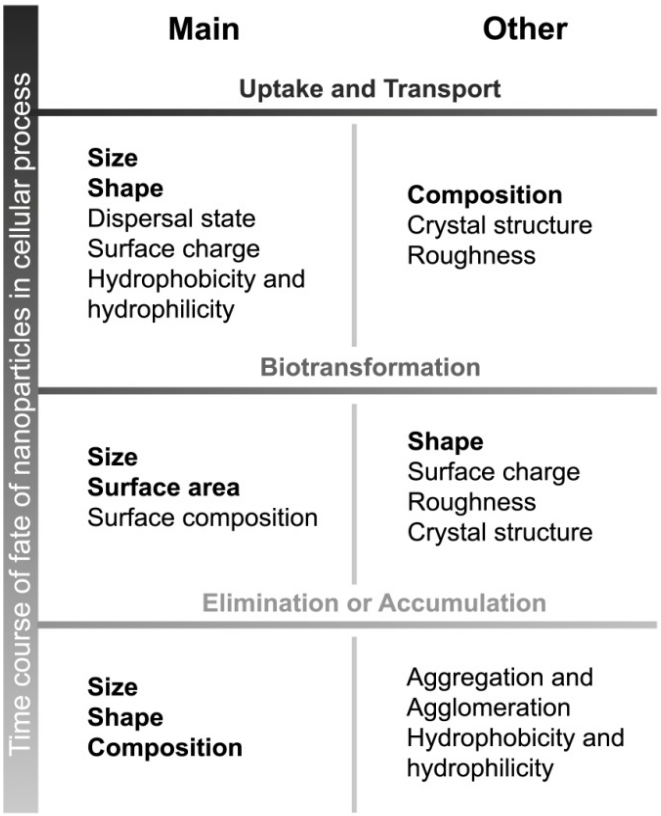

Figure 1.3 The major physicochemical properties of nanoparticles that impact the fate of nanoparticles and their biological interactions at the cellular level. Figure adapted from Zhu *et al.* (2013) (slightly modified).

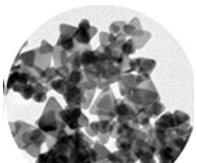

1.3.1 Size

The size of a given nanomaterial plays an important role in determining cellular uptake, transport and accumulation (Zhu *et al.*, 2013). The importance of the size among many physical properties may explain why most definitions of NMs solely focused on the size aspect as mentioned in Section 1.1.1. Many studies have investigated the toxicity of different-sized NPs using Ag NPs (Bar-Ilan *et al.*, 2009; Jiang *et al.*, 2008b; Lee *et al.*, 2012), Au NPs (Bar-Ilan *et al.*, 2009), Si NPs (Tenzer *et al.*, 2011), and Ni NPs (Ispas *et al.*, 2009). Bar-Ilan *et al.* (2009) reported that all sizes of Ag NP cause toxic effects to zebrafish embryos and that the smaller particles were more toxic. Similarly, Ivask *et al.* (2014b) also found that biological effects of Ag NPs were size-dependent. Smaller Ag NPs (10 nm) displayed more efficient cell-particle contact and higher intracellular bioavailability of silver than in case of larger sized NPs (Ivask *et al.*, 2014b). In addition, Au particles with larger size have been commonly considered to induce no toxicity, but Au NPs with size of 1.4 nm were found to induce toxicity in different cell lines (Tsoli *et al.*, 2005). However, scientific debate is going on about the relationship between size and the induced toxicity response. For example, Ispas *et al.* (2009) found that there was no significant difference in LC_{50} of different sizes of Ni NPs.

1.3.2 Shape

The shape of particles can also affect the toxicity of NPs. Many studies have been conducted to investigate the toxicity of various shapes of NPs. For example, Ag NPs (George *et al.*, 2012), Au NPs (Chithrani and Chan, 2007), Ni NPs (Ispas *et al.*, 2009), Si NPs (Huang *et al.*, 2011; Tenzer *et al.*, 2011), and Fe_2O_3 NPs (Lee *et al.*, 2014). George *et al.* (2012) found that Ag nanoplates were considerably more toxic than Ag nanospheres and Ag nanowires in a fish gill epithelial cell line (RT-W1) and in zebrafish embryos. Rod-shaped Au NPs showed a lower uptake in mammalian cells in comparison to spherical Au NPs (Chithrani and Chan, 2007). Lee *et al.* (2014) found that Fe_2O_3 nanorods were more toxic than Fe_2O_3 nanospheres to murine macrophage cells. Larger nanodiscs and rods had higher uptake rates compared with the smallest particles tested for mammalian cells (Agarwal *et al.*, 2013).

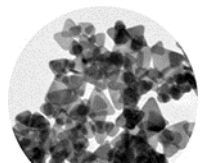

1.3.3 Solubility and ion release

Dissolved metal ions from NPs ($NP_{(ion)}$) also play an important role in inducing acute or chronic toxicity of NPs to aquatic organisms, and thus solubility should be taken into account in toxicity assessment (Zhu *et al.*, 2013). The dissolution rate of a given nanomaterial could be dependent on the surface area of particles, and NMs are expected to have higher dissolubility in terms of rate and extent of dissolution than large particles of the same material (Dobrovolskaia *et al.*, 2007; Zhu *et al.*, 2013). Cho *et al.* (2012) assessed the inflammability of various metal/metal oxide NPs and found that toxicity was strongly correlated with zeta potential under acid conditions for low-solubility NPs and solubility for high-solubility NPs. However, the problem in recently studies is that most of the studies have directly compared the toxicity of nanoparticle colloids with the effect of their compartment salts (Xia *et al.*, 2008; Zhu *et al.*, 2008; Lin *et al.*, 2011). The clear differentiation between the effects of the particle form of NPs and of ion release from NPs in the observed toxic properties is often difficult to prove experimentally by this general approach (Ivask *et al.*, 2014a). Therefore, it is of utmost importance to propose a general approach that can overcome these difficulties and that allows us to make a quantitative assessment of the relative contribution to toxicity of ions and particles.

1.3.4 Other physicochemical characteristics

There are also various other physicochemical characteristics for NMs, including the chemical composition, aggregation state, surface charge and surface coating (Monteiro-Riviere and Tran, 2007) that influence NMs fate and chemical behavior as described in Section 1.2.

The chemical composition relates to elemental composition, chemical structure, and chemical purity. Different NMs can have a different chemical composition, and chemical composition determines many aspects such as the surface chemistry, surface energy, redox status, photoactivation potential, surface charge, and surface reactivity (Zhu *et al.*, 2013). Hence chemical composition could induce differences in biological behavior and toxicity.

NPs generally have a high tendency to form aggregates in a range of different phases (solution, powder and gas phases) as described in Section 1.2. The type and

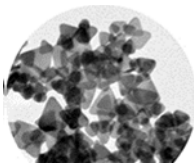

degree of aggregation may affect the stability of NMs colloids (Monteiro-Riviere and Tran, 2007) and further toxic effects. For example, Zhu *et al.* (2009) reported more effective macrophage clearance for larger aggregated particles compared with smaller ones. Single and aggregated NPs have different uptake patterns for different cell types (Albanese *et al.*, 2011). For example, for HeLa and A549 cells the uptake of aggregated Au NPs decreased by 25% when compared to single and monodisperse Au NPs. In contrast, for MDA-MB 435 cells, the uptake of the largest synthesized Au aggregates increased by 2-fold (Albanese *et al.*, 2011). Gilbert *et al.* (2009) found that the aggregation mechanism has a great effect on aggregate morphology and thus on the net sorption/retention of ions from NPs suspensions.

The surface of NPs may have an electric charge, and surface charge could strongly affect the uptake of NPs (Nordberg *et al.*, 2014). It is shown that NPs with positive surface charge are taken up faster by cells than those with a negative surface charge typically due to the overall net negative surface charge of cells. As a result, the NPs with positive surface charge have a potential to induce a higher toxicity because of elevated cellular uptake (Oh *et al.*, 2010; Nordberg *et al.*, 2014).

Some NPs could be coated with different chemicals to achieve particular functions (Monteiro-Riviere and Tran, 2007). The coating and chemical properties of the surface for given NPs can affect the wettability, suspension stability, solubility, shedding of toxic ions, and durability (Zhu *et al.*, 2013), and thus have a direct influence on their biological behavior and toxicity.

1.4 Dose metrics assessment of nanoparticles

In the risk assessment of chemicals, the dose metrics is one of the foundations. For conventional chemicals (*i.e.* chemicals that are not present as particles), risk is commonly expressed on the basis of dose metric “mass”. However, ‘mass’ as a dose metric is not ideal for the expression of responses induced by NPs (Oberdörster, 2000; Wittmaack, 2007a).

For a better assessment of dose metrics of NPs, the physicochemical characteristics of NPs should be taken into account. It was found by Oberdörster *et al.* (2007) that

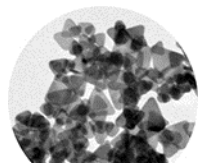

particle surface area is a better dose metric than particle mass or particle number, when evaluating dose-response relationships of NPs. Other investigators have also considered surface area as an appropriate dose metric (Donaldson *et al.*, 2000; Oberdörster, 1996; Oberdörster *et al.*, 2005; Stoeger *et al.*, 2006). By contrast, Wittmaack (2007a) suggested that particle number was the optimal metric. In addition, Delmaar *et al.* (2015) showed a systematic and unbiased approach to determine the best dose metric for spherical-shaped NPs, and apply the approach to datasets from *in vitro* and *in vivo* experiments with Ag NPs and SiO_2 NPs. For most of the datasets, a single parameter (*e.g.* surface area, volume) is adequate to describe the dose metric of the NPs considered (Delmaar *et al.*, 2015). For different NPs and different systems, the dose metric was not the same.

1.5 Metal-based nanoparticles

The most common NPs are metallic oxides NPs (titanium dioxide, silicon dioxide, antimony pentoxide), metal NPs (silver, magnesium, zinc), and carbon nanotubes. The toxicology of metals has been the subject of investigation for many years. However, as particle size decreases, some metal-based materials may display increased toxicity compared to the same material in its bulk form. For some metal or metal oxide NPs (such as Cu/CuO or Ni/NiO), particle dissolution and the release of toxic metal ions may be the principle driving force underlying toxicity. NPs cause oxidative stress, DNA damage, and apoptosis (Nel *et al*., 2013), but there is a striking variation in the levels of toxicity reported in different studies. Most likely these differences can be explained by differences in size, shape, surface coating, and release of metal ions, as well as the species as described in Section 1.3.

In this section, we will highlight recent opinions on the possible risks of some of the metal/metal oxide NPs that are most commonly studied and/or produced in largest quantities (Ag NPs, Cu NPs, ZnO NPs, and TiO_2 NPs)

1.5.1 Silver NPs (Ag NPs)

Due to their antibacterial properties, Ag NPs have been used to prevent bacterial growth in cosmetics, personal care products, clothing, wound plasters. Ag NPs also

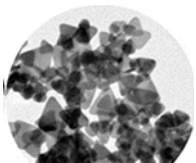

have been used extensively in food packaging, food supplements, water treatment, and medical devices. The toxicity of Ag NPs may exceed the toxicity of the most toxic silver compound in its standard form (Pal *et al.*, 2007). Indeed, silver has been shown to be relatively more toxic than other metals when in nanoparticle form (Zeng *et al.*, 2007).

1.5.1.1 *In vivo* toxicity studies

There have been some studies into the toxicity of Ag NPs *in vivo*. Researchers have shown that Ag NPs can destroy the ability of bacterial DNA to replicate or can damage DNA (Hwang *et al.*, 2007). Low concentrations of Ag NPs will harm aquatic invertebrates and fish. Ag NPs administered *in vivo* to zebrafish embryo increased malformation rates and mortality. Individual Ag NPs were found inside embryos at each developmental stage (Landsdown, 2007). Lee *et al.* (2007) found that Ag NPs can induce altered physiology to zebrafish, including the degeneration of body parts, inhibition of hatching and an increase in mortality. Ag NPs are transported into zebrafish embryos through chorion pore canals (Lee *et al.*, 2007). The growth and reproductive ability of nematodes can be weakened by Ag NPs (Asharani *et al.*, 2008). Li *et al.* (2015b) demonstrated that released Ag^+ and particulate Ag of NPs were both toxic to earthworm. Wang *et al.* (2012) also reported that both particulate Ag and released Ag^+ were toxicity to algae (*Raphidocelis subcapitata*), cladocerans (*Chydorus sphaericus*), and fish (*Danio rerio*), these being species of different trophic levels.

1.5.1.2 *In vitro* toxicity studies

Ag NPs are also toxic to mammalian cell cultures, such as cultured neuroendocrine cell lines, which are a model for human brain cells, and rat cells used as a model for human toxicity after inhalation (Hussain *et al.*, 2005; 2006). Ag NPs induce oxidative stress-mediated cytotoxicity in human hepatoma cells (Kim *et al.*, 2009). Carlson *et al.* (2008) found that the smallest Ag NPs generated more ROS and caused a more pronounced deleterious effect on cell viability compared to the larger particles. Shape of Ag NPs rather than the amount of released Ag ions are important for the toxicity of Ag NPs in A549 cells (Stoehr *et al.*, 2011).

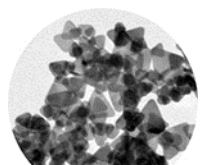

1.5.2 Copper NPs (Cu NPs)

Cu NPs are widely used in catalysis and in electronic applications, and they are the major constituent of conductive inks and pastes (Griffitt *et al.*, 2007; Lee *et al.*, 2008; Radi *et al.*, 2010). Cu_2O NPs and CuO NPs, have various potentially useful physical properties, and are widely used in semiconducting compounds that attracted particular attention (Nordberg *et al.*, 2014). These semiconductors are used in many applications such as in gas sensors, batteries, and catalysis (Yin *et al.*, 2005; Griffitt *et al.*, 2007; Radi *et al.*, 2010; Nordberg *et al.*, 2014).

1.5.2.1 *In vivo* toxicity studies

Cu and CuO NPs have shown high toxicity *in vivo* when compared to other metal-based NPs in many studies. Cu NPs (23.5 nm) induce toxic effects and kidney, liver, and spleen injury in mice (Chen *et al.*, 2006). However, 17 μm Cu micron-sized particles (MPs) were found not to be toxic to mice (Chen *et al.*, 2006). Meng *et al.* (2007) found that Cu NPs were extremely reactive in the stomach of mice. Yokohira *et al.* (2008) reported that CuO particles, especially CuO NPs, were the most toxic to the lung of rats compared to other types of particles. Cu NPs were observed to be acutely toxic to the gills of zebrafish (Griffitt *et al.*, 2007).

1.5.2.2 *In vitro* toxicity studies

In line with *in vivo* studies, *in vitro* studies also highlight the high toxicity of Cu NPs and CuO NPs. Prabhu *et al.* (2010) found neurotoxic effects from Cu NPs on rat DRG neuron cell cultures, with smaller size Cu NPs producing the maximum toxic effects. Karlsson *et al.* (2008) showed that the CuO NPs displayed the highest potency in causing higher intracellular ROS levels and DNA damage when compared to other metal oxide NPs following exposure of A549 cells. CuO NPs induced dose-dependent toxicity in human H4 neuroglioma cells (Li *et al.*, 2007). Song *et al.* (2014) reported that Cu NPs were toxic to two mammalian (H4IIE and HepG2) and two piscine (PLHC-1 and RTH-149) cell lines. The results showed that the size, shape, and ion release all should be taken into account when investigating the toxicity of Cu NPs.

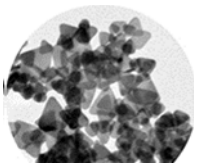

1.5.3 Zinc oxide NPs (ZnO NPs)

Zinc oxide is considered relatively safe in its bulk form. ZnO NPs are widely used in products such as a pigment for paints and cosmetics, semiconductor, food packaging, food additives, wall coatings, sunscreens, polymer fillers, and UV absorbents (Xia *et al.*, 2008). It can also exhibit antibacterial properties. It is known that ZnO NPs are toxic to organisms, and ZnO particles have been considered as "extremely toxic" in the environment (Kahru and Dubourguier, 2010).

1.5.3.1 *In vivo* toxicity studies

There have been some studies into the effects of ZnO NPs to various species *in vivo*. ZnO NPs caused death, anemia, and damage in kidney, liver, heart, spleen and pancreas in mice (Wang *et al.*, 2006; 2008). The released ions from ZnO NPs are an important factor in the toxicity of ZnO NPs, and reduced dissolution would be expected to cause less toxicity (Xia *et al.*, 2011). Iron-doped ZnO NPs, showed less dissolution than non-doped ones, and induced less lung toxicity and inflammation in rats (Xia *et al.*, 2011). Some studies report the toxicity of ZnO NPs in bacteria and vertebrates (Brayner *et al.*, 2006; Heinlaan *et al.*, 2008); inhibition of seed germination and root growth in plants (Lin and Xing, 2007). ZnO NPs are also toxic to roundworms and can inhibit their growth and reproductive capabilities (Wang *et al.*, 2009). Microorganisms and plants may be able to modify and concentrate ZnO NPs that can then bioaccumulate (or even biomagnify) along the food chain (Wang *et al.*, 2009). Zhu *et al.* (2009) reported that ZnO NPs induce toxicity to zebrafish embryos, including malformation, hatching delay and mortality.

1.5.3.2 *In vitro* toxicity studies

ZnO NPs are also toxic to human and rat cells *in vitro* (Brunner *et al.*, 2006). ZnO NPs have been reported to induce cytotoxicity in L2 cells (Sayes *et al.*, 2007), in BEAS-2B cell lines (Huang *et al.*, 2010a). George *et al.* (2010) found that ZnO NPs induced cytotoxicity in BEAS-2B cells and RAW264.7 murine macrophages using a cytotoxicity screening approach.

1.5.4 Titanium dioxide NPs (TiO_2 NPs)

Titanium dioxide (TiO_2) NPs (rutile, anatase and brookite in three crystalline

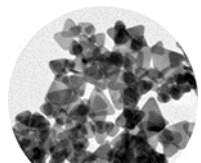

phases) have been widely used as a pigment and in paints, ointments, and toothpaste (Pfaff and Reynders, 1999; Salvador *et al.*, 2000; Zallen and Moret, 2006), as well a UV filter in sunscreens (Zallen and Moret, 2006).

1.5.4.1 *In vivo* toxicity studies

TiO_2 NPs were reported less toxic compared to other kinds of metal-based NPs. Nano and bulk TiO_2 were not toxic even at very high concentration (20 g/L) to Daphnia magna (Heinlaan *et al.*, 2008). Ferin *et al.* (1992) reported that TiO_2 NPs induced a higher pulmonary inflammatory response than their bulk counterpart. Smaller sized TiO_2 NPs were observed to stay in the lung for 501 days following inhalation, compared to larger TiO_2 particles for 174 days, indicating that clearance is far more slower for the NPs. Van Ravenzwaay *et al.* (2009) found that TiO_2 NPs accumulated in the lungs of male rats following inhalation.

1.5.4.2 *In vitro* toxicity studies

Various studies have been performed using different types of cell lines in order to assess the *in vitro* toxicity of TiO_2 NPs. The size and crystal phase influenced the toxicity: the smaller the size and greater the anatase content of the TiO_2 NPs, the greater its ability to induce cell death (Jiang *et al.*, 2008a; Simon-Deckers *et al.*, 2008). Gurr *et al.* (2005) demonstrated that toxic effects of TiO_2 NPs were size and shape dependent, and had the tendency to increase levels of ROS, cellular nitric oxide, hydrogen peroxide in BEAS-2B human bronchial epithelial cell line.

1.5.5 Toxicology of NPs mixtures

Toxicity of metal-based NPs has received considerable attention in recent years due to the massive increasing application of various products containing metal-based NPs that can induce adverse effects on human health and the environment. Such attention resulted in a large amount of publications on the assessment of toxicity of various metal-based NPs. However, new generation NPs are more often composites or mixtures. A limited number of studies considered mixtures of NPs. Li *et al.* (2015a) investigated the toxic effect of ZnO NPs and Cu NPs, and they found that ZnO NPs at non-toxic concentrations enhance Cu NPs toxicity *in vitro*. Kim *et al.* (2010) studied the toxic effect of a combination of copper and single-walled carbon nanotubes on Daphnia magna. However, to our knowledge

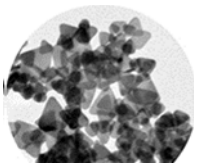

there are no other publications on the toxicity of mixtures of various metal-based NPs.

In the practical situation, both humans and ecosystems are typically exposed to mixtures of NPs. The NPs will inevitable dissolve in air, water, sediment and soil as described in Section 1.2, therefore, the NPs colloids can be treated as a mixture of dissolved metal ions from NPs ($NP_{(ion)}$) and particulate metal-based NPs ($NP_{(particle)}$) and other types of metal species. Nevertheless, it is very important to assess the toxicity induced by mixtures of NPs or different metal species of NPs. A better understanding is needed about: whether the toxicity of the mixture is equal to the sum of toxicities of individual components; whether there exist synergistic or antagonistic effects resulting in higher or lower toxicity than the sum of toxicities of individual components, respectively.

Concentration Addition (CA) (also known as Similar Action (SA)) and Response Addition (RA) (also known as Independent Action (IA)) are the two main conceptual models that are available for calculating the toxicity of mixtures (Loewe and Muischnek, 1926; Bliss, 1939).

1.5.5.1 Concentration addition

The CA model is used to predict the effect of substances with the same or a similar mode of action or mechanism of action (Loewe and Muischnek, 1926). Mechanisms of action are the specific means by which chemicals induce effects in organisms. Modes of action are more general and phenomenological. Note that the terms mechanism of action and mode of action are not used consistently in the literature, and there is no agreed dividing line between them (Suter II, 2006). In addition, the mode of action of toxicity of metal-based NPs is still unclear. We therefore refer in our study with regard to MoA to the mechanism of action. In the concentration addition model, the effect of the mixture can be calculated by the following equation:

$$\sum_{i=1}^{n} \frac{c_i}{E(c_i)} = 1 \qquad (1.1)$$

where n is the number of mixture substances, c_i is the actual exposure concentration of substance *i*, $E(c_i)$ is the effective concentrations of substance *i*.

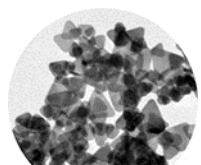

1.5.5.2 Response addition

The RA model is used to predict the effect of components with different or dissimilar modes of action or mechanisms of action (MoAs) (Bliss, 1939). Here, we also refer in our study with regard to MoAs to mechanisms of action. In the response addition model, the effect of the total mixture can be calculated by summing the effects of each component, using the following equation:

$$E(c_{mix}) = 1 - \prod_{i=1}^{n}(1 - E(c_i)) \quad (1.2)$$

where $E(c_{mix})$ is the total effect of the mixture (scaled from 0 to 1), $E(c_i)$ is the extent of effect induced by component *i*.

1.6 Zebrafish

Zebrafish (*Danio rerio*) is a small tropical freshwater fish. The zebrafish adults are about 2 cm long and have a generation time of around 3 months (Basu and Sachidanandan, 2013). They can be easily maintained and be bred in freshwater tanks at 28 °C in the laboratory. Females are highly prolific egg layers with one individual capable of laying hundreds of eggs in a day, on a weekly basis (Basu and Sachidanandan, 2013). It has been considered as a 'gold standard' for toxicity assessment in the environment (Scholz *et al.*, 2008).

Numerous advantages have made zebrafish an attractive *in vivo* model for environmental health and safety studies with NPs (Basu and Sachidanandan, 2013; Lin *et al.*, 2013a). The early life stages of zebrafish embryos offer a rapid, high-throughput screening platform for noninvasive real-time assessments of toxicity, due to their small size, transparency and ability to absorb compounds through the water (Kimmel *et al.*, 1995; Bar-Ilan *et al.*, 2009; Lin *et al.*, 2013a). In addition, embryos develop most of their major organ systems, including the cardiovascular, neural and digestive systems, in less than one week (Rubinstein, 2006).

The advantages of embryos have been already mentioned above as an *in vivo* model compared to other *in vivo* organisms. Furthermore, compared to *in vitro* cellular assays, zebrafish embryos also have the following advantages: they offer

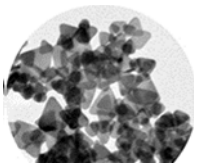

higher biological relevance and complexities while maintaining high throughput and high volume data generation capabilities (Lin *et al.*, 2013a).

The Organization for Economic Cooperation and Development (OECD) is developing standards for using zebrafish to assess chemical toxicity (McGrath and Li, 2008; McGrath, 2012), and the OECD provides support for the wider use of zebrafish for toxicity testing. A series of test guidelines have been established by OECD, *i.e.*, "Validation Report (Phase 1) for the Zebrafish Embryo Toxicity Test, Series on Testing and Assessment, No. 157" (OECD, 2011), "Validation Report (Phase 2) for the Zebrafish Embryo Toxicity Test, Series on Testing and Assessment, No. 179" (OECD, 2012), and "Fish Embryo Acute Aquatic Toxicity (FET) Test guideline for the testing of chemicals" (OECD, 2012). The EU recently enacted Registration, Evaluation, Authorisation and Registration of Chemicals (REACH) legislation, also providing support for wider use of zebrafish as the model organism for toxicity assessment (McGrath, 2012).

1.7 Objectives and research questions of the thesis

The SRA describes the present conditions and the research requirements for the next several years: 1) nanomaterial identification and classification; 2) nanomaterial exposure and transformation; 3) assessment of toxic mechanisms related to effects on human health and the environment; and 4) development of tools for predictive risk assessment and management.

In the context of the SRA research requirements, the general objective of this thesis was to assess the physicochemical-dependent toxicity of nanoparticles and assess the proper dose metrics of metal-based nanoparticles. Three specific goals of this thesis were:

(1) To determine how physicochemical properties (size, shape, and ion release) of metal-based nanoparticles affect the toxicity of the nanoparticles to zebrafish embryos;
(2) To develop a generic dose calculation method and determine which property or properties are the most appropriate as a dose metric when assessing dose-response relationships of different metal-based nanoparticles.

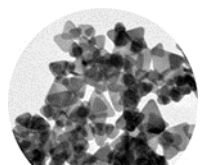

(3) To assess the toxicity of mixtures of metal-based nanoparticles at different component ratios and concentration levels.

To achieve these goals, several main research questions were formulated:

(1) Is the toxicity of metal-based NPs to zebrafish embryos related to NPs' size or shape? What properties of NPs should also be considered when assessing the toxicity of NPs? (Chapter 2, 3 and 4)
(2) Are the ions released from nanoparticles or the particle itself the main factor causing toxicity? How to make a quantitative assessment of the relative contribution to toxicity of ions and particles? (Chapter 2, 3 and 5)
(3) Which physicochemical property of nanoparticles (such as surface area, volume, or number) is an appropriate dose metric of NPs? (Chapter 4)
(4) How does a mixture of metal-based nanoparticles (ZnO NPs and TiO_2 NPs) impact the overall toxicity as compared to the toxicity of the individual particles? (Chapter 5)

1.8 Outline of the thesis

Chapter 1 provides an overview of the nanomaterials and nanotechnology, exposure and risks of nanoparticles in the environment, physicochemical characterization of nanoparticles, dose metrics assessment of nanoparticle, and some of the commonly studied metal/metal oxide nanoparticles are briefly summarized

Chapter 2 deals with different-sized spherical copper nanoparticles. Toxic effects of different sized copper nanoparticles to zebrafish embryos were assessed, showing whether nanotoxicity is size-dependent. The response addition model was used to calculate the contribution to toxicity of Cu ions and Cu particles.

Chapter 3 focuses on differently shaped zinc oxide nanoparticles. Both the concentration addition model and the response addition model were used to calculate the contributions to toxicity of Zn ions and ZnO particles. We also determined whether the toxicity of ZnO NPs to zebrafish embryos is related to the shape of the NPs.

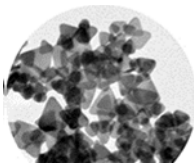

In Chapter 4 a general model was developed to assess the dose metrics for differently shaped and sized metal-based nanoparticles. Laboratory data from different origin were also collected to validate the general model.

Chapter 5 focuses on the interactions of ZnO NPs and TiO_2 NPs in an aquatic exposure system and on the impact of mixtures of ZnO NPs and TiO_2 NPs on the toxicity to zebrafish embryos (*Danio rerio*) as compared to the impact of the individual particles.

Finally, Chapter 6 summarizes and concludes the main findings of this thesis. The recommendations for future research are also provided in this final chapter.

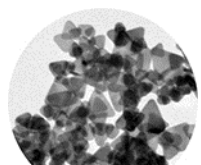

Prague, Czech Republic

Photo by Jing HUA

2

Toxicity of different-sized copper nano- and submicron particles and their shed copper ions to zebrafish embryos[1]

2.1 Introduction

Copper nanoparticles (Cu NPs) are widely used in catalysis and in electronic applications (Radi *et al.*, 2010; Cioffi *et al.*, 2005; Griffitt *et al.*, 2007). The manufacture, use, and disposal of Cu NPs may lead to the exposure of humans and environmental receptors. Therefore, the potential risks of Cu NPs should be investigated. Various studies have reported that Cu NPs and CuO NPs have lethal and sublethal toxicity to fish (Griffitt *et al.*, 2007; Lin *et al.*, 2011; Zhu *et al.*, 2008; Manusadzianas *et al.*, 2012; Lubick, 2007; Bai *et al.*, 2010a; Shaw and Handy, 2011). It was, for instance, shown that Cu NPs decreased the Na^+/K^+-ATPase activity of zebrafish and rainbow trout (Shaw *et al.*, 2012). The zebrafish has been widely selected as an attractive *in vivo* model for environmental health and safety studies with nanoparticles because of its small size, transparency, and rapid growth (Lin *et al.*, 2013a). It has been shown that Cu NPs are more acutely toxic to juvenile zebrafish than is dissolved Cu^{2+}, whereas this trend was reversed in adult fish (Griffitt *et al.*, 2008).

Particle size has been suggested as an important physicochemical characteristic

[1] Based on: Hua, J., Vijver, M. G., Ahmad, F., Richardson, M. K. and Peijnenburg, W. J.G.M. (2014), Toxicity of different-sized copper nano- and submicron particles and their shed copper ions to zebrafish embryos. *Environmental Toxicology and Chemistry*, 33: 1774–1782. doi: 10.1002/etc.2615.

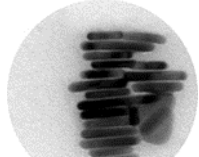

when assessing the toxicity of nanoparticles, although the underlying mechanism has not been fully understood (Oberdorster *et al.*, 2005; Nel *et al.*, 2006). Many studies have investigated the toxicity of different-sized nanoparticles using Ag NPs (Jiang *et al.*, 2008b; Lee *et al.*, 2012), Au NPs (Bar-Ilan *et al.*, 2009), Si NPs (Tenzer *et al.*, 2011), and Ni NPs (Ispas *et al.*, 2009). However, little attention has been paid to the toxicity of different-sized Cu NPs in zebrafish embryos. Griffitt *et al.* (2007; 2008) indicated that smaller Cu NPs were more toxic than larger Cu NPs to adult zebrafish. Therefore, our first research aim was to deduce whether the toxicity of Cu NPs is size-dependent and, in particular, the extent to which particle size might have adverse effects on the development of zebrafish embryos. To evaluate toxicity, zebrafish embryos were exposed to either Cu as $Cu(NO_3)_2$ or Cu NPs or to Cu submicron-sized particles, and the effects on the development of the embryos were recorded. It should be noted that in previous studies the death of zebrafish embryos was in all cases caused by metal suspensions (designated as Cu $NP_{(total)}$ hereafter), including dissolved Cu ions from Cu NPs (designated as Cu $NP_{(ion)}$ hereafter) and the particle form of Cu NPs and submicron-sized particle (designated as Cu $NP_{(particle)}$ hereafter), and not by Cu $NP_{(particle)}$ only. To fill this gap, we calculated the combined toxic effects to embryos of Cu $NP_{(particle)}$ and Cu $NP_{(ion)}$ following exposure to a suspension of Cu NPs. Our second research aim was to determine the relative contributions of Cu $NP_{(ion)}$ when exposed to zebrafish embryos and of Cu $NP_{(particle)}$ in inducing toxic effects to zebrafish embryos.

2.2 Materials and methods

2.2.1 Preparation of Cu suspensions

Copper nanoparticles were purchased from IoLiTec and had initial nominal sizes of 25 nm (specific surface area 30–50 m^2/g, purity 99.9%), 50 nm (specific surface area 6–8 m^2/g, purity 99.5%), and 100 nm (purity 99.9%) (according to the manufacturer's information). The 400-nm submicron-sized particles (purity 99%) were purchased from NanoAmor. The Cu particles were all uncoated. Dry powder Cu particles were weighed (8 mg/L) and added into 100 mL of egg water (0.21 g Instant Ocean® salt in 1 L Milli-Q water and 1 µL 0.25% methylene blue, pH 6.5–7.0). The Cu ion concentration in egg water was 0.002 mg/L. All stock solutions (100 mL) were freshly prepared and sonicated for 10 min in an S40 h Elmasonic water bath sonicator; diluted to 0.25 mg/L, 0.5 mg/L, 1 mg/L, 2 mg/L, 4

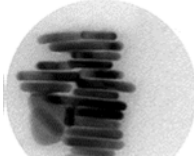

mg/L, and 8 mg/L of copper particle suspensions or $Cu(NO_3)_2$ using egg water and then exposed to embryos immediately and to other physicochemical characterization measurements after 1 h of incubation.

2.2.2 Physicochemical characterization of Cu NPs

The size and morphology of the Cu NPs and submicron-sized particles (8 mg/L) were characterized using transmission electron microscopy (JEOL 1010) after drying the suspension (required for this microscopic technique) in egg water after 1 h of incubation. The primary particle sizes of Cu NPs were analyzed by Nano Measurer 1.2 (Department of Chemistry, Fudan University, China). Size analysis was performed only when individual well-defined nanoparticles could be determined. Dynamic light scattering assessments were executed on a Zetasizer Nano-ZS instrument (Malvern Instruments) and performed for detecting the size distribution and zeta-potential of copper suspensions in egg water (1 mg/L, 2 mg/L, and 8 mg/L) at 1 h and 24 h. Three independent measurements for dynamic light scattering were taken, with each measurement consisting of 6 measurements at each time point and at each concentration. We assessed the properties only in the exposure medium without embryos. The embryos may affect the size distribution of Cu particles, which is out of the scope of our present study and needs further investigation. Copper particles often have a layer of CuO on the surface because of their reactivity, which could influence the dissolution rate. We assumed that dissolved Cu was fully converted to Cu^{2+} (Cu $NP_{(ion)}$), and we did not take any other Cu species into account. The Cu particle suspension (Cu $NP_{(total)}$) is composed of Cu $NP_{(ion)}$ and Cu $NP_{(particle)}$. The Cu $NP_{(ion)}$ and Cu $NP_{(total)}$ in egg water were analyzed by atomic absorption spectroscopy (AAS; Perkin Elmer 1100B) after 24 h of equilibration of the samples. To determine Cu $NP_{(ion)}$ concentrations in the particle suspensions, 5 mL of the suspensions was sampled after 24 h of incubation and centrifuged at 13 300 *g* for 20 min to remove Cu NPs and submicron-sized particles from suspensions. There were still some particles present in the supernatant during this procedure, but the lower Cu ion concentrations can be neglected. Nitric acid was added to digest the samples at pH 2 for at least 1 d. Then, the samples were analyzed using AAS.

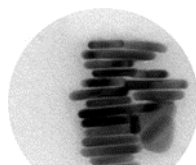

2.2.3 Waterborne exposure of zebrafish embryos to Cu NPs

Fertilized zebrafish eggs were obtained from an AB wild-type zebrafish. Adult zebrafish were maintained at 25 ± 5 °C in a 14 h light: 10 h dark cycle. An acute exposure regime of 96 h was used, from 24 h post fertilization (hpf) to 120 hpf, thus including exposure during the major stages of organ development. The background mortality at 24 hpf was less than 10% (data not shown). At 24 hpf zebrafish embryos were distributed, 1 embryo per well, into 96-well plates in 250 µL of freshly prepared egg water containing 0.25 mg/L, 0.5 mg/L, 1 mg/L, 2 mg/L, 4 mg/L, and 8 mg/L of copper particle suspensions and $Cu(NO_3)_2$. Throughout all procedures, embryos and solutions were kept at 28 °C. The exposure media were replaced with a freshly prepared suspension of nanoparticles every day according to Organisation for Economic Co-operation and Development (OECD) guideline 157. The test suspension was replaced according to Ali *et al.* (2011a). This replacement procedure could increase the actual copper concentrations over time in the fluid in the 96-well plate because of the possibility of continued sedimentation of particles in between 2 fluid renewals. To verify this possibility, the actual concentrations of the remaining Cu NP suspensions were measured after 120 hpf, and the actual concentrations in the 96-well plates 120 hpf deviated by 96 ± 0.5% from the actual concentrations of the suspensions.

Zebrafish embryos were exposed in triplicate to either a control or different concentrations of Cu as $Cu(NO_3)_2$, Cu NPs, or Cu submicron-sized particles, each replicate contained 16 embryos for each treatment (48 embryos in total). Mortality and hatching rates were assessed at 48 hpf, 72 hpf, 96 hpf, and 120 hpf using a dissecting stereomicroscope. Embryos were scored as dead according to OECD guideline 157: coagulation of the embryo, nondetachment of the tail, nonformation of somites, and nondetection of the heartbeat. The median lethal concentration (LC_{50}) was determined based on cumulative mortality obtained from 3 independent experiments at 120 hpf. The LC_{50} values of zebrafish caused by Cu NPs ($E_{(total)}$) were calculated using GraphPad Prism 5 (Supplemental data 2.1).

2.2.4 Contribution to toxicity of Cu $NP_{(particle)}$ and Cu $NP_{(ion)}$

The toxicity of Cu $NP_{(total)}$ to zebrafish embryos was determined as the sum of the contributions of both Cu $NP_{(particle)}$ and Cu $NP_{(ion)}$. The toxicity of Cu $NP_{(ion)}$ in Cu

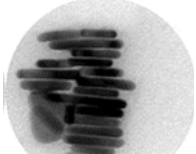

$NP_{(total)}$ can be calculated by the concentration–response curve of $Cu(NO_3)_2$. The actual concentrations of Cu $NP_{(ion)}$ and Cu $NP_{(total)}$ were measured by AAS. To calculate the individual contributions of Cu $NP_{(particle)}$ and of Cu $NP_{(ion)}$ to the total toxicity of Cu $NP_{(total)}$, it was assumed that the mode of action of Cu $NP_{(ion)}$ is dissimilar with the mode of action of Cu $NP_{(particle)}$. This assumption is in line with the assumption of response addition, which is one of the basic concepts of mixture toxicity (Backhaus. Therefore, mortality of embryos induced by Cu $NP_{(particle)}$ ($E_{(particle)}$) was calculated on the basis of the response addition model (Backhaus *et al.*, 2000):

$$E_{(total)} = 1 - \left[\left(1 - E_{(ion)}\right)\left(1 - E_{(particle)}\right)\right] \quad (2.1)$$

where $E_{(total)}$, $E_{(ion)}$, and $E_{(particle)}$ represent the mortality of zebrafish embryos caused by the copper suspensions, Cu $NP_{(ion)}$, and Cu $NP_{(particle)}$ (scaled from 0 to 1), respectively.

2.2.5 Behavioral analysis and morphological assessment

All living embryos tested were subjected to the light–dark challenge test at 120 hpf following Ali *et al.* (2011a). Switching from light (basal phase) to dark (challenge phase) and back to light (recovery phase) had a substantial effect on the activity of zebrafish embryos. Zebrafish embryos have a low locomotor activity under light exposure. Sudden transition to dark induces a sharp spike of fast swimming activity lasting less than 2 s (Burgess, 2007; Rihel *et al.*, 2010; Ali *et al.*, 2011b). A total of 14 min of recording was used (Supplemental data 2.2) (Ali *et al.*, 2011a). Swimming pattern and movement distance of each zebrafish embryo were recorded and analyzed in the ZebraBox recording apparatus with VideoTrack software (both from Viewpoint). After behavioral analysis, all living embryos were rinsed, stained, and stored as described by Ali *et al.* (2011a), then evaluated using a stereo dissecting microscope in terms of normal development and morphological defects at 120 hpf (Supplemental data 2.3).

2.2.6 Statistical analysis

Data are presented as mean ± standard error of the mean (SEM). Mortality data obtained at 120 hpf were used to calculate LC_{50} values. Statistical analysis was used to compare the significant difference between treatments and controls. One-way

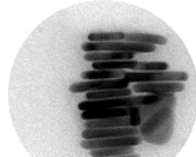

analyses of variance (ANOVA) with Tukey's multiple comparison posttest were performed when necessary. The homogeneity of variance was checked before one-way ANOVA. The significance level in all calculations was set at $p < 0.05$.

2.3 Results

2.3.1 Physicochemical characterization of suspended copper particles

Transmission electron microscopic images of Cu NPs and of the submicron-sized particle demonstrated that the majority of particles were spherical in shape (Figure 2.1). The particles aggregated to a high extent and showed broad size distributions by dynamic light scattering (Table 2.1). Most primary particles of 25-nm, 50-nm, and 100-nm Cu NPs and submicron-sized particles were within 20 nm to 40 nm, 30 nm to 50 nm, 120 nm to 200 nm, and 200 nm to 500 nm, respectively. However, in the case of the 25-nm Cu NPs, some larger particles (>150 nm) also were detected (Figure 2.1).

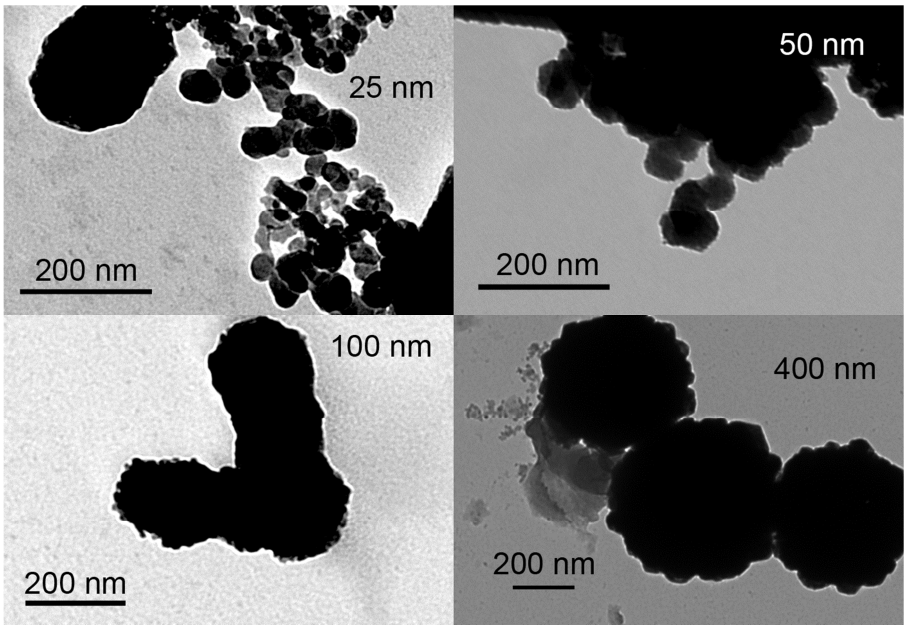

Figure 2.1 Transmission electron microscopic micrographs of the aggregate of 25-nm, 50-nm, and 100-nm Cu nanoparticles and the 400-nm submicron-sized particles used in the present study.

Table 2.1 Size distribution, zeta-potential of multisized CuNPs and SMPs after 1 and 24 h of incubation, the total copper particle suspension concentrations (Cu $NP_{(total)}$) and shed Cu^{2+} from the copper particle suspensions (Cu $NP_{(ion)}$) measurement and pH value after 24 h of incubation

Size (nm)	Nominal conc. (mg/L)	Particle size distribution (nm)[a]		Zeta-potential (mV)[a]		Cu $NP_{(total)}$ conc. (mg/L)[b]	Cu $NP_{(ion)}$ conc. (mg/L)[b]	pH
		1 h	24 h	1 h	24 h			
25	1	380±121	536±35	-20.9±2.7	-20.5±4.9	0.90 ± 0.00	0.42 ± 0.15	6.10
	2	464±28	491±31	-16.5±1.6	-19.3±3.1	1.79 ± 0.00	0.62 ± 0.26	6.32
	8	424±25	803±72	15.3±1.4	-5.6±2.2	7.35 ± 0.04	0.84 ± 0.12	6.38
50	1	551±76	345±26	-16.7±3.1	-8.2±4.4	0.96 ± 0.01**	0.23 ± 0.11	6.28
	2	643±24	498±44	-21.0±1.6	-15.9±2.3	1.87 ± 0.04*	0.38 ± 0.18	6.32
	8	545±19	896±72	-14.1±1.2	3.2±1.4	7.56 ± 0.08*	0.61 ± 0.22	6.49
100	1	396±46	578±97	-16.3±0.8	-1.3±0.9*	0.91 ± 0.03	0.24 ± 0.08	6.80
	2	368±47	641±105	-26.5±1.0	-6.6±2.3	1.96 ± 0.02***	0.41 ± 0.11	6.76
	8	438±42	647±30	-18.0±5.9	-8.1±0.7	7.92 ± 0.02	0.84 ± 0.19	6.79
400	1	832±207**	435±23	-16.6±2.4	-4.9±1.8	0.38 ± 0.01***	0.14 ± 0.05*	6.45
	2	980±170**	736±291	-21.0±4.9	-13.9±6.8	0.65 ± 0.02***	0.24 ± 0.10	6.91
	8	1518±431**	1683±124***	-32.6±2.6	-22.4±4.7	3.64 ± 0.41***	0.75 ± 0.11	6.91

[a] Particle size distribution and zeta-potential in suspensions were determined by dynamic light scattering (DLS). Particle size was expressed as intensity-based average hydrodynamic diameter ± SEM (standard error of the mean). Zeta-potential was expressed as mean ± SEM (n=3). [b] Cu^{2+} concentrations were determined by atomic adsorption spectroscopy (AAS). Concentrations are expressed as mean ± SEM (n=3). Statistical analysis was used to compare the significant difference between Cu particles and copper nitrate at the same concentration. * $p < 0.05$, and ** $p < 0.01$, and *** $p < 0.001$.

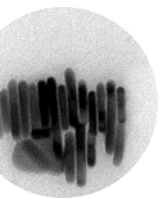

Dynamic light scattering was performed for determining the hydrodynamic diameter of particles suspended in egg water. Data on size distributions after 1 h and 24 h are given in Table 2.1. The measurements revealed that Cu NP aggregates had sizes varying from 200 nm to several thousand nanometers in diameter. Initial particle sizes changed as soon as the particles were submerged in egg water.

Flame AAS measurements of the concentration of total copper (including Cu $NP_{(ion)}$ and Cu $NP_{(particle)}$) and Cu $NP_{(ion)}$ in egg water at 24 h are shown in Table 2.1. The total copper concentrations in egg water ranged from 91% to 96% of the nominal concentrations depending on the Cu NPs. The submicron-sized particle concentrations showed the largest deviations, and only 39% of the nominal concentration was actually detected. The reason for this deviation could be partly attributed to the observation that the submicron-sized particles adhered to the flask and did not disperse well in egg water.

2.3.2 Survival and hatching rate over time

Mortality increased with the duration of exposure (Figure 2.2). Embryos exposed to the highest concentration (nominal 8 mg/L) of 25-nm, 50-nm, and 100-nm Cu NPs and the 400-nm submicron-sized particle showed different rates of mortality of 85%, 31%, 31%, and 100% at 48 hpf, respectively. In the case of $Cu(NO_3)_2$, it was found that 56% and 83% of the embryos died when exposed to nominal concentrations of 4 mg/L and 8 mg/L at 48 hpf, respectively. For all sizes of Cu NP colloids, the percentage of mortality of zebrafish exposed to high concentrations (≥1 mg/L) of Cu NP colloids was significantly different from that of the control at 120 hpf (one-way ANOVA, $p < 0.05$).

The time courses of hatching of zebrafish embryos (survivors only) exposed to Cu NPs, the submicron-sized particle, and $Cu(NO_3)_2$ are shown in Figure 2.2. Compared with the controls, the hatching rates associated with all treatments of Cu NPs were delayed during the 96-h exposure time. Although embryos were delayed in hatching at 0.25 mg/L, after 96 hpf, all surviving zebrafish embryos hatched. At concentrations of 0.5 mg/L and higher, embryos exposed to all different-sized Cu NPs had a significantly lower hatching success (>50%) than embryos in egg water.

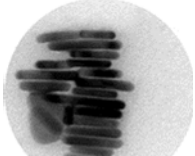

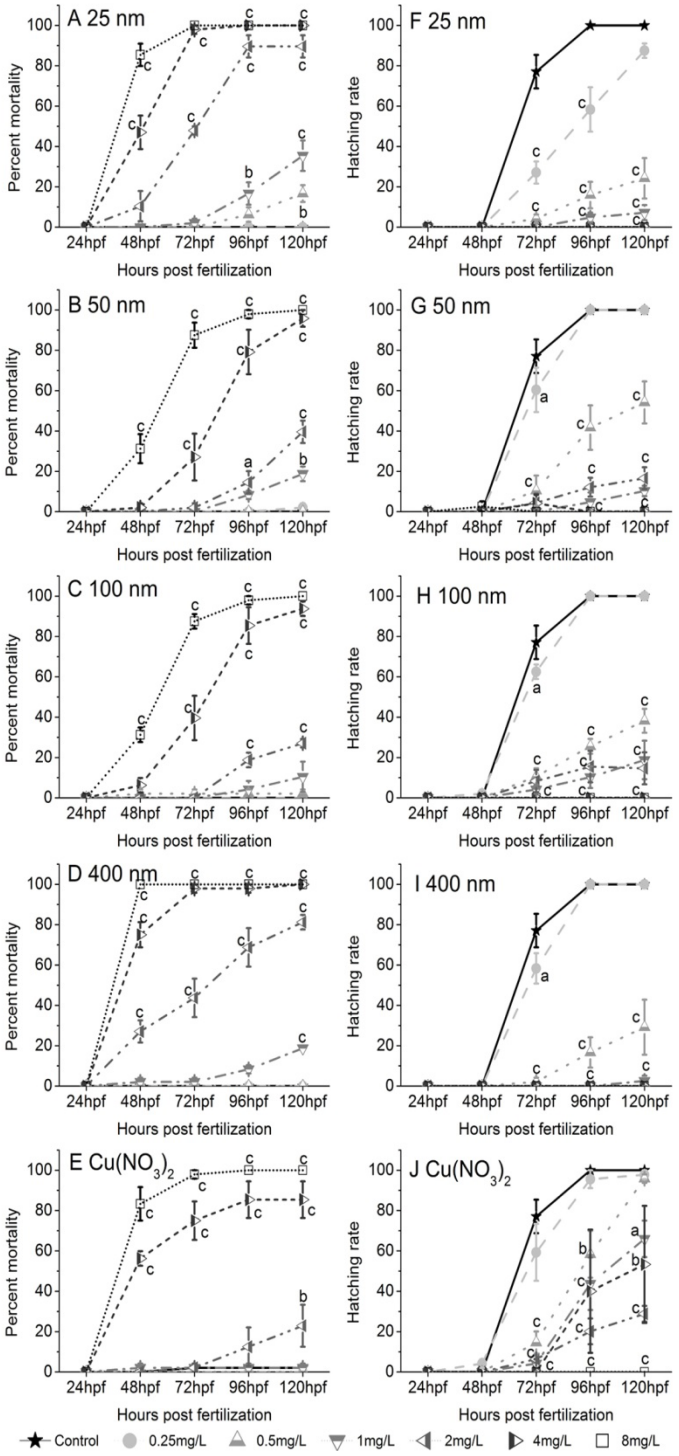

Figure 2.2 Time course of mortality (**A–E**) and hatching rate of surviving zebrafish embryos (**F–J**) exposed to egg water and nominal concentrations 0.25 mg/L to 8 mg/L Cu nanoparticles of 25 nm, 50 nm, and 100 nm; submicron-sized particles; and $Cu(NO_3)_2$ from 24 h to 120 h post fertilization (hpf). The nominal concentration rather than the actual concentration (see Table 2.1) was used in this instance for clear figure presentation. Data presented as mean ± standard error of the mean, with lower-case letters (a–c) denoting statistical differences in lethality and hatching delay from control (one-way analysis of variance, $p < 0.05$).

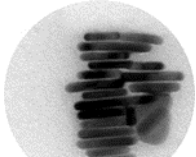

2.3.3 Lethal toxic effects induced by Cu NPs, submicron-sized particles, and Cu^{2+}

The mortality rates of zebrafish embryos following exposure to $Cu(NO_3)_2$ solutions and all different-sized Cu NPs and submicron-sized particle colloids at 120 hpf are given in Figure 2.3. The LC_{50} values and 95% confidence intervals of 25-nm, 50-nm, and 100-nm Cu NPs; submicron-sized particle suspensions; and Cu^{2+} were 1.03 (0.85–1.25) mg/L, 1.99 (1.60–2.48) mg/L, 2.33 (2.02–2.68) mg/L; 0.55 (0.54–0.56) mg/L; and 0.70 (0.68–0.72) mg/L, respectively. From LC_{50} values, it was demonstrated that Cu NP toxicity is size-dependent in the nano-sized range. However, the death of the zebrafish embryos in all cases was caused by Cu NP suspensions (not by Cu $NP_{(particle)}$ only).

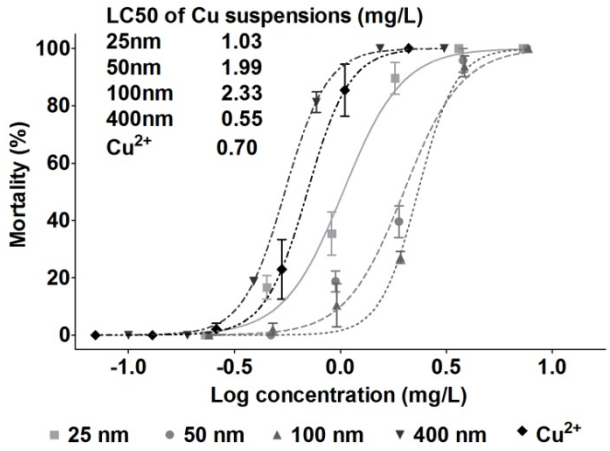

Figure 2.3 Dose–response curves of mortality of zebrafish embryos at 120 h post fertilization following exposure to Cu^{2+} ($Cu(NO_3)_2$), submicron-sized particles, and Cu nanoparticles of 25 nm, 50 nm, and 100 nm. Actual log-transformed Cu concentrations are plotted on the *x* axis. Data are presented as means of 3 independent replicates ± standard error of the mean. LC_{50} = median lethal concentration.

2.3.4 Relative contribution to toxicity of Cu $NP_{(particle)}$ and Cu $NP_{(ion)}$

The LC_{50} values of solely Cu $NP_{(particle)}$, solely Cu $NP_{(ion)}$, and total Cu NP suspensions are listed in Table 2.2. The LC_{50} values of Cu $NP_{(particle)}$ (25 nm, 50 nm,

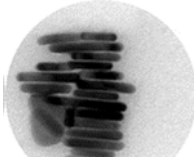

and 100 nm) were 0.58 mg/L, 1.65 mg/L, and 1.90 mg/L, respectively, indicating again the size dependence of toxicity. We found that the 120-hpf LC_{50} value of Cu^{2+} ($Cu(NO_3)_2$) was 0.70 mg/L, indicating that Cu^{2+} is more toxic than Cu NPs. The submicron-sized particle was more toxic compared with all Cu NPs and Cu^{2+}, with a 120 hpf LC_{50} value of 0.35 mg/L.

Table 2.2 The LC_{50} value of the Cu particle suspensions, the particle form of the Cu particles (Cu $NP_{(particle)}$), and of Cu^{2+} ($Cu(NO_3)_2$) in zebrafish at 120 h post fertilization (hpf)

Particle size (nm)	LC_{50} (95% confidence interval) (mg/L)	
	Cu $NP_{(total)}$	Cu $NP_{(particle)}$
25 nm	1.03 (0.85-1.25)	0.58 (0.49-0.70)
50 nm	1.99 (1.60-2.48)	1.65 (1.46-1.86)
100 nm	2.33 (2.02-2.68)	1.90 (1.72-2.10)
400 nm	0.55 (0.54-0.56)	0.35 (0.34-0.36)
Cu^{2+}	0.70 (0.68-0.72)	

Figure 2.4 shows the relative mortality of zebrafish embryos caused by Cu $NP_{(particle)}$ and the particle form of the submicron-sized particle and Cu $NP_{(ion)}$. For each different-sized Cu $NP_{(particle)}$, the relative contribution (>71%) could predominantly be ascribed to the particles and a minor contribution (<29%) to Cu $NP_{(ion)}$. The toxic contribution of Cu $NP_{(particle)}$ increased with decreasing concentration of Cu NP colloids. The smaller Cu NPs (25 nm) were more toxic to embryos than the larger ones (100 nm).

2.3.5 Behavioral analysis and morphological assessment

The total distance moved in the light–dark challenge test, following exposure to Cu NPs, the submicron-sized particle, and $Cu(NO_3)_2$, is shown in Figure 2.5. At all exposure concentrations of Cu NP colloids except 0.25 mg/L, a clear increase in the zebrafish total distance moved was observed for 25 nm, 50 nm, and 100 nm, as seen in Figure 2.5. Exposure to 0.25 mg/L of 25-nm Cu NPs caused a reduction in the total distance moved in all phases compared with the control (Figure 2.5A). Embryos swam slightly more at 0.25 mg/L and 0.5 mg/L of 50-nm and 100-nm Cu NPs and submicron-sized particles than embryos in the controls (Figures 2.5A and

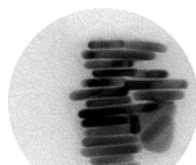

B). However, the distance moved by the embryos decreased with increasing concentrations (Figures 2.5C and D). With Cu NP size held constant, there is a clear dose-dependent inhibition effect on total distance moved (Figures 2.5E–H). Copper nitrate also had a clear dose-dependent effect on embryos' behavior (Figure 2.5I). Embryos treated with $Cu(NO_3)_2$ moved less compared with embryos exposed to 50-nm, 100-nm, and 400-nm Cu particle colloids. The detailed number of abnormalities of exposed embryos is given in Supplemental data 2.4.

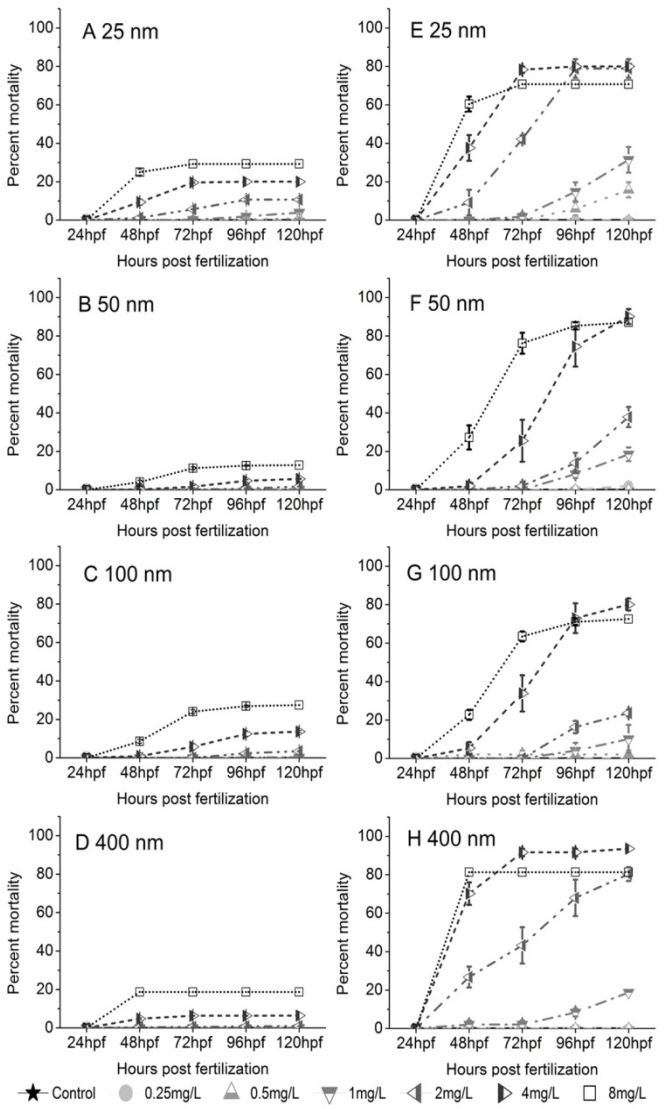

Figure 2.4 Toxic contribution of the shed Cu^{2+} from Cu nanoparticles (Cu NP) (**A – D**), the particle form of Cu NP (**E – H**) in Cu NP colloid exposure of zebrafish embryos from 24 h to 120 h post fertilization (hpf). The nominal concentration rather than the actual concentration (see Table 2.1) was used in this instance for clear figure presentation. Each size of the particle form of Cu NP contributed mainly to the toxicity to zebrafish embryos compared to that of the shed Cu^{2+} from Cu NP. Data presented as mean ± standard error of the mean.

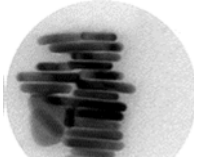

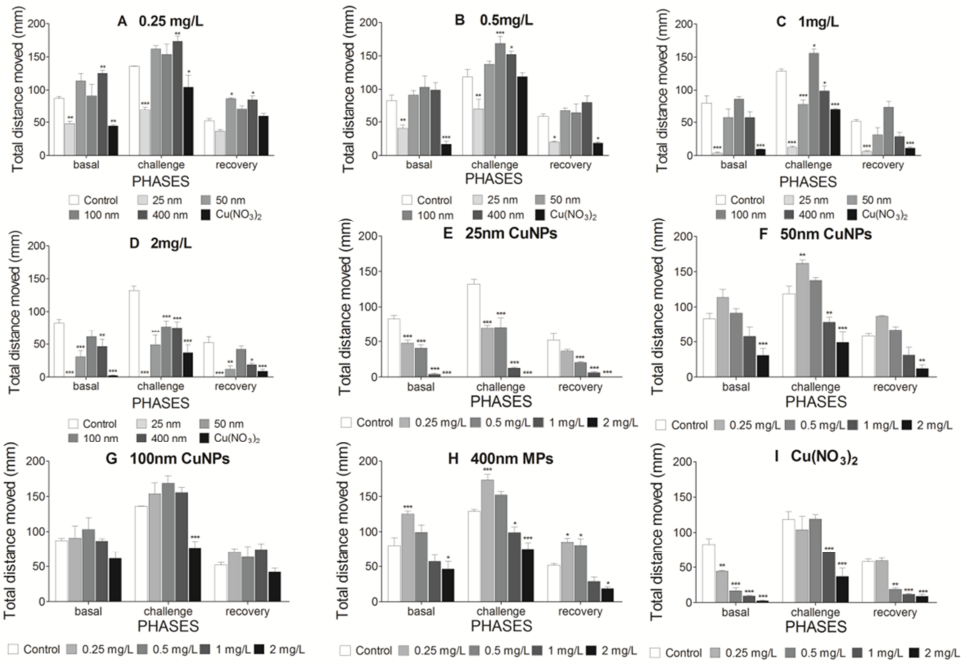

Figure 2.5 Behavioral performance in the light-dark challenge test. Constant nominal concentration of Cu nanoparticles (Cu NPs), submicron-sized particles (MPs), and $Cu(NO_3)_2$ - (**A**) 0.25 mg/L, (**B**) 0.5mg/L, (**C**) 1mg/L, and (**D**) 2 mg/L—and constant Cu particle size - (**E**) 25 nm, (**F**) 50nm, (**G**) 100nm, (**H**) 400nm, and (**I**) $Cu(NO_3)_2$. The nominal concentration rather than the actual concentration (see Table 2.1) was used in this instance for clear figure presentation. Data presented as mean ± standard error of the mean. One-way analyses of variance with Tukey's multiple comparison posttest were performed. Differences between treatment groups and control: * $p < 0.05$, ** $p < 0.01$, and *** $p < 0.001$.

2.4 Discussion

2.4.1 Hatching rate over time

Zebrafish embryos normally hatch at approximately 72 hpf (Kimmel *et al.*, 1995). Compared with the controls, the hatching rates associated with all treatments of Cu NPs were delayed during the 96-h exposure time (Figure 2.2). Increasing Cu NP concentrations had an inhibitory effect on hatching. It is known that Cu ions interfere with hatching, compromising the activity of the hatching enzyme (Lin *et*

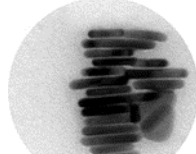

al., 2011). The Cu NP suspension has also been shown to inhibit the secretion and activity of the hatching enzyme chorionase of zebrafish and other fish (Lin *et al.*, 2011). It was observed that exposure to 0.03 mg/L to 1.00 mg/L Cu ions and above decreased hatching success of zebrafish embryos (Bai *et al.*, 2010a). This concentration is close to what we used (0.25 mg/L and above) in the present study. In addition, previous studies demonstrated that other kinds of nanoparticles retarded the hatching of zebrafish embryos (Bar-Ilan *et al.*, 2009; Xia *et al.*, 2011; Zhu *et al.*, 2011).

2.4.2 Lethal toxic effects induced by Cu NPs, submicron-sized particles, and Cu^{2+}

The LC_{50} values demonstrated that Cu NP toxicity is size-dependent (Table 2.2). It can be concluded that suspensions of smaller Cu NPs were more toxic than larger ones, which might be related to the larger surface-to-volume ratio of the smaller particles, which is in line with other studies (Bar-Ilan *et al.*, 2009; Griffitt *et al.*, 2007; 2008). Specifically, Griffitt *et al.* (2007; 2008) assessed the acute toxicity of Cu NPs to zebrafish, and they found that the 48-h LC_{50} values of Cu NPs in adult zebrafish were 1.56 mg/L for 80-nm Cu NPs and 0.94 mg/L for 26.7-nm Cu NPs, indicating that the smaller particles were more toxic, which is consistent with our finding in the present study. In addition, Bar-Ilan *et al.* (2009) reported that all sizes of Ag NP (3 nm, 10 nm, 50 nm, and 100 nm) caused toxic effects to zebrafish embryos and that the smaller particles were more toxic. Ispas *et al.* (2009) found that there was no significant difference in LC_{50} of different sizes of Ni NPs. Considering our results, that smaller Cu NPs were more toxic than larger ones to zebrafish embryos, these findings suggest that there is size-dependent toxicity of nanoparticles for certain metal constituents and for specific end points of toxicity assessment.

In the present study, exposure to the submicron-sized particle was included to compare the toxicity of nano- and submicron particles and $Cu(NO_3)_2$ solution. The submicron-sized particle and ionic Cu were in general more toxic than Cu NPs (Table 2.2). One possible reason for this could be the fact that submicron-sized particles have rough surfaces in egg water (Figure 2.1); thus, they have large effective surface areas. The surface area has been widely considered as a main

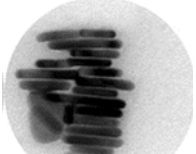

factor in the toxicity of nanoparticles (Oberdorster *et al.*, 2007; Nel *et al.*, 2006). The high toxicity of submicron-sized particles could also be caused by other factors, which is beyond the scope of the present study and requires further investigation.

2.4.3 Relative contribution to toxicity of Cu $NP_{(particle)}$ and Cu $NP_{(ion)}$

It should be noted that previous studies were performed *in vitro*, and mortality of the zebrafish embryos was in all cases caused by metal suspensions (not by solely the particle form of NPs) in the cases of Cu NPs (Griffitt *et al.*, 2007; 2008), Ag NPs (Bar-Ilan *et al.*, 2009; Griffitt *et al.*, 2008), Au NPs (Bar-Ilan *et al.*, 2009), Ni NPs (Griffitt *et al.*, 2008; Ispas *et al.*, 2009), Al NPs (Griffitt *et al.*, 2008), Co NPs (Griffitt *et al.*, 2008), and TiO_2 NPs (Griffitt *et al.*, 2008). In addition, most previous studies did not test the contribution of the ions potentially released from nanoparticles during exposure versus the particle form of the nanoparticles tested on embryo toxicity.

Our results showed that particles dominated the explanation of toxicity (Figure 2.4). The higher contribution to toxicity by Cu $NP_{(particles)}$ could be caused by the existence of a particle-mediated mechanism (Griffitt *et al.*, 2008; Asharani *et al.*, 2011). Similar findings were reported for Ag NPs by Wang *et al.* (2012). These authors found that the main contribution to the toxicity to zebrafish embryos was from Ag NPs rather than from Ag^+. Both larger and smaller Ag NPs were shown to enter zebrafish embryos through chorionic pore canals by passive diffusion and were reported to stay inside the embryos (Lee *et al.*, 2007; 2012). Nanoparticles can be accumulated in the zebrafish embryo chorion to block pore canals (Lee *et al.*, 2012). During the present experiments, it was observed by microscopy that Cu particles, both Cu NPs and submicron-sized particles, adhered to the chorion of the embryos at higher concentrations. On the other hand, the diameter of embryonic chorion pore canals was small, approximately 0.5 μm to 0.7 μm (Lee *et al.*, 2012). As a consequence, smaller metal NPs can easily penetrate into the embryos via chorion pore canals, but the larger metal NPs cannot be transported directly through chorionic canals. If the aggregate metal NPs on the surface of embryos were formed by relatively weak cohesive bonds, they could be separated into smaller metal NPs and pass into the chorion (Bai *et al.*, 2010a). The exact uptake

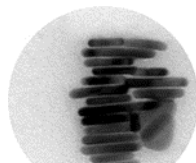

mechanism of Cu NPs should be investigated in future studies.

2.4.4 Behavioral analysis

Behavioral analysis results showed that zebrafish behavior, as influenced by Cu NPs, was size-dependent (Figure 2.5). It was concluded that suspensions of smaller nanoparticles were more toxic than suspensions of larger nanoparticles, which was consistent with the mortality results. Surprisingly, for submicron-sized particles the behavioral analysis result was not consistent with the mortality result. Treatment of embryos with submicron-sized particles at any concentration resulted in severe toxic effects (*e.g.*, hatching delay, morphological abnormalities, and death). However, submicron-sized particles had less effect on the total distance moved in the behavioral assay (Figure 2.5). Previous studies have reported the effects of copper on swimming behaviors in fish. For example, Handy *et al.* (1999) found that trout exposed to dietary copper will reduce locomotion. Campbell *et al.* (2002) reported that Cu-exposed trout decreased swimming speed. Recently, Boyle *et al.* (2013) found that swimming speed was significantly decreased when rainbow trout were exposed to TiO_2 nanoparticles. They attributed such decreased swimming speed mainly to gill injury and respiratory hypoxia. However, the gill injury may not be the reason for the swimming behavior found in zebrafish embryo in the present study because the gills of zebrafish become functional after approximately 14 d post fertilization (Chen *et al.*, 2014). Given that Cu particles induced hatching interference, lethality, and various morphological abnormalities, the behavioral alteration of 120-hpf larvae could be a result of morphological abnormalities or some neuronal toxicity exerted by Cu particles or their combined effects. The swimming behavior of zebrafish and its alteration in light–dark–light challenge tests was dependent on an intact visual system, central and peripheral nervous systems, and locomotor systems. It is therefore a nonspecific physiological readout of embryo normality and, indeed, can be influenced by malformations.

2.5 Conclusions

All sizes of Cu $NP_{(total)}$ were toxic to zebrafish embryos. In the case of Cu NPs, the toxic effects of Cu $NP_{(total)}$ were size-dependent. The smaller Cu NPs were more toxic than larger Cu NPs in zebrafish; however, the 400-nm submicron-sized

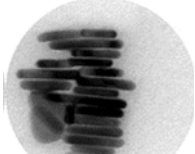

particle and Cu ions in turn were more toxic than the Cu NPs. The main contribution to the toxicity in zebrafish embryos was from Cu $NP_{(particle)}$ rather than from Cu $NP_{(ion)}$. All sizes of Cu $NP_{(total)}$ and Cu ions inhibited hatching success even at low concentrations. Higher concentrations of Cu suspensions induced a lower total distance moved in the light–dark challenge test.

Supplemental data

Supplemental data 2.1 The LC_{50} value calculation

The LC_{50} value of zebrafish caused by CuNPs ($E_{(total)}$) was calculated using GraphPad Prism 5 with the equation:

$$E_{(total)} = \frac{1}{1 + 10^{(\log EC_{50,(total)} - \log C_{(total)})\rho}} \quad \text{(S2.1)}$$

where $E_{(total)}$ is the mortality of zebrafish embryos caused by the suspensions (scaled from 0 to 1), $C_{(total)}$ describes the initial actual exposure concentration of Cu particle suspensions and ρ represents the steepness of the curve.

Supplemental data 2.2 Behavioral analysis

All living embryos tested were subjected to the light-dark challenge test at 120 hpf. This test constituted a behavioral test relying on the integrity of both eye and locomotor/skeletal system development. This test consists of frequent alternations between periods of light and dark. A total of 14 minutes recording was used as follows: for the first 2 minutes the light was on, this being a pre-test adaptation period. For the next 4 min. the light remained on, and behavior was recorded (the basal activity). For the next 4 min. the light was off, this sudden pulse of darkness (challenge phase) being a potent stressor. For the last 4 min. the light was turned on again (recovery phase) (Ali *et al.*, 2011a). Swimming patterns and movement distance of each living zebrafish embryos was recorded and analyzed in the ZebraBox recording apparatus with VideoTrack software (both from Viewpoint S.A., Lyon, France).

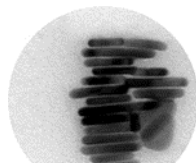

Supplemental data 2.3 The procedure of cleaning, staining and storing embryos for morphological assessment

Living embryos at 120 hpf were fixed in 4% paraformaldehyde (PFA) in phosphate- buffered saline at pH 7.2 at 4°C overnight. They were then rinsed five times in distilled water and dehydrated in a graded series of ethanol (25, 50, and 70%) for 5 min each. Embryos were rinsed in acid alcohol (1% concentrated hydrochloric acid in 70% ethanol) for 10 min, and then placed in filtered Alcian blue solution (0.03% Alcian blue in acid alcohol) overnight. Embryos were subsequently differentiated in acid alcohol for 1 h and washed 2×30 min in distilled water. Finally, they were cleared and stored in glycerol (Ali *et al.*, 2011a).

Supplemental data 2.4 The number of morphological malformations at 120 hpf for egg water, actual concentrations of Cu particles (25, 50, 100, and 400 nm) and Cu^{2+} ($Cu(NO_3)_2$).

It was seen that expose to the Cu NPs lead to a series of sublethal toxicological responses. Single malformations were observed at low CuNP concentrations. Multiple deformities were observed at Cu NP concentrations ranging from 0.5 mg/L to 4 mg/L. The high percentage of malformation embryos in untreated controls were range 29% to 50% (14 to 24 out of 48 fish). We found that the high percentage malformation 50% did happen in the case of copper nitrate, and low percentage malformation was observed in the case of Cu particles. The copper nitrate solution may be easier to be transferred by the evaporation, thereby causing more effects (high percentage malformation) on the controls. In addition, during the last steps to the procedures of "Embryos were subsequently differentiated in acid alcohol for 1 h and washed 2×30 min in distilled water" (Supplemental data 2.3), some embryos inevitably adhered to the well-plates. When we detached the embryos from the well-plates, it was quite easy to damage their body, especially their tails and spines. However, the above procedure is necessary. Given the large number of animals left at the end to the experiment, this procedure is necessary as we analyzed every alive embryo for their malformations, which took several days. This procedure might also have affected the malformations found in the controls.

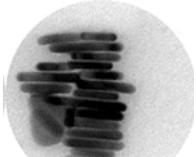

Particle size (nm)	Actual conc. (mg/L)	D	N	Y	P	T	B	YT	YP	TB	YB	PB	PT	YPB	YPT	YTB	PTB	YPTB	E
	0	0	32	3	0	6	2	2	0	0	0	0	0	0	0	0	2	1	0
	0.45	8	5	1	0	6	3	1	0	4	2	0	0	3	0	4	6	5	0
25	0.91	17	0	1	0	0	0	2	0	2	0	1	0	1	3	6	3	11	1
	1.81	43	0	0	0	0	0	0	0	0	0	0	0	0	0	0	0	0	5
	3.62	48	0	0	0	0	0	0	0	0	0	0	0	0	0	0	0	0	0
	0	1	33	2	0	9	0	1	0	1	1	0	0	0	0	0	0	0	0
	0.47	0	4	2	1	7	4	12	0	1	0	2	1	0	4	0	6	4	0
50	0.95	9	0	1	0	0	0	4	0	1	0	0	0	1	3	3	1	23	2
	1.89	19	0	0	0	0	0	2	0	0	0	0	0	0	2	1	1	23	0
	3.79	46	0	0	0	0	0	0	0	0	0	0	0	0	0	0	0	0	2
	0	0	34	3	1	7	0	2	0	1	0	0	0	0	0	0	0	0	0
	0.48	1	0	2	0	7	3	5	1	7	1	2	2	1	3	2	5	6	0
100	0.96	5	0	0	2	4	0	0	0	3	0	4	6	0	1	0	18	5	0
	1.92	13	0	0	0	0	0	1	0	1	0	1	2	0	1	0	12	17	0
	3.85	45	0	0	0	0	0	0	0	0	0	0	0	0	0	0	0	0	3
	0	0	30	1	0	11	4	0	0	1	1	0	0	0	0	0	0	0	0
	0.19	0	0	1	0	0	0	5	0	0	5	0	0	0	1	23	0	13	0
400	0.39	9	0	0	0	0	0	0	0	0	0	0	0	0	0	4	0	34	1
	0.77	39	0	0	0	0	0	0	0	0	0	0	0	0	0	0	0	6	3
	1.54	48	0	0	0	0	0	0	0	0	0	0	0	0	0	0	0	0	0
	0	1	24	6	1	4	2	5	0	1	0	0	0	0	1	1	0	0	2
	0.13	0	1	11	2	0	0	9	10	1	2	0	0	1	7	0	1	1	2
Cu^{2+}	0.26	1	0	2	0	0	0	2	5	0	0	0	0	4	15	0	0	18	1
	0.53	11	0	0	0	0	0	0	0	0	0	0	0	3	7	0	0	27	0
	1.05	41	0	0	0	0	0	0	0	0	0	0	0	0	2	0	0	5	0

Key: N, normal; D, dead; E, empty; Y, yolk sac edema; P, pigmentation dispersion; T, tail malformation; B, bent spine; YT, embryos with yolk sac edema and tail malformation; YP, embryos with yolk sac edema and pigmentation dispersion; TB, embryos with tail malformation and bent spine; YB, embryos with yolk sac edema and bent spine; PB, embryos with pigmentation dispersion and bent spine; PT, embryos with pigmentation dispersion and tail malformation; YPB, embryos with yolk sac edema, pigmentation dispersion and bent spine; YPT, embryos with yolk sac edema, pigmentation dispersion and tail malformation; YTB, embryos with yolk sac edema, tail malformation and bent spine; PTB, embryos with pigmentation dispersion, tail malformation and bent spine; YPTB, embryos with yolk sac edema, pigmentation dispersion, tail malformation and bent spine.

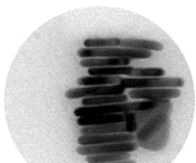

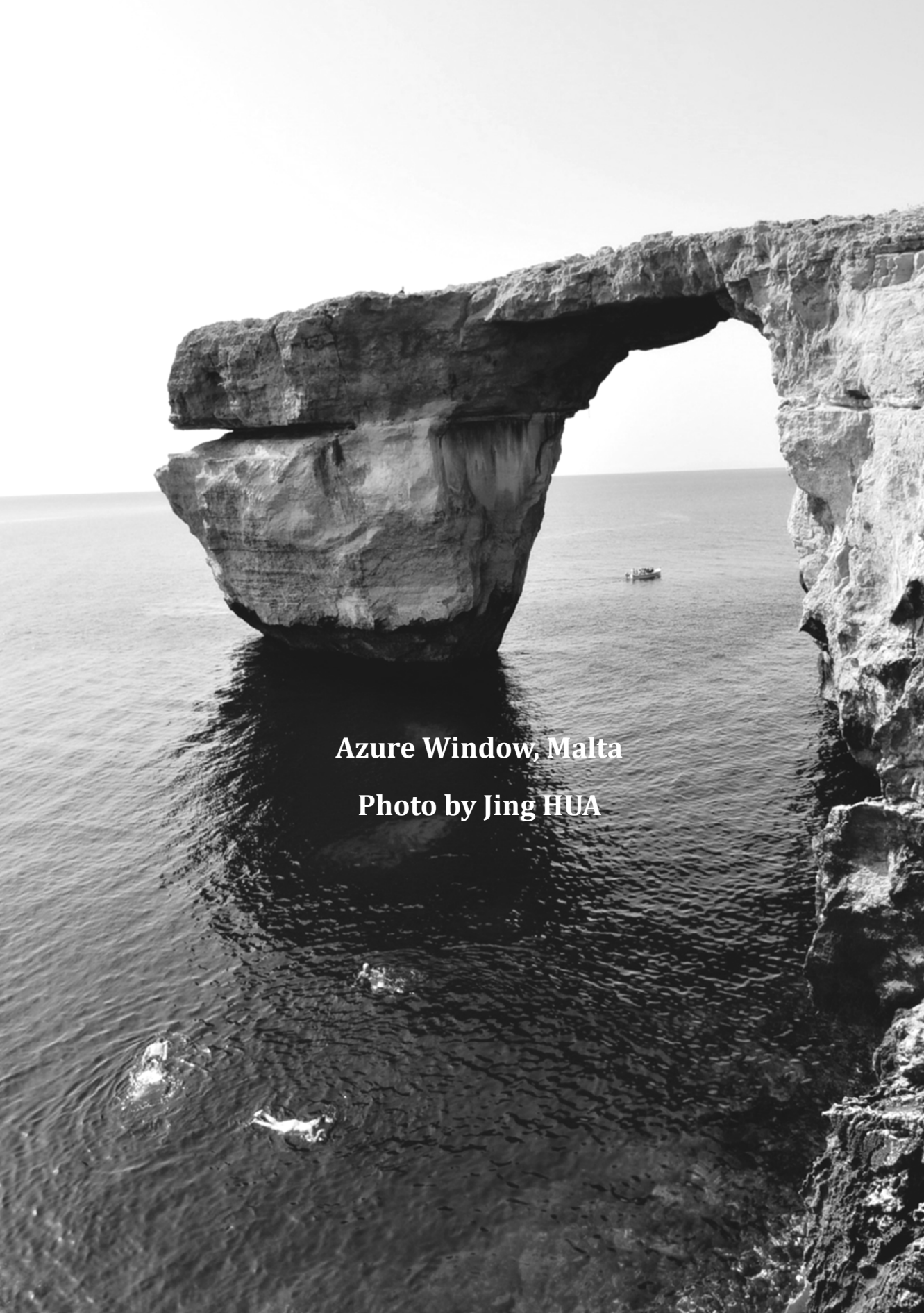

Azure Window, Malta

Photo by Jing HUA

3

Particle-specific toxic effects of differently shaped zinc oxide nanoparticles to zebrafish embryos[2]

3.1 Introduction

ZnO nanoparticles (NPs) are widely used in products such as sunscreens, polymer fillers and UV absorbents (Xia *et al.*, 2008). It is known that ZnO NPs are toxic to organisms, and ZnO particles have been considered as "extremely toxic" in the environment (Kahru and Dubourguier, 2010). Zebrafish embryos have been widely selected as an attractive *in vivo* model for demonstrating toxicological effects of chemicals, due to their small size, transparency and rapid growth (Lin *et al.*, 2013a).

In assessing the toxicity of NPs, besides chemical concentrations the physical properties should also be taken into account (Nel *et al.*, 2006; Buzea *et al.*, 2007 Zhu *et al.*, 2013; Hua *et al.*, 2014a). Many studies have been conducted to investigate the toxicity of various shapes of NPs, *e.g.* Ag NPs (Bar-Ilan *et al.*, 2009; George *et al.*, 2012), Au NPs (Bar-Ilan *et al.*, 2009; Chithrani and Chan, 2007), Ni NPs (Ispas *et al.*, 2009) and Si NPs (Huang *et al.*, 2011; Tenzer *et al.*, 2011). In general, evidence was found that particle shape is closely correlated

[2] Based on: Hua, J., Vijver, M. G., Richardson, M. K., Ahmad, F. and Peijnenburg, W. J.G.M. (2014), Particle-specific toxic effects of differently shaped zinc oxide nanoparticles to zebrafish embryos (Danio rerio). *Environmental Toxicology and Chemistry*, 33: 2859–2868. doi: 10.1002/etc.2758.

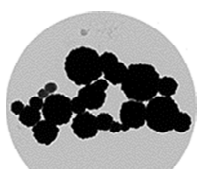

with toxicity. This relationship is not conclusive, because the toxic effects also are species-specific and composition dependent (Zhu *et al.*, 2013; Hua *et al.*, 2014a; George *et al.*, 2012; Tenzer *et al.*, 2011; Oberdorster *et al.*, 2007).

Dissolved Zn ions from ZnO NPs (designated as $NP_{(ion)}$ hereafter) also play an important role in inducing acute or chronic toxicity of ZnO NPs to aquatic organisms (Xia *et al.*, 2008; 2011; Bai *et al.*, 2010b; Adam *et al.*, 2014). The ZnO $NP_{(ion)}$ was found to interfere in the functioning of the zebrafish hatching enzyme 1 (ZHE1) (Lin *et al.*, 2013b). Nonetheless, the particle form of ZnO NPs (designated $NP_{(particle)}$ hereafter) also has an effect on zebrafish embryos. A previous study reported that ZnO $NP_{(particle)}$ caused much more toxicity to zebrafish embryos than the ZnO $NP_{(ion)}$, as it was found that zebrafish embryos treated with ZnO NPs failed to upregulate their anti-oxidant genes (Gstp2 and Nqo1) as well as their oxidative stress responses to counteract the reactive oxidative species (ROS) formed (Zhu *et al.*, 2009). There is no consistency on the main factor causing toxicity of ZnO NPs suspensions (designated $NP_{(total)}$ hereafter) in particular and for metallic nanoparticles generating metal ions in general. Most studies directly compared the toxicity of ZnO $NP_{(total)}$ with the effect of Zn salts (*e.g.* $ZnSO_4$, $Zn(NO_3)_2$) (Xia *et al.*, 2008; 2011; Bai *et al.*, 2010b; Zhu *et al.*, 2008; 2009; Lin *et al.*, 2011). The clear differentiation between the effects of $NP_{(particle)}$ and of $NP_{(ion)}$ in the observed toxic properties is often difficult to prove experimentally by this general approach (Ivask *et al.*, 2014a). We here propose a general approach that can overcome these difficulties and allows to make a quantitative assessment of the relative contribution to toxicity of ions and particles, in this case ZnO $NP_{(ion)}$ and ZnO $NP_{(particle)}$.

The first research aim of our study was to determine the relative contribution of ZnO $NP_{(ion)}$ versus ZnO $NP_{(particle)}$ to the toxicity of differently shaped ZnO $NP_{(total)}$ to zebrafish embryos. In our study, we treated ZnO $NP_{(total)}$ as being a toxic mixture of ZnO $NP_{(ion)}$ and ZnO $NP_{(particle)}$. Since mechanisms of action (MOAs) of ZnO $NP_{(ion)}$ and ZnO $NP_{(particle)}$ are not fully understood, we used two different addition models to calculate the toxic effects of ZnO $NP_{(ion)}$ and ZnO $NP_{(particle)}$. The ZnO $NP_{(ion)}$ was quantified during the exposure of the zebrafish embryos and a $Zn(NO_3)_2$ solution was used as a reference to assess the toxicity of zinc ions generated during exposure of zebrafish embryos to a suspension of ZnO $NP_{(total)}$

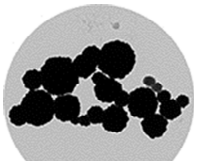

containing ZnO $NP_{(particle)}$ and $NP_{(ion)}$.

The second research aim was to determine whether the toxicity of ZnO $NP_{(total)}$ and ZnO $NP_{(particle)}$ to zebrafish embryos is related to the shape of the NPs. We further investigated what factors control the dependency of toxicity on shape. If the ZnO $NP_{(ion)}$ is the main factor causing toxicity to zebrafish embryos (research aim 1), then the toxicity of differently shaped ZnO NPs should be related mainly to the dissolved Zn^{2+} concentrations in the suspensions tested. It is in this respect further assumed that dissolution levels of differently shaped ZnO NPs are different, as dissolution levels are assumed to depend on the shape of the particles. On the other hand, if the ZnO $NP_{(particle)}$ is the main factor causing toxicity to zebrafish embryos, then after ruling out the toxicity of the ZnO $NP_{(ion)}$, we can explicitly relate the toxic impacts of differently shaped ZnO $NP_{(particle)}$ to the morphology and size of the particles. The toxicity endpoints studied were: mortality rate, hatching rate, and assessment of the behavioral profile of the embryos. We tested various ZnO particles, namely: nanospheres, nanosticks, and ZnO submicron particles (SMPs).

3.2 Materials and methods

3.2.1 Preparation of ZnO particle suspensions

The three different types of ZnO particles were purchased from IoLiTec GmbH (Heilbronn, Germany). $Zn(NO_3)_2$ was purchased from Sigma Aldrich (Zwijndrecht, The Netherlands). Dry powdered ZnO particles were weighed (32 mg Zn/L) and suspended in 100 mL egg water (0.21 g 'Instant Ocean®' salt in 1 L of Milli-Q water and 1µL of methylene blue, pH 6.5 - 7.0) using sonication for 10 min in a water bath sonicator and then diluted with egg water to obtain the desired concentrations. Stock solutions were freshly prepared every day.

3.2.2 Physicochemical characterization of ZnO NPs

Transmission electron microscopy (TEM) (JEOL 1010, JEOL Ltd., Japan) analysis was used to characterize the particle size and morphology of ZnO suspensions after 1 h of incubation in egg water. The particle size distribution was analyzed using a Nano Measurer 1.2 (Fudan University, China). Size distribution

analysis was only performed when individual well defined NPs could be determined. Dynamic light scattering (DLS) was measured on a Zetasizer Nano-ZS instrument (Malvern Instruments Ltd., UK) and was performed to detect the size distribution of aggregates and zeta-potential of ZnO particles in egg water. The dissolved Zn ions and the ZnO $NP_{(total)}$ concentration in egg water were analyzed using flame atomic absorption spectroscopy (AAS) (Perkin Elmer 1100B) after 24 h of equilibration of the samples. To determine concentrations of dissolved Zn ion in the particle suspensions, 5 mL of the suspensions was sampled after 1 h and after 24 h of incubation and centrifuged at 13.300 g for 20 min to remove (aggregated) nanoparticles (Fernández-Cruz *et al.*, 2013). The supernatants were analyzed using DLS to confirm that (aggregated) ZnO NPs were removed. There were still some particles presented in supernatant during this proceed, but the lower Zn ions concentrations can be neglected. Nitric acid was added to digest the samples at pH 2 for at least 1 day at room temperature. Then, the samples were analyzed using AAS.

3.2.3 Waterborne exposure of zebrafish embryos to ZnO NPs

Zebrafish embryos were obtained from AB wild type zebrafish. Embryos were assessed for quality, and healthy ones were distributed into 96 well-plates with one embryo per well. An acute exposure regime of 96 h was used, from 24 hours post-fertilization (hpf) to 120 hpf, thus including the major stages of organ development. The embryos were exposed to 250 µL/well of ZnO particles in egg water. In order to determine the contributions to toxicity of the ZnO $NP_{(particle)}$ and the $NP_{(ion)}$, embryos were exposed to suspensions of ZnO NPs as well as to $Zn(NO_3)_2$ solutions. Solutions containing ZnO NPs were prepared in egg water as detailed above. After a range finding experiment, a geometric series of concentrations lying in the range between 0% and 100% mortality were selected, namely: 2, 4, 8, 16, and 32 mg Zn/L for all ZnO NPs., and 3.5, 7, 14, 28 and 55 mg Zn/L for $Zn(NO_3)_2$ solutions. Throughout all procedures, the embryos and solutions were kept at 28.5°C. The exposure medium (containing NPs) was replaced with a fresh suspension of nanoparticles every day up to 120 hpf according to OECD guideline 157. This replacement procedure could increase the actual zinc concentrations over time in the liquid in the 96-well plate because of the possibility of continued sedimentation of particles in between 2 fluid renewals.

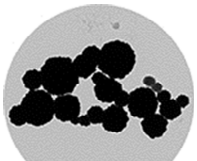

To verify this possibility, the actual concentrations of the remaining ZnO NP suspensions were measured after 120 hpf. These actual concentrations of refreshed ZnO $NP_{(total)}$ in the 96-well plates after 120 hpf were equal to 94 ± 2% of the actual concentrations of the suspensions, hence no impact of sedimented particles was found to be present. Triplicate trials involved 16 embryos per treatment group (totally 48 embryos). Mortality and hatching rate were assessed at 24, 48, 72, 96 and 120 hpf. Embryos were scored as dead according to OECD guideline 157 (OECD, 2011).

The median lethal concentration (LC_{50}) and the median effect concentration (EC_{50}) of hatching inhibition and behavioral inhibition of zebrafish caused by ZnO NPs can be calculated using GraphPad Prism 5 (California, USA) according to the dose-response curve:

$$E = \frac{\text{Bottom} + (\text{Top} - \text{Bottom})}{1 + 10^{(LogEC_{50} - LogC)\rho}} \quad (3.1)$$

where E is the effect (mortality, hatching and behavioral inhibition) on zebrafish embryos caused by ZnO NPs (scaled from 0 to 1), Top and Bottom are plateaus in the units of the Y axis, The Top and Bottom of mortality and hatching are 100% and 0%, respectively. The Top of behavioral inhibition are 1 (the most total moved distance divided by the most total moved distance in the same phase), the Bottom of behavioral inhibition are 0. C describes the initial actual exposure concentration of ZnO NPs and ρ represents the steepness (slope) of the curve.

3.2.4 Behavioral analysis

For screening NPs for neurotoxicity, we also tested the behavioral activity of zebrafish embryo's that survived after 96 h of exposure. This test relies on the integrity of both eye and locomotor/skeletal system development. Alterations in locomotor activity in this period can be used to provide an index of physiological alterations. Zebrafish embryo activity is low during exposure to light. Sudden transition to dark induces a sharp spike of fast swimming activity lasting less than 2 sec (Burgess and Granato, 2007; Rihel *et al.*, 2010; Ali *et al.*, 2011a).

At 120 hpf, all living embryos were subjected to the light-dark challenge test. A total of 14 minutes of recording was used similar to Ali *et al.* (2011c). In brief, for

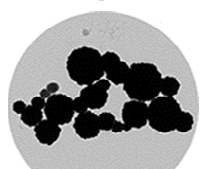

the first 2 minutes the light was on, this being a pre-test adaptation period. For the next 4 min. the light remained on, and the behavior was recorded (basal phase). For the next 4 min. the light was off, this sudden pulse of darkness (challenge phase) being a potent stressor. For the last 4 min. the light was turned on again (recovery phase). During the 14 min, swimming patterns and movement distance were recorded and analyzed in the ZebraBox recording apparatus with VideoTrack software (both from Viewpoint S.A., Lyon, France).

3.2.5 Mixture toxicity of ZnO $NP_{(particle)}$ and ZnO $NP_{(ion)}$

Zebrafish embryos were exposed to ZnO $NP_{(total)}$ which mainly contained a mixture of ZnO $NP_{(particle)}$, ZnO $NP_{(ion)}$, and other types of Zn species (*e.g.* $Zn(OH)_n^{2-n}$, $ZnCO_3^0$). For toxic chemicals, the combined effects of various chemical species present in solution can be categorized based on their similarity of mode of action or mechanism of action (MOA) (Altenburger *et al.*, 2003; Faust *et al.*, 2003). If Zn species have a similar MOA, the concentration addition model (CA) can be used to estimate the combined effects, while the response addition model (RA) should be used in the case of dissimilar MOAs (Altenburger *et al.*, 2003). Mechanisms of action are the specific means by which chemicals induce effects in organisms. Modes of action are more general and phenomenological. Note that the terms mechanism of action and mode of action are not used consistently in the literature, and there is no agreed dividing line between them. In addition, the mode of action of toxicity of metal-based NPs is still unclear. We therefore refer in our study with regard to MOA to mechanism of action. Some reported MOAs of free Zn^{2+} ions are: (a) low as well as high levels of Zn^{2+} can disrupt homeostatic mechanisms, and toxicity is described to occur once homeostasis variation surpasses the range of physiological tolerance (Chang *et al.*, 012); (b) severe inhibition of calcium uptake (Hogstrand *et al.*, 1996); (c) inhibition of the hatching enzyme (ZHE1) activity (Lin *et al.*, 2013b). The MOAs of ZnO $NP_{(particle)}$ are not fully understood, but recent studies reported some mechanistic pathways: (a) membrane damage (Ivask *et al.*, 2014a); (b) mitochondrial damage (Ivask *et al.*, 2014a); (c) hatching delay, probably due to hypoxia induced by NPs (Bai *et al.*, 2010b). Some studies reported some mechanistic pathways of free Zn^{2+} ions and $NP_{(particle)}$: (a) inducing a higher level of reactive oxidative species (ROS) and/or compromise the cellular oxidative

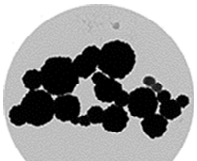

stress response (Zhu *et al.*, 2008); (b) DNA damage (Ivask *et al.*, 2014a); (c) lipid peroxidation (Ivask *et al.*, 2014a); Please note that Zn^{2+} is reported to be capable of inducing a higher level of ROS, DNA damage and lipid peroxidation, but $NP_{(particle)}$ was shown to play a dominant role in this respect (Zhu *et al.*, 2009). Hence, our first assumption is that the MOAs of ZnO $NP_{(particle)}$ and ZnO $NP_{(ion)}$ are likely to be dissimilar, so we used the RA to explicitly account for the toxic impacts of ZnO $NP_{(particle)}$ in this study.

In the response addition model, the effect of the total mixture can be calculated by summing the effects of each type of Zn species, using the following equation:

$$E(c_{mix}) = 1 - \prod_{i=1}^{n}(1 - E(c_i)) \qquad (3.2)$$

where $E(c_{mix})$ is the total effect of the mixture and $E(c_i)$ is the extent of effect induced by Zn species i.

Due to some potential different mechanistic pathway of free Zn^{2+} ions and $NP_{(particle)}$ are similar: (a) inducing a higher level of reactive oxidative species (ROS) (Zhu *et al.*, 2008); (b) DNA damage (Ivask *et al.*, 2014a); (c) lipid peroxidation (Ivask *et al.*, 2014a). Therefore, we also used the CA to explicitly account for the toxic impacts of ZnO $NP_{(particle)}$. In the concentration addition model, the effect of the mixture can be calculated by the following equation:

$$\sum_{i=1}^{n}\frac{c_i}{E(c_i)} = 1 \qquad (3.3)$$

where c_i is the actual exposure concentration of Zn species *i*, $E(c_i)$ is the median effect concentrations of Zn species *i*.

The ZnO $NP_{(ion)}$ plays a key role in the ZnO $NP_{(total)}$ toxicity to zebrafish embryos (Xia *et al.*, 2008; 2011; Bai *et al.*, 2010b; Adam *et al.*, 2014). Zn speciation is strongly related to the pH of the medium, at pH values below 8 it is the free Zn^{2+}-ion that dominates aqueous zinc speciation in the absence of nanoparticles (Bervoets and Blust, 2000). In our study, the pH of the suspensions of all types of ZnO NPs in egg water was below 7.5. $Zn(NO_3)_2$ solutions and ZnO NPs suspensions were all prepared in egg water, and have similar pH, thus the activity

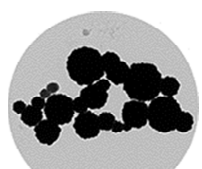

of dissolved Zn-species fraction is likely to be similar in solutions with or without nanoparticles present. The effect of any other Zn species on zebrafish embryos was out of our scope and might need further investigation. Hence, our second modeling assumption is that the toxicity of the ZnO $NP_{(total)}$ to zebrafish embryos is composed mainly of the sum of the contributions of the ZnO $NP_{(particle)}$ and of the ZnO $NP_{(ion)}$, and no other Zn species were accounted for. This assumption is realistic as we used the toxicity of Zn^{2+} at the same composition of the $Zn(NO_3)_2$ solutions as the positive reference.

The actual concentrations of ZnO $NP_{(ion)}$ and of ZnO $NP_{(total)}$ were measured by AAS. The actual concentrations of ZnO $NP_{(particle)}$ were calculated as the difference of the actual concentrations of ZnO $NP_{(total)}$ and the actual concentrations of ZnO $NP_{(ion)}$. After 1 h of incubation, concentrations of dissolved ions of all types of ZnO particles reached a platform, and increased slowly afterwards to 24 h (Table 3.2). As we replaced the test medium every day, the third assumption is that concentrations of ZnO $NP_{(ion)}$ to which the zebrafish embryos were exposed, were the average concentrations of ZnO $NP_{(ion)}$ in egg water after 1 and after 24 h. The toxicity of ZnO $NP_{(ion)}$ can be quantified by the concentration-response curve of $Zn(NO_3)_2$. The total toxicity of ZnO $NP_{(total)}$ was assessed experimentally.

Therefore, using the RA, the toxic effects (mortality, hatching inhibition, and behavioral inhibition) of embryos induced by ZnO $NP_{(particle)}$ ($E_{(particle)}$) can be computed as follows:

$$E_{(total)} = 1 - \left[\left(1 - E_{(ion)}\right)\left(1 - E_{(particle)}\right)\right] \quad (3.4)$$

where $E_{(total)}$ and $E_{(ion)}$ represent the effect of zebrafish embryos caused by the ZnO $NP_{(total)}$ and ZnO $NP_{(ion)}$ (scaled from 0 to 1), respectively. This leaves $E_{(particle)}$ as the only unknown, allowing for direct calculation of the effect caused by the particles at any specific initial actual particle concentration.

For the concentration addition model, the toxic effects of embryos induced by ZnO $NP_{(particle)}$ ($E_{(particle)}$) can be computed as follows:

$$E_{(particle)} = c_{(particle)}/(1 - c_{(ion)}/E_{(ion)}) \quad (3.5)$$

where $E_{(ion)}$ represent the median effect of zebrafish embryos caused by the ZnO $NP_{(ion)}$ (scaled from 0 to 1). $c_{(ion)}$ and $c_{(particle)}$ is the actual exposure concentration

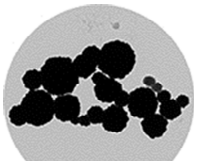

of ZnO $NP_{(ion)}$ and ZnO $NP_{(particle)}$, respectively. This leaves $E_{(particle)}$ as the only unknown, allowing for direct calculation of the effect caused by the particles at median lethal concentration.

3.2.6 Statistical analysis

All of the above experiments were repeated three times independently. Data are presented as mean with 95% confidence intervals (95% CI) or standard error of the mean (SEM). The LC_{50} values, the EC_{50} values and 95% CI were calculated (Eq.3.1) using GraphPad Prism 5. Statistical analyses were performed using one-way analysis of variance (ANOVA) with Tukey's multiple comparisons to compare among different ZnO particles treatments. For behavioral performance, one-way ANOVA was performed with Tukey's multiple comparisons. The significance level in all calculations was set at $p < 0.05$.

3.3 Results

3.3.1 Physicochemical characterization of ZnO particles

The primary sizes and shapes of the particles were estimated from TEM images (Figure 3.1) and are listed in Table 3.1. DLS was performed for determining the hydrodynamic diameter of aggregated particles suspended in egg water. Data on size distributions and zeta-potential are given in Table 3.1. We tested various ZnO particles: nanospheres (~27 nm, size variation of 11 - 51 nm), nanosticks (width: ~32 nm, size variation of 11 - 78 nm; length: ~81 nm, size variation of 27 - 157 nm), and ZnO SMPs (~202 nm, size variation of 47 - 571 nm). All ZnO NPs were present as aggregates in egg water. Initial particle sizes changed as soon as the particles were submerged in egg water. ZnO particles were partially dissolved after 24 h of incubation in egg water (Table 3.2). Results of AAS measurements of the concentration of total zinc (including ZnO $NP_{(ion)}$ plus ZnO $NP_{(particle)}$) and ZnO $NP_{(ion)}$ after 1 h and 24 h of incubation in egg water are shown in Table 3.2. The total zinc concentrations in egg water ranged from 67% to 92% of the nominal concentrations (mg Zn/L) depending on the ZnO NPs. The concentrations of ZnO $NP_{(ion)}$ increased with the total zinc concentrations, ranging from 1.0 to 3.5 mg Zn/L. In general, ions were released rather quickly as soon as the particles were submerged in egg water. A comparison of concentrations of ZnO $NP_{(ion)}$ after

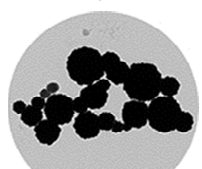

1 h and 24 h of exposure showed that hardly any additional dissolution was observed in between 1 and 24 h of exposure (Table 3.2). The relative amounts of dissolved zinc ions were different for differently shaped ZnO NPs at high concentration, with nanospheres (smaller particles) releasing more Zn ions, whereas dissolution from ZnO SMPs (larger particles) was the least.

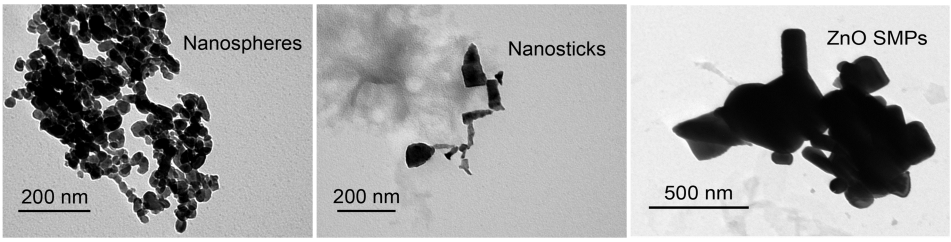

Figure 3.1 TEM images of ZnO particles in egg water at 1 h of incubation. The ZnO particles could aggregate to large particles. Pictures were taken with a JEOL 1010 TEM at 70 kV.

Table 3.1 Particles characterization

Particle	Average size [a]	Size variation using TEM	Size distribution using DLS	ζ-potential using DLS
nanospheres	43 nm	~27 nm (11-51 nm)	>1000 nm	-18.7 mV
nanosticks	150 nm	W:~32 nm (11-78 nm); L:~81 nm (27-157 nm)[b]	600 nm	-25.7 mV
ZnO SMPs	900 nm	~202 nm (47-571 nm)	>1200 nm	-23.1 mV

[a] According to the manufacturer information. [b] W: width; L:length.

3.3.2 Lethality of nanoparticles and zinc ions

Exposure of embryos to the ZnO $NP_{(total)}$ suspensions and zinc nitrate solutions induced a range of mortality, from 2 to 100% at 120 hpf. The LC_{50} values and 95% CI of suspensions of ZnO nanospheres, nanosticks, ZnO SMPs, and Zn^{2+} (zinc nitrate) were 11.9 (10.3 - 13.7), 7.1 (6.8 – 7.5), 10.0 (8.9 - 11.1), and 7.9 (7.1 - 8.8) mg Zn/L at 120 hpf, respectively (Figure 3.2A). The LC_{50} values of these ZnO $NP_{(total)}$ and zinc nitrate solutions showed that a suspension of Zn^{2+} was significantly more toxic than a suspension of most of the ZnO $NP_{(total)}$. Suspensions of ZnO nanospheres were least toxic as compared to suspensions of any of the other ZnO particles with regard to mortality to zebrafish embryos.

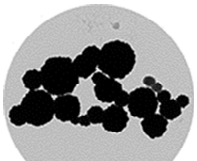

Table 3.2 The total ZnO particle suspension concentrations ($NP_{(total)}$) and shed Zn^{2+} from the ZnO particles ($NP_{(ion)}$) as measured after 1 h and 24 h of incubation in egg water (mean ± SEM)

Particle	Nominal conc. (mg Zn/L)	$NP_{(total)}$ conc. (mg Zn/L)*	$NP_{(ion)}$ conc. (mg Zn/L) *	
			1 h	24 h
nanospheres	4	3.1	1.0[a]	1.1[a]
	32	29.7	3.3[a]	3.5[a]
nanosticks	4	2.7	1.0[a]	1.2[a]
	32	28.8	2.7[b]	2.8[b]
ZnO SMPs	4	2.7	1.2[a]	1.2[a]
	32	28.9	1.6[c]	1.8[c]
$Zn(NO_3)_2$	7	4.5		
	55	35.7		

* Zn^{2+} concentrations were determined by atomic adsorption spectroscopy (AAS). Significant differences are indicated with different letters in dissolution of Zn for the different shaped nanoparticles at the same concentrations (Tukey's multiple comparisons, one-way ANOVA). Significant differences are indicated with different letters.

Using RA to quantify the toxicity of the ZnO $NP_{(particle)}$ to zebrafish embryos, we corrected for the toxicity caused by the ZnO $NP_{(ion)}$. The concentrations of ZnO $NP_{(total)}$ and ZnO $NP_{(ion)}$ present in the dispersions that were tested, are shown in Table 3.2. The LC_{50} values and the corresponding 95% CI of the ZnO $NP_{(particle)}$ nanospheres, nanosticks, and ZnO SMPs were 16.2 (12.4 – 21.2), 8.4 (7.3 – 9.5), and 9.6 (8.8 – 10.6) mg Zn/L, respectively (Figure 3.2B). We found that the 120 hpf LC_{50} value of Zn^{2+} ($Zn(NO_3)_2$) was 7.9 (7.1 - 8.8) mg Zn/L, indicating that Zn^{2+} was more lethal than any of the ZnO $NP_{(particle)}$. After ruling out the toxicity caused by ZnO $NP_{(ion)}$ to embryos, nanosticks and ZnO SMPs induced significantly more lethality than nanospheres (Figure 3.2B).

The LC_{50} and EC_{50} of hatching inhibition of embryos to ZnO $NP_{(particle)}$ using RA and CA are shown in Table 3.3, The LC_{50} values of the ZnO $NP_{(particle)}$ nanospheres, nanosticks, and ZnO SMPs were 12.5, 6.9, and 10.5 mg Zn/L, respectively.

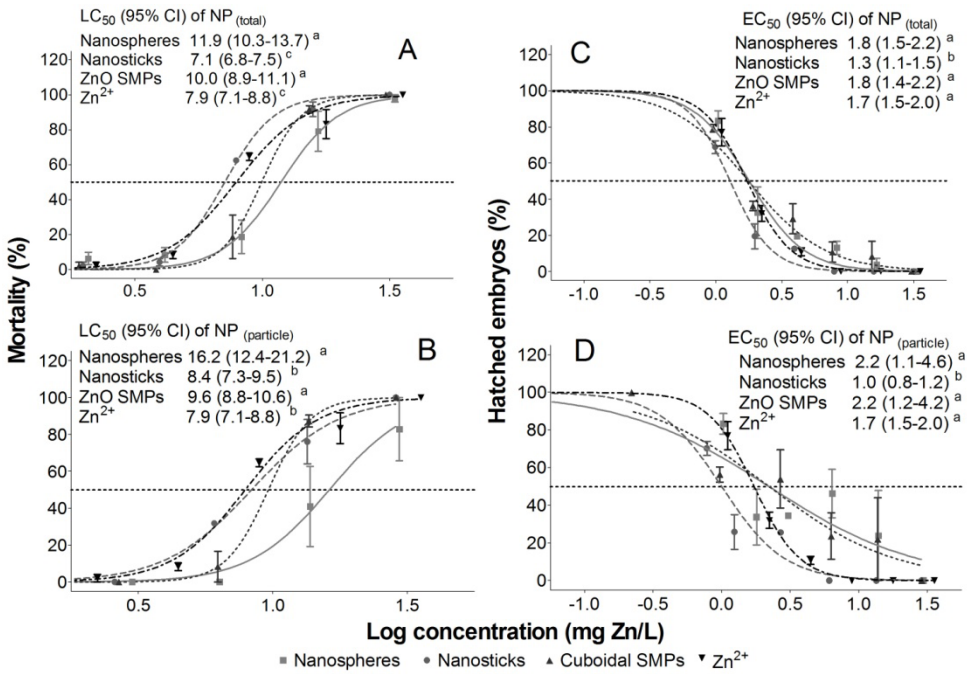

Figure 3.2 Dose response curves of mortality of zebrafish embryos exposed to ZnO $NP_{(total)}$ (A) and ZnO $NP_{(particle)}$ (B) at 120 hpf, dose response curves of hatching of zebrafish embryos exposed to ZnO $NP_{(total)}$ (C) and ZnO $NP_{(particle)}$ (D) at 72 hpf, following exposure to ZnO nanospheres, nanosticks, ZnO SMPs, and Zn^{2+} ($Zn(NO_3)_2$). Actual log-transformed Zn concentrations (mg Zn/L) are plotted on the X-axis. Data are presented as mean of three independent replicates ± SEM. One-way ANOVA with Turkey's multiple comparisons was used to detect significant differences between $L(E)C_{50}$ values of differently shaped ZnO NPs and Zn salt treated groups. Significant differences are indicated with different letters.

3.3.3 Hatching rate

The hatching rates associated with all four kinds of ZnO particles were reduced during the 96-h exposure time compared to the controls (Figure 3.3). Control groups of embryos developed normally, in the sense that all of the embryos hatched after 72 hpf. There was a clear concentration-dependence of exposure of embryos to different ZnO $NP_{(total)}$ and zinc nitrate solutions (Figure 3.2C). The EC_{50} values of $ZnO_{(total)}$ (nanospheres, nanosticks, ZnO SMPs) and $Zn(NO_3)_2$ for

hatching of zebrafish embryos were 1.8 (1.5 - 2.2), 1.3 (1.1 - 1.5), 1.8 (1.4 - 2.2), and 1.7 (1.5 - 2.0) mg Zn/L, respectively (Figure 3.2C). When taking only the ZnO $NP_{(particle)}$ into account by RA, the EC_{50} of hatching inhibition of zebrafish embryos after exposure to $ZnO_{(particle)}$ (nanospheres, nanosticks, ZnO SMPs) were 2.2 (1.1 – 4.6), 1.0 (0.8 - 1.2), and 2.2 (1.2 - 4.2) mg Zn/L, respectively (Figure 3.2D), which showed that ZnO nanosticks have a significantly higher effect on hatching than any of the other ZnO $NP_{(particle)}$ tested. The EC_{50} of hatching inhibition of embryos to ZnO $NP_{(particle)}$ using CA are shown in Table 3.3, The EC_{50} values of the ZnO $NP_{(particle)}$ nanospheres, nanosticks, and ZnO SMPs were 1.8, 1.2, and 1.9 mg Zn/L, respectively.

Table 3.3 The $L(E)C_{50}$ values of ZnO $NP_{(particle)}$ and of Zn^{2+} ($Zn(NO_3)_2$) after exposure to zebrafish embryos at 120 hpf using the response addition model (RA) and the concentration addition model (CA)

Particle	LC_{50} of $NP_{(particle)}$ (mg Zn/L)		EC_{50} of $NP_{(particle)}$ (mg Zn/L)	
	RA	CA	RA	CA
nanospheres	16.2	12.5	2.2	1.8
nanosticks	8.4	6.9	1.0	1.2
ZnO SMPs	9.6	10.5	2.2	1.9
Zn^{2+}	7.9		1.7	

3.3.4 Behavioral analysis

The total distance moved in the light/dark challenge test in three phases: basal, challenge, and recovery, following exposure to ZnO particle suspensions and $Zn(NO_3)_2$, is shown in Figure 3.4. The total distance moved by the embryos decreased with increasing concentrations. Some embryos swam slightly more at low concentrations (*e.g.* 2 and 4 mg Zn/L) than embryos in the controls in the basal and recovery phases. However, embryos swam less when exposed to all kinds of ZnO $NP_{(total)}$ than those in controls in the challenge phases (Figure 3.4). The EC_{50} values of $ZnO_{(total)}$, $ZnO_{(particle)}$ (nanospheres, nanosticks, ZnO SMPs), and $Zn(NO_3)_2$ are listed in Table 3.4. The EC_{50} values of Zn^{2+} ranged from 4.8 to 6.1 mg Zn/L in the different phases. For the three shapes of the ZnO $NP_{(total)}$, the EC_{50} values ranged from 0.01 to 6.1 mg Zn/L. In terms of the particle form of ZnO NPs, the EC_{50} values of ZnO $NP_{(particle)}$ ranged from 0.002 to 3.9 mg Zn/L.

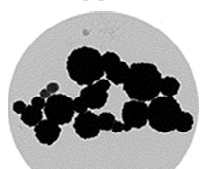

There are no significant differences among the three shapes of the ZnO NP and Zn^{2+} because of the wide range of the 95% CIs.

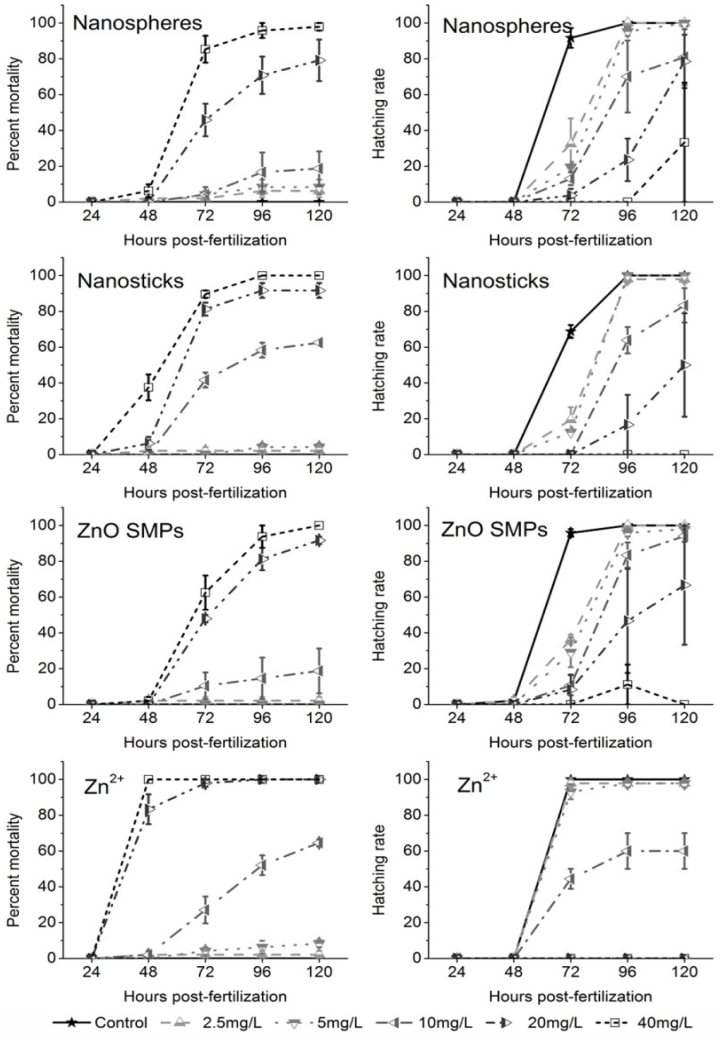

Figure 3.3 Time course of mortality (left column) and hatching rate of survived zebrafish embryos (right column) exposed to ZnO particle suspensions from 24 to 120 hours post-fertilization (hpf). Data presented as mean of three independent replicates ± SEM.

The EC_{50} values of ZnO $NP_{(particle)}$ for the hatching of embryos (1.0 - 2.2 mg Zn/L) was a more consistent endpoint than were the behavioral profiles of embryos albeit that overall, the most sensitive endpoint was the impact of ZnO-nanosticks on the behavior of the embryos in the basal phase. Embryo mortality of ZnO $NP_{(particle)}$ was the least sensitive endpoint among all of the three endpoints in our study, with LC_{50} values ranging from 8.4 to 16.2 mg Zn/L.

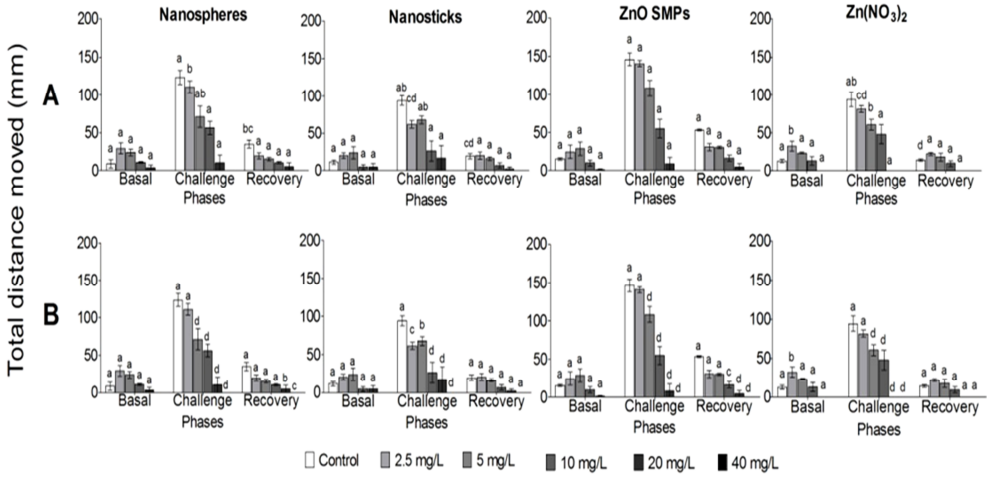

Figure 3.4 Behavioral performance of zebrafish embryos in the light-dark challenge test, as a function of the nominal concentrations of ZnO $NP_{(total)}$ and $Zn(NO_3)_2$. Data are presented as mean of three independent replicates ± SEM. One-way ANOVA with Turkey's multiple comparisons was used to detect significant differences. Significant differences of total distance moved are indicated with different letters in the same phase (A) significant differences between different particles in the same concentration and (B) significant differences between different concentrations exposed to same particles.

Table 3.4 The EC_{50} values of ZnO $NP_{(total)}$, ZnO $NP_{(particle)}$ and of Zn^{2+} ($Zn(NO_3)_2$) on behavioral performance after exposure to zebrafish embryos at 120 hpf

Particle	EC_{50} in different phases (mg Zn/L)					
	Basal phase		Challenge phase		Recovery phase	
	EC_{50}	95% CI	EC_{50}	95% CI	EC_{50}	95% CI
ZnO $NP_{(total)}$						
nanospheres	4.2	1.9-9.4	4.8	3.7-6.3	1.1	0.3-3.6
nanosticks	0.01	0.001-0.2	3.8	2.4-5.9	3.8	2.3-6.1
ZnO SMPs	0.02	0.001-7.0	5.3	4.5-6.2	3.2	2.3-4.4
Zn^{2+}	4.8	2.6-9.2	5.4	4.0-7.2	6.1	3.9-9.6
ZnO $NP_{(particle)}$						
nanospheres	0.04	0.01-9.0	5.6	3.9-8.1	1.2	0.2-6.3
nanosticks	0.002	0.001-2.8	4.6	2.4-8.5	3.9	2.1-7.2
ZnO SMPs	0.02	0.001-1.8	5.5	4.6-6.6	3.2	2.1-5.1

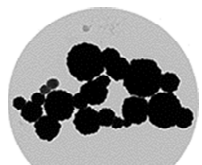

Table 3.5 Relative contribution to toxicity of ZnO $NP_{(particle)}$ and ZnO $NP_{(ion)}$ at the LC_{50}-value of the suspensions and at the EC_{50}-value of the suspensions for hatching inhibition using response addition (RA) and concentration addition (CA) models

Particle	Median conc. (mg Zn/L)	Relative toxic contribution using RA (%)		Relative toxic contribution using CA (%)	
		$NP_{(ion)}$	$NP_{(particle)}$	$NP_{(ion)}$	$NP_{(particle)}$
LC_{50}					
nanospheres	11.9	48	52	14	86
nanosticks	7.1	39	61	22	78
cuboidal SMPs	10.0	28	72	18	82
EC_{50}					
nanospheres	1.8	17	83	1	99
nanosticks	1.3	18	82	25	75
cuboidal SMPs	1.8	62	38	54	46

3.3.5 Relative contribution to toxicity of ZnO $NP_{(particle)}$ and ZnO $NP_{(ion)}$

The relative contribution to toxicity of ZnO $NP_{(particle)}$ and ZnO $NP_{(ion)}$ to zebrafish embryos using RA and CA is given in Table 3.5. For RA, at the LC_{50} of the suspensions of each particle, the contributions of the particle form of ZnO nanospheres, nanosticks, and SMPs to the lethal effects observed after exposure to suspensions of nanoparticles were 52%, 61%, and 72%, respectively. In the case of the 50% hatching inhibition concentration of each particle suspension, the particle contribution to hatching inhibition of suspensions of ZnO nanospheres, nanosticks, and SMPs was 83%, 82%, and 38%, respectively. For CA, at the LC_{50} of the suspensions of each particle, the contributions of the particle form of ZnO nanospheres, nanosticks, and SMPs to the lethal effects observed after exposure to suspensions of nanoparticles were 86%, 78%, and 82%, respectively. In the case of the 50% hatching inhibition concentration of each particle suspension, the particle contribution to hatching inhibition of suspensions of ZnO nanospheres, nanosticks, and SMPs was 99%, 75%, and 46%, respectively. The particle form of nanospheres and nanosticks was thus found to be the main factor causing inhibition of hatching of zebrafish embryos after exposure to suspensions of ZnO particles.

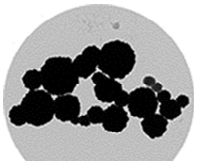

3.4 Discussion

3.4.1 Lethality of ZnO $NP_{(total)}$

We exposed zebrafish eggs to two kinds of ZnO NPs and one type of ZnO SMP. The average size and size variation of the two ZnO NPs, namely the nanospheres and nanosticks, were similar in one dimension (Table 3.1), but with different shape (Figure 3.1, the top two pictures). We also used one kind of ZnO SMPs, which was cuboidal of shape (Figure 3.1). The ZnO SMPs were used to test the impact of a third shape on embryo toxicity. Moreover, ZnO SMPs were used to extend the range of sizes tested, enabling us to compare the toxicity of nano- and submicron-particles. When comparing the LC_{50} values of suspensions of ZnO $NP_{(total)}$, it was found that Zn^{2+} and nanosticks were more lethal to zebrafish embryos than the ZnO SMPs and nanospheres suspensions.

In previous studies, Zn^{2+} was reported to induce various adverse cellular outcomes in the lysosome and the intracellular environment, such as reactive oxidative species (ROS) production, lysosome damage, mitochondrial perturbation, excitation of pro-inflammatory cytokine and chemokine production (Xia *et al.*, 2008; Zhu *et al.*, 2009; Nel *et al.*, 2009; George *et al.*, 2010; 2011a). However, as seen from our results (Table 3.5), ZnO particle dissolution only partially contributed to the toxicity of ZnO particle suspensions. These findings are in line with other studies (Bai *et al.*, 2010b; Xia *et al.*, 2011; Zhu *et al.*, 2008). However, the extend of toxicity and the relative toxic contribution of ZnO $NP_{(particle)}$ cannot be deduced from these and other studies. We therefore investigated this aspect as described in the following section.

3.4.2 Lethality of ZnO $NP_{(particle)}$

Several studies suggested that mixtures of contaminants with dissimilar MOAs tend to be best modeled by the response addition model (Altenburger *et al.*, 2003; Faust *et al.*, 2003). The MOAs of ZnO $NP_{(particle)}$ and ZnO $NP_{(ion)}$ are described in the Section 3.2.5. The effects of ZnO $NP_{(particle)}$ and ZnO $NP_{(ion)}$ using the RA (eq. 3.3) gave the LC_{50} values of ZnO $NP_{(particle)}$ and Zn^{2+} (Figure 3.2B) and indicated that Zn^{2+} and ZnO nanosticks were more lethal to zebrafish embryos than the $NPs_{(particle)}$ of ZnO SMPs and nanospheres. At the 50% mortality concentration of

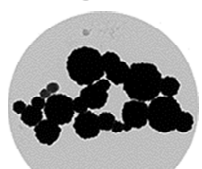

suspensions of nanospheres, nanosticks, and ZnO SMPs, the relative contribution to lethality of ZnO $NP_{(particle)}$ was higher than that of the ZnO $NP_{(ion)}$ present in suspensions at the LC_{50}-level (Table 3.5). This indicates that, despite the relative high intrinsic lethality of Zn^{2+}, the ZnO $NP_{(particle)}$ was the main factor inducing lethality to zebrafish embryos for all particle shape suspensions tested.

Comparing the LC_{50} of $NP_{(particle)}$ calculated by RA and CA, we found that the LC_{50} calculated using CA of the particle form of nanospheres and nanosticks were smaller than those calculated by RA. This means more toxic effects by using CA than by using RA and therefore the increased relative contribution of the particle form of nanospheres (Table 3.5). It is also the case for the EC_{50} of hatching inhibition to $NP_{(particle)}$. Both results from CA and RA allowed us to conclude that the ZnO $NP_{(particle)}$ was the main factor in inducing lethality to zebrafish embryos for all particle shape suspensions tested.

Taken together, our results show that the lethality of solutions of Zn^{2+} to zebrafish embryos was higher than the lethality induced by exposure of zebrafish embryos to most of the suspensions of ZnO NPs at equal mass concentrations, the exception being ZnO nanosticks. This finding is due to the fact that the concentrations of dissolved Zn^{2+} in the ZnO particle suspensions were low (for instance: < 3.5 mg Zn/L for the 32 mg Zn/L actual concentration of ZnO $NP_{(total)}$) (Table 3.2), and such low concentrations were insufficient to exert considerable lethality in suspensions of ZnO particles. Consequently, the contribution of ZnO $NP_{(ion)}$ was lower than the contribution of ZnO $NP_{(particle)}$.

During the present experiments, it was observed by microscopy that all types of aggregated ZnO particles adhered to the chorion of the embryos at higher concentrations (Supplemental data 3.1). This is consistent with Zhu *et al.* (2009). Some studies have reported on the route of uptake of nanoparticles into embryos. One possibility is that ZnO NPs are taken up into embryos directly. TEM images show that the ZnO NPs were aggregated in egg water (Figure 3.1). The aggregation of ZnO NPs in egg water changed their size distribution. Smaller ZnO NPs aggregates can easily penetrate into the perivitelline space of embryos *via* the chorion pore canals, the diameter of which is around 0.5-0.7 μm (Lee *et al.*, 2007; 2012). Larger ZnO NPs aggregates cannot be transported directly through

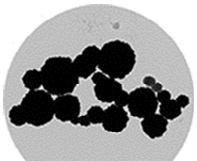

chorionic canals. The aggregated ZnO NPs might subsequently block the pore canals of the chorion, and no more ZnO NPs and Zn^{2+} (and maybe also oxygen) could enter into the embryo chorion (Zhu *et al.*, 2009). If the ZnO NPs were loosely aggregated, they could be separated into smaller ZnO NPs and still pass into the chorion (Bai *et al.*, 2010b). Another possibility is that ZnO NPs were concentrated in the chorionic fluid of zebrafish embryos, which could be possibly due to passive diffusion and the high osmotic pressure of the protein-rich fluid (Xia *et al.*, 2011).

3.4.3 Comparison of lethality of ZnO $NP_{(particle)}$ with different shape

In the current study, ZnO nanosticks (which are similar to rod shaped NPs) were more toxic than ZnO SMPs (nearly cuboidal), whereas ZnO SMPs in turn were more toxic than nanospheres (Figure 3.2B). These findings may be explained by the fact that stick-shaped NPs have a larger direct contact area with embryos than spherical NPs as the longitudinal axis of the rods interacts with embryos (Huang *et al.*, 2010b). Similarly, ZnO SMPs also have a larger direct contact area with embryos as one face of the cube interacts with embryos (Figure 3.1), which might explain why SMPs are more toxic than nanospheres. Moreover, the uptake of rod-shaped NPs in mammalian cells (which are similar to stick-shaped NPs in this study) was found to depend mainly on the width of the NPs (Chithrani and Chan, 2007). Another explanation of the overall toxicity patterns is the observation that ZnO nanospheres as well as ZnO SMPs form larger aggregates as compared to ZnO nanosticks aggregates, as may be deduced from TEM images (Figure 3.1). This will lead to reduced effective exposure and hence reduced toxicity of ZnO nanospheres and ZnO SMPs. The aggregation of nanoparticles in water is an important factor in assessing their toxicity, also due to a more effective macrophage clearance for larger particles compared to smaller ones (Buzea *et al.*, 2007; Zhu *et al.*, 2009). Taken together, the toxicity of ZnO NPs depends on multiple factors including ZnO particle dissolution, shape, as well as aggregation state.

In previous studies, the toxicity of different NP shapes was found to be also species-specific and composition dependent, although the findings are not conclusive. Chithrani and Chan (2007) found that rod-shaped Au NPs showed a

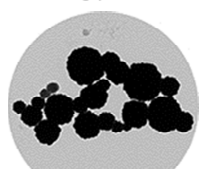

lower uptake in mammalian cells in comparison to spherical shaped Au NPs. The rates of uptake were higher with a decreasing aspect ratio. Agarwal *et al.* (2013) reported that larger nanodiscs and rods had higher uptake rates compared to the smallest particles tested for mammalian cells. In another study, there was no significant difference in toxicity to zebrafish embryos between strip-shaped ZnO NPs and bulk ZnO with spherical/elliptical shape (Zhu *et al.*, 2008).

3.4.4 Sub-lethal toxicity of ZnO $NP_{(total)}$ and $NP_{(particle)}$

Our results on behavioral performance showed no significant differences among all the types of ZnO $NP_{(total)}$ as well as all types of the ZnO $NP_{(particle)}$. Therefore, behavior is not a response that distinguishes with regard to particle shape. The behavioral changes in 120 hpf larvae could be due to (i) morphological abnormalities; previous studies showed that exposure to ZnO NPs shortened the body length and induced tail malformation, pericardial and yolk sac edemas in zebrafish embryos and larvae (Bai *et al.*, 2010b; Zhu *et al.*, 2009), (ii) neuronal toxicity exerted by ZnO particles or (iii) combined effects. In our study, we also observed tail malformation, pericardial and yolk sac edemas in zebrafish embryos and larvae exposed to each type of ZnO NPs (data not shown). Serious malformations were not observed in our studies.

The results further showed that hatching was in general the most sensitive endpoint in the case of exposure of embryos to ZnO NPs. Small changes in hatching reduced fish reproduction. Zn^{2+} concentrations in the media used for assessing the impact of ZnO NPs on hatching were low. After ruling out the toxic effect of Zn^{2+}, we explicitly accounted for the toxic impacts of ZnO $NP_{(particle)}$. The stick-shaped ZnO $NP_{(particle)}$ was significantly more toxic as compared to the $nanospheres_{(particle)}$ and ZnO $SMP_{(particle)}$ (Figure 3.2D).

ZnO SMPs were more lethal than nanospheres, but they showed similar hatching inhibition. One possible reason is the relative toxic contribution of $NP_{(particle)}$ and $NP_{(ion)}$ of lethality and hatching inhibition are different (Table 3.5). $NP_{(particle)}$ are more toxic than $NP_{(ion)}$. However, their contribution of the particle form of nanospheres and SMPs of lethality are 52% and 72%, respectively. The contribution of the particle form of nanospheres and SMPs of hatching inhibition

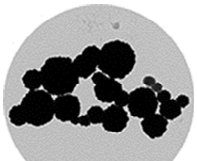

are 83% and 38%, respectively. Taken together, the toxicity effect of the particle form of nanospheres and SMPs are different in lethality and hatching inhibition. In addition, the MOA of lethality and MOA of hatching inhibition of NPs to zebrafish embryos may be different. Therefore, ZnO SMPs were more lethal than nanospheres, but they showed similar hatching inhibition.

At the 50% hatching inhibition concentration of each of the ZnO $NP_{(total)}$, the particle form of ZnO sticks and spheres was mostly responsible for the effects observed on hatching of zebrafish embryos (Table 3.5). Again, this is due to the quite low concentrations of dissolved Zn^{2+} in the ZnO particle suspensions at the EC_{50}-level (Table 3.2). In the case of the particle form of SMPs, the relative contribution of ZnO $NP_{(particle)}$ was lower than that of the ZnO $NP_{(ion)}$ at the EC_{50} concentration of each ZnO $NP_{(total)}$.

3.5 Conclusions

ZnO nanosticks induced higher toxicity than nanospheres and cuboidal SMPs for zebrafish embryos when mortality and hatching inhibition were used as endpoints. Hatching of the embryos was in general the most sensitive endpoint. The contribution to toxicity of ZnO $NP_{(particle)}$ was dominant over the contribution of ZnO $NP_{(ion)}$ when explaining toxicity of all ZnO $NP_{(total)}$ tested for zebrafish embryos.

Supplemental data

Supplemental data 3.1 Aggregated ZnO particles adhered to the chorion of the embryos at higher concentration.

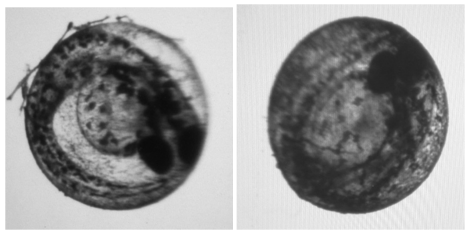

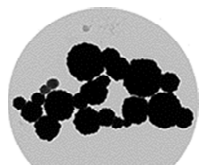

Budapest, Hungary

Photo by Jing HUA

4

Dose metrics assessment for differently shaped and sized metal-based nanoparticles[3]

4.1 Introduction

Dose-response relationships are one of the main parameters in conventional ecotoxicology. The dose metric for expressing the effective dose is very important. Researchers generally use mass of test compound in describing the dose because of its convenience. However, physicochemical properties of nanoparticles, including size, morphology, number, surface state, can all influence their biological activity (Alivisatos *et al.*, 1996; Jiang *et al.*, 2008a; Nel *et al.*, 2006; Oberdörster *et al.*, 2005; Rushton *et al.*, 2010). 'Mass' is not the only optimal metric for nanoparticles (NPs) (Oberdörster, 2000, Oberdörster *et al.*, 2007; Wittmaack, 2007b).

One study showed that the surface area of TiO_2 nanoparticles is a better dose metric than particle mass or particle number, when evaluating dose-response relationships of TiO_2 nanoparticle bioactivity toward lung tissue (Oberdörster *et al.*, 2007). Others have considered surface area as an appropriate dose metric (Donaldson *et al.*, 2000; George *et al.*, 2012; Oberdörster, 1996; Oberdörster *et al.*, 2005; Rushton *et al.*, 2010; Stoeger *et al.*, 2006). Yet other studies have suggested that particle number is the optimal metric of NP exposure when considering their bioactivity

[3] Based on: Hua, J., Vijver, M. G., Chen, G., Richardson, M. K., and Peijnenburg, W. J.G.M. Dose metrics assessment for differently shaped and sized metal-based nanoparticles. Submitted.

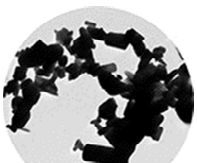

(Wittmaack, 2007b). Taken together, these studies show that there is yet no consensus on the most appropriate dose metric when assessing dose-response relationships of nanoparticles.

However, all these studies used human lung injury as the readout of toxicity. A limited number of studies focused on ecologically relevant species (other than human) (Tuttle, 2012; Delmaar *et al.*, 2015). A generic species-independent method for assessing the best way to express a dose is needed. Tuttle (2012) used the mean primary particle diameter (*d*) of Ag NPs plotted against the median lethal concentration (LC_{50}) and found that surface area was a better predictor than mass and particle number to describe zebrafish embryos response data after NP-exposure. The particle diameter *d* was used by Delmaar *et al.* (2015) to plot against the theoretical total particle number at the LC_{50} value of each type of NPs to obtain an equi-response curve and, based on the slope of the curve, to determine the best dose metric for various species. However, these studies only focused on spherical NPs. Clearly, the particle diameter is not applicable for non-spheric shaped NPs, as the diameter of these particles is not defined. In our study, we used the mean primary particle surface area to volume ratio (SA/V, nm^{-1}) instead of *d*. The reasons are: parameters of sizes of NPs are easy to quantify by TEM, SEM and DLS, and geometrical methods can then easily be applied to calculate surface area (SA) and volume (V) of NPs as described in Supplemental data 4.5; SA/V is applicable for non-spherically shaped NPs.

The aim of this study was to develop a generic dose calculation method and determine which property is the most appropriate as a dose metric when assessing dose-response relationships of differently shaped metal nanoparticles and submicron particles. We exposed zebrafish embryos not only to spherical but also to non-spherical NPs and to a range of sizes of Cu NPs and ZnO NPs to assess toxicity. We also collected data on the toxicity of NPs from peer-reviewed scientific papers to construct a comprehensive dataset for model verification. Considering that the majority of literature investigated Ag NPs and ZnO NPs, which are more toxic than other types of metal-based NPs (*e.g.* Au NPs), we therefore only focus on Ag NPs and ZnO NPs from literature dataset. We applied our generic dose calculation method to our data and secondary data from a range of species from aquatic biota *in vivo* to mammalian cells *in vitro*. With deriving

this dose calculation method, we aimed to assess the dose metrics for all kinds of shaped and sized metal-based NPs and for various biological species.

4.2 Materials and methods

4.2.1 Nanoparticles properties and toxicity to zebrafish embryos

The Cu and ZnO nanoparticles data sets were obtained from our previous studies and shown in Supplemental data 4.1 to 4.3 (Hua *et al.*, 2014a, 2014b). The data sets were used in two ways. Firstly, we used the data in our generic dose calculation method to find the best dose metric of NPs for differently shaped and sized NPs (Section 4.2.2). Secondly, we applied the data to modified dose-response curves as described by Oberdörster *et al.* (2005) (Supplemental data 4.4). Both results from the different calculation approaches were then compared, enabling us to evaluate the consistency and robustness of both modeling approaches.

4.2.2 Generic dose calculation method for differently shaped and sized NPs

Delmaar *et al.* (2015) used the mean primary particle diameter (*d*) plotted against total number of particles (N) as the basis for deducing dose metrics, and reported that the slope of the equi-response curve (hereafter labels as S_{curve}) in the log(N) versus log(*d*) plot derived from experimental data can describe the dose. However, the *d* is not ideal for differently shaped NPs. In our study, we used mean primary particle surface area to volume ratio to plot against the theoretical total particle number at the $L(E)C_{50}$ value of each type of NP and performed a linear regression, then the S_{curve} was used to assess the best dose metric of NP. The SA/V was selected because of the following reasons: 1) The SA/V of these particles are easy to quantify using TEM, SEM, and other technology; 2) Besides spherically shaped NPs, the SA/V is also suited for non-spherically shaped NPs; 3) The SA/V is an intensive property (*e.g.* no matter how many uniform particles are involved, the SA/V always remains the same). As particles get smaller, their SA/V gets larger. The particles with larger surface area for the same volume react much faster because larger surface area provides more reaction sites for the same volume, leading to more chemical reactivity.

The parameters of the differently shaped NPs used in the calculations, are shown in Supplemental data 4.5. For easier calculation of the SA and V of differently shaped and sized NPs, we assumed that the shape and size are uniform with the same mean primary parameters in each type of NPs suspension. The mean primary particle surface area (nm^2/particle) and the mean primary particle volume (nm^3/particle) were calculated using the geometric equations (Supplemental data 4.5).

If administered surface area is an adequate dose metric, a large number of small nanoparticles will give the same response as a smaller number of larger nanoparticles of the same shape and with the same total surface area. The constant total surface area (S) of total number (N) of particles is given by:

For nanospheres:

$$S = N\pi d^2 = \text{constant, and thus:}$$

$$N = \frac{C_1}{d^2}$$

where C_1 is a particular constant that, in the equi-response curve, depends on the response level of the test. Taking the logarithm of both sides of the equation allows for a more convenient comparison of curves:

$$\log(N) = \log(C_2) + 2\log(\tfrac{6}{d}) \text{ , or:}$$

$$\log(N) = C_3 + 2\log(SA/V)$$

This has the form of the equation describing a straight line:

$$y = ax + b$$

where *a* is slope of the line and *b* is the intercept when x=0. It follows that the equation describing the curve for constant surface area of nanospheres has a slope that also equals 2.

For nanorods and nanosticks:

$$S = N[2\pi\left(\frac{d}{2}\right)^2 + \pi dl] = \text{constant, and thus:}$$

$$N = \frac{C_4}{d(2l + d)}$$

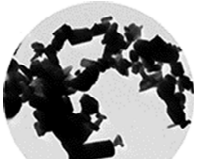

For easy calculation, we set $l = C * d$, where C is a constant and equals the mean primary aspect ratio of one type of NP measured in TEM images, thus:

$$N = \frac{C_4}{d(2l+d)} = \frac{C_4}{d(2Cd+d)} = \frac{C_5}{d^2}$$, or:

$$\log(N) = C_6 + 2\log(SA/V)$$

It follows that the equation describing the curve for constant surface area of nanorods or nanosticks has a slope that also equals 2.

For cuboidal particles:

$S=N*6*l^2$=constant, and thus:

$$N = \frac{C_7}{l^2}$$

$$\log(N) = C_8 + 2\log(SA/V)$$

It follows that the equation describing the curve for constant surface area of cuboidal particles has a slope that also equals 2.

Generally, on the logarithmic scale, the equation describing the curve for constant surface area of different shaped NPs has a slope that equals 2. For all kinds of different sized and shaped NPs for which surface area is an adequate dose metric in a specific test system, the equi-response curve will be parallel to this curve, which will also have a slope that equals 2.

In a similar way, if volume is an adequate dose metric, the curve for constant total volume (V) of total number (N) of particles is:

For nanospheres:

$V=N*1/6*\pi*d^3$=constant.

For nanorods and nanosticks:

$V=N*(\pi*(d/2)^2*l)$=constant.

For cuboidal particles:

$V=N*l^3$=constant.

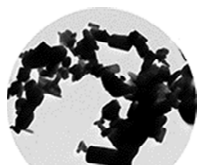

And thus:

$$\log(N) = C_9 + 3\log(SA/V)$$

It follows that the equation describing the curve on a logarithmic scale for constant volume of nanospheres, nanorods and nanosticks, and nanocuboids has a slope of 3. Generally, for all kinds of different sized and shaped NPs, the equation describing the curve on the logarithmic scale for constant particle volume has a slope of 3.

Finally, the curve of constant particle number N is independent of SA/V and is given by

N=constant, or:

$$\log(N) = C_{12}$$

Hence, the equation describing the curve for constant particle number has a slope of 0 in a log (N) versus log (SA/V) plot and is thus a horizontal line.

For other shapes of NPs, we also can use this method to calculate their SA/V and calculate their slopes for dose metrics.

4.2.3 Database from literature survey

We also collected the toxicity data from previous literature that contained physicochemical characteristics of NPs and toxicity data of these NPs to different species (*e.g.* algae, crustaceans, fish, nematode, and mammalian cells). During literature survey, we found that only the toxicity of Ag NPs and ZnO NPs have a sufficient number (greater than 3) of data points for a more accurate modeling. Other types of metal-based NPs did not have a sufficient number of data points for the modeling. Therefore, the data of Ag NPs and ZnO NPs were chosen to evaluate the consistency and robustness of both modeling approaches. Because previous studies only show the toxicity of $NP_{(total)}$, and some of the studies did not show the actual concentrations of dissolved metal ion, it is not possible to calculate the toxic effect induced by $NP_{(particle)}$. So the toxicity data were only for $NP_{(total)}$ to different species. However, from our results, the S_{curve} of $NP_{(particle)}$ and $NP_{(total)}$ are quite similar, especially for the endpoints of mortality. In the case of hatching rate as the endpoint, the S_{curve} of $NP_{(particle)}$ are smaller than those of $NP_{(total)}$ (Figure 4.1). For

most of the cases, the NPs sizes were based on mean primary sizes of TEM, SEM images, DLS and information provided by the manufacturer. There are two studies only provided a range for size (*e.g.* 40-60 nm) not the mean primary sizes of NPs, then we assumed that the size distribution is normal distribution and we used the mean value of the upper range value and lower rang value (*e.g.* 50 nm). For algae, the endpoints are different, including 4.5 h EC_{50}, 72 h EC_{50} and 96 h EC_{50} of growth inhibition. The endpoint for crustaceans is 48 h LC_{50}. For fish, 96 h LC_{50} is used as the endpoint (same with our endpoint). The endpoint for nematodes testing is 72 h EC_{50}. For mammalian cells, 24 h IC_{50} of viability is the endpoint.

4.3 Results

4.3.1 Generic dose calculation method for differently shaped and sized NPs

In our experimental dataset of zebrafish embryos, the base-10 logarithm of the theoretical total particle number at each $L(E)C_X$ value of each type of NPs were used to plotted against the base-10 logarithm of the surface area to volume ratio (SA/V) for linear regression of the equi-response curves (Figure 4.1). The S_{curve} was determined and subsequently used to indicate the best dose metric. If the S_{curve} approaches 3, 2, or 0, the best dose metrics of NPs are volume, surface area, or number of particles, respectively (Section 4.2.2). The S_{curve} and intercept obtained from spherical and non-spherical $NP_{(particle)}$ and $NP_{(total)}$ (mean±95% CI) are listed in Supplemental data 4.7.

As a start, we calculated the S_{curve} of spherical $NP_{(particle)}$ and $NP_{(total)}$ and determined the best dose metric. We then extended our modeling to differently shaped $NP_{(particle)}$ and $NP_{(total)}$. Comparing those results can give indication whether using particle morphology related attributes are suitable as a generic calculation method for expressing toxicity for different shaped and sized NPs. Our experimental dataset of zebrafish embryos contained five types of Cu NPs and five types of ZnO NPs, of which four spherical Cu NPs were present with different sizes, and two spherical ZnO NPs used. For the spherical Cu NPs, 11 out of the 12 endpoints investigated for $NP_{(total)}$ and $NP_{(particle)}$ had slopes (mean ± 95% CI) of the equi-response curve of around 3 (2.6~3.0), except for the slope of the EC_{20} of Cu $NP_{(particle)}$ (slope=2.3±0.3) (Figure 4.1, Supplemental data 4.7). This indicates that volume is in general an

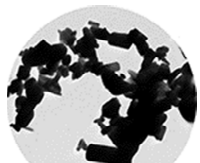

adequate dose descriptor when assessing the toxicity of spheric Cu NPs to *Danio rerio*. We excluded the spherical ZnO NPs for modeling, because we only had data on 2 types of spheric ZnO NPs, which is not sufficient for meaningful modeling.

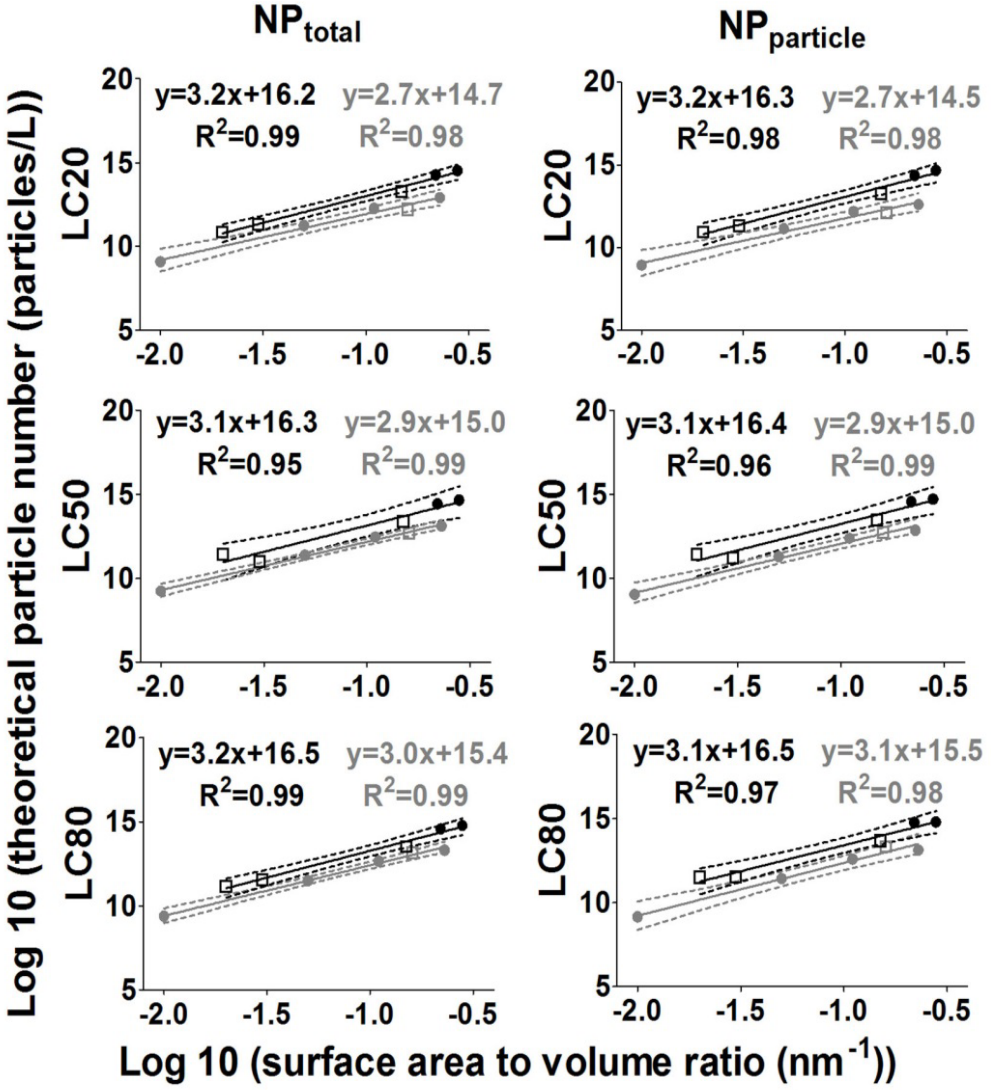

(Continued)

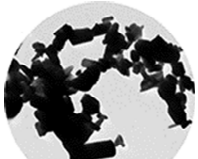

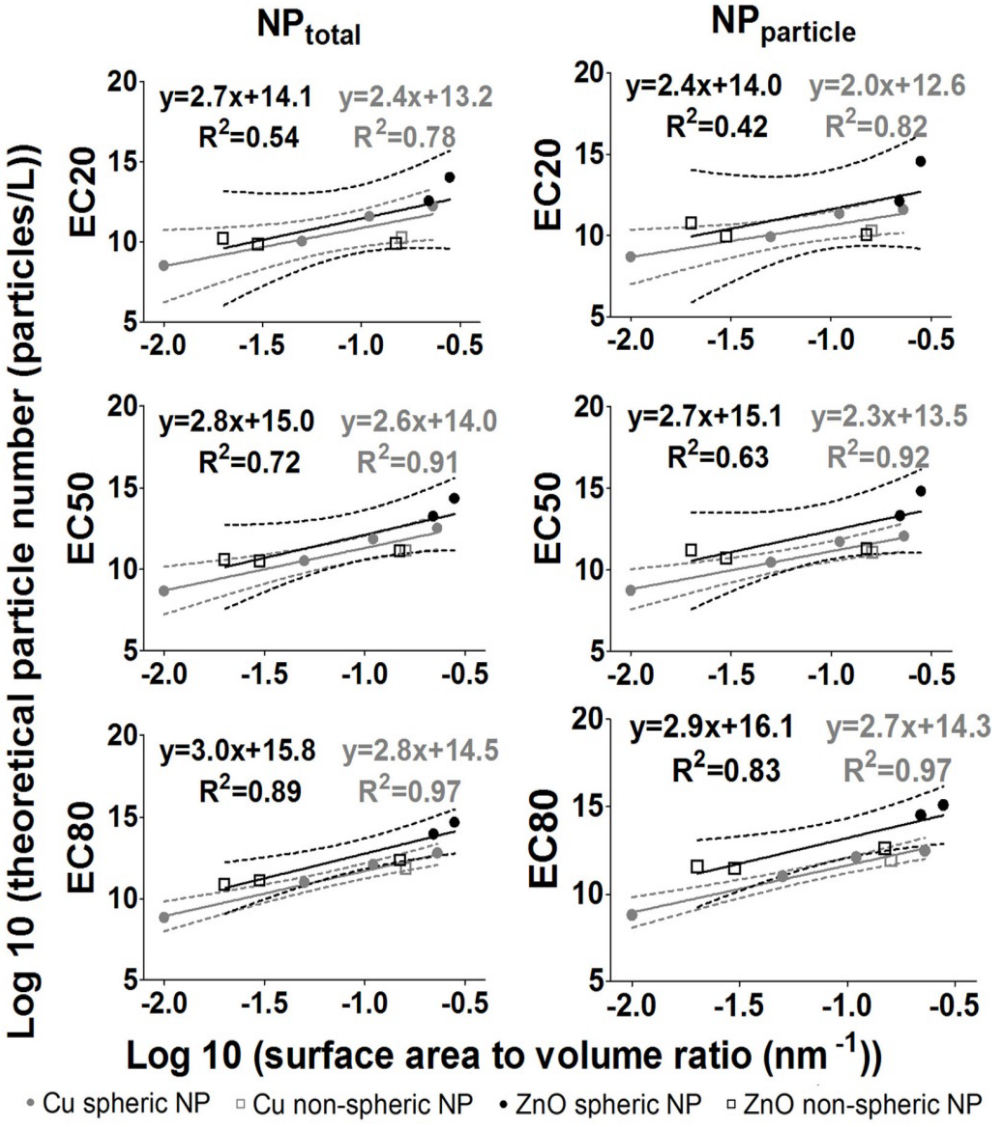

Figure 4.1 Estimated logarithm of LC_{20}, LC_{50}, and LC_{80} values, EC_{20}, EC_{50}, and EC_{80} values of hatching inhibition plotted against logarithm of surface area to volume ratio for particle number of Cu spheric NPs, Cu non-spheric NPs, ZnO spheric NPs, and ZnO non-spheric NPs. The best-fit lines from linear regression analysis are displayed (solid lines) as well as their associated 95% CIs (dashed lines).

For all spherical and non-spherical Cu NPs and ZnO NPs, most the S_{curve} (mean±95% CI) were around 3 (2.6~3.1), except for the slopes of EC_{20} of Cu $NP_{(total)}$ (slope=2.4±0.7), EC_{20} (slope=2.0±0.5) and EC_{50} (slope=2.3±0.4) of Cu $NP_{(particle)}$, EC_{20} (slope=2.4±1.6) of ZnO $NP_{(particle)}$. It should be noted that in 2 out of the 4 cases, the confidence interval of the S_{curve} encompassed 3 as well as 2. This indicates that volume is in general an adequate dose descriptor when assessing the toxicity of ZnO NPs and Cu NPs to zebrafish embryos. As the calculation results for spheric NPs and non-spheric NPs showed to be consistent over the different shapes, we conclude that this calculation approach is suitable for all types of metal-based NPs.

Using the dose-response curve modeling method by Oberdörster *et al.* (2005) resulted in the same conclusion with that by our generic dose calculation method. Thus, this supports the validity of our proposed modeling method and our results of modeling (Supplemental data 4.4).

The intercept of the equi-response curve reflects the base-10 logarithm of the theoretical particle number at $L(E)C_{50}$ values where the base-10 logarithm of SA/V equals 0 (SA/V=1). A smaller value of the intercept indicates an increased intrinsic toxicity of the NPs. The intercept of the equi-response curve of Cu NPs and ZnO NPs ranged from 12.6 to 15.5 and from 14.0 to 16.5, respectively (Figure 4.1). This indicated that when their size and shape are similar, Cu NPs are more toxic than ZnO NPs to zebrafish embryos. On average, this difference in toxicity of Cu NPs and ZnO NPs is a factor of 24. The difference in toxicity of Cu^{2+} (0.7 mg/L) and Zn^{2+} (7.9 mg/L) is a factor of 11 (Hua *et al.*, 2014a, 2014b).

4.3.2 Database from literature survey

We constructed an extensive dataset (covering diverse specifies and different nanoparticles) by collecting published data from literature. This dataset was used to further evaluate and extend the applicability of our proposed modeling method. Values of the base-10 logarithm of $L(E)C_{50}$ expressed as particle numbers plotted against the base-10 logarithm of surface area to volume ratio for the pristine Ag NPs and ZnO NPs are shown in Figure 4.2 (more than 3 data points), the results with two or three data points are shown in Supplemental data 4.8. The S_{curve} and

intercept (mean±95% CI) are listed in Table 4.1.

In the case of Ag NPs, the S_{curve} differ according to the species. For mammalian cells, the S_{curve} showed wide variation, ranging from 0.9 to 5.9 (Table 4.1). For crustaceans (*Daphnia magna* and *Chydorus sphaericus*) and for the zebrafish *Danio rerio*, the S_{curve} are very close to 3 (Table 4.1). For other fish species, different species have different slopes: *Oryzias latipes* (slope=4.1±1.0, *i.e.* including 3), *Pimephales promelas* (slope=1.8±0.6). For the nematodes, the slope is 2.6±1.0 (with 2 and 3 included).

For ZnO NPs, all the S_{curve} are 3, or slightly larger than 3, which means that particle volume seems to be a more appropriate dose metric for different sized and shaped nano- and sub-micron ZnO particles to various species.

The intercept of the equi-response curve of Ag NPs and ZnO NPs ranged from 12.8 to 18.8 and from 14.4 to 17.1, respectively (Table 4.1). The intercept of the equi-response curves are significantly different between Ag NPs and ZnO NPs for different species. As some of the endpoints of Ag NPs and ZnO NPs are different, we only compared the intercept of models with the same endpoint for Ag NPs and ZnO NPs. The intercept of the Ag NPs and ZnO NPs curve to *Danio rerio* are 16.0±0.03 and 15.6±0.3, respectively. For *Daphnia magna* and A549 cells, the intercept of ZnO NPs curve are larger than that of Ag NPs curve, which indicates that ZnO NPs are less toxic than Ag NPs to *Daphnia magna* and A549 cells when the SA/V of particles are similar.

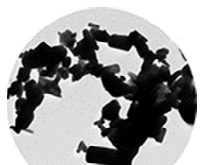

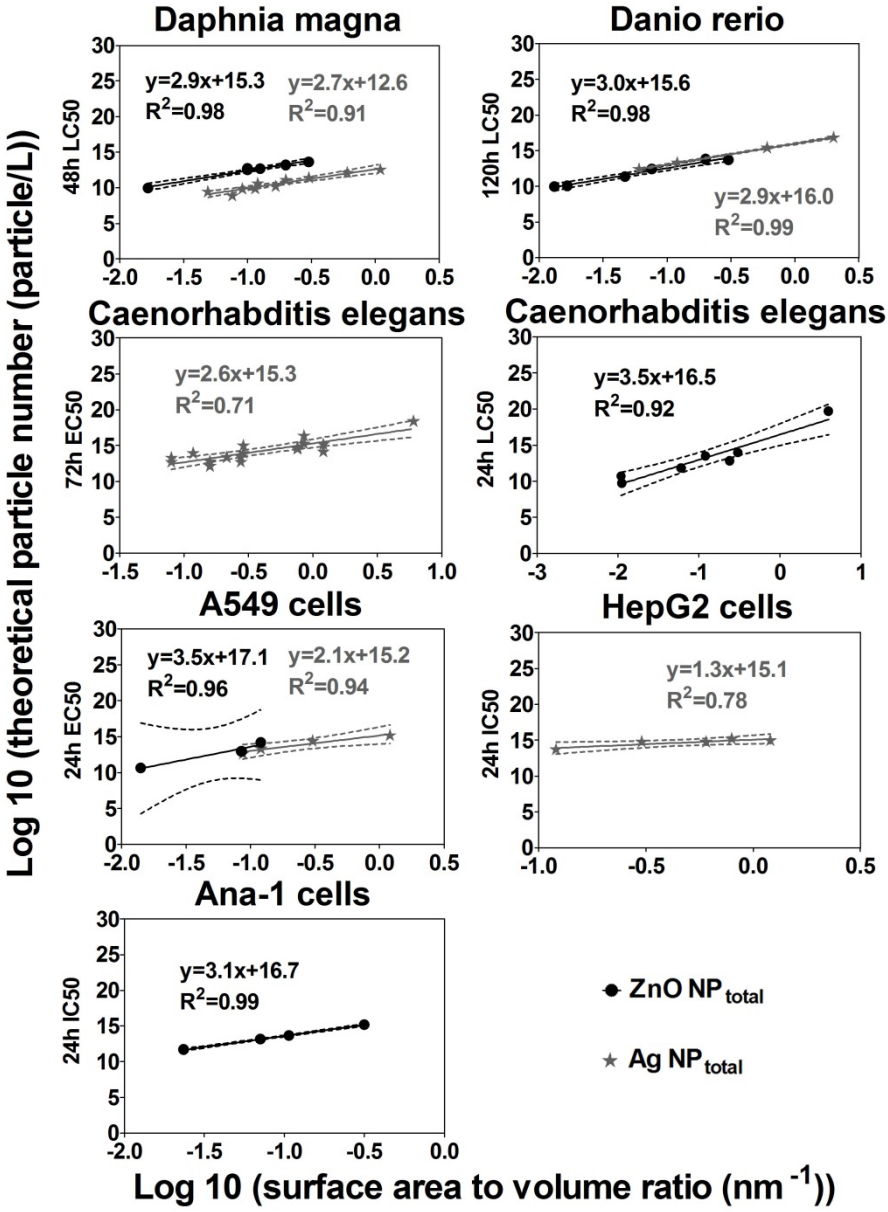

Figure 4.2 Estimated logarithm of $L(E)C_{50}$ values plotted against logarithm of surface area to volume ratio for particle number of Ag NPs (star) and ZnO NPs (dot). The best-fit lines from linear regression analysis are displayed (solid lines) as well as their associated 95% CIs (dashed lines).

Table 4.1 The slope and intercept of the equi-response curve (mean ± SEM) of Ag NPs and ZnO NPs for different species from peer-reviewed papers

Species		Endpoint	Ag NPs			ZnO NPs		
			Slope	Intercept	n	Slope	Intercept	n
Algae	*Pseudokirchneriella subcapitata*	72h IC_{50}				3.5±0.4	14.4±0.3	3[a]
	Pseudokirchneriella subcapitata	4.5h EC_{50}	2.1±1.7	14.9±1.4	3[a]			
Crustaceans	*Daphnia magna*	48h LC_{50}	2.7±0.3	12.6±0.3	11	2.9±0.2	15.3±0.2	6
	Chydorus sphaericus	48h EC_{50}	2.8±0.7	13.0±0.6	3[a]			
	Ceriodaphnia dubia	48h LC_{50}	2.5±1.5	12.8±1.3	3[a]			
Fish	*Danio rerio*	120h LC_{50}	2.9±0.03	16.0±0.03	4	3.0±0.2	15.6±0.3	6
	Oryzias latipes	96h LC_{50}	4.1±1.0	15.0±0.7	3[a]			
	Pimephales promelas	96h LC_{50}	1.8±0.6	13.8±0.5	3[a]			
Nematode	*Caenorhabditis elegans*	72h EC_{50}	2.6±0.4	15.3±0.3	17			
	Caenorhabditis elegans	24h LC_{50}				3.5±0.5	16.5±0.6	7
Mammalian cells	*A549 cells*	24h EC_{50}	2.1±0.4	15.2±0.3	4	3.5±0.7	17.1±1.0	3[a]
	HepG2 cells	24h IC_{50}	1.3±0.4	15.1±0.2	5			
	THP-1 cells	24h IC_{50}	5.9±2.2	18.8±1.8	3[a]			
	MCF-7 cells	24h EC_{50}	1.0±0.3	14.9±0.2	3[a]			
	SGC-7901 cells	24h IC_{50}	0.9±0.5	15.2±0.3	3[a]			
	Ana-1 cells	24h IC_{50}				3.1±0.06	16.7±0.06	4

[a] Higher SEM for slope were due to the limited number of data point (n).

4.4 Discussion

4.4.1 Generic dose calculation method for differently shaped and sized NPs

Nanoparticle properties, such as size, shape, number, surface area, volume, and crystal phase, can impact their toxicity (Alivisatos *et al.*, 1996; Jiang *et al.*, 2008a; Nel *et al.*, 2006; Oberdörster *et al.*, 2005; Rushton *et al.*, 2010). To find an appropriate property as a dose metric of NPs is of utmost importance. Most studies have focused on one type of NPs and one kind of test species. From single experiments, the dosimetry issue cannot be solved. Furthermore, spherical NPs

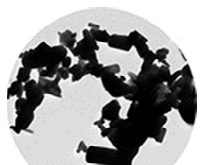

are more often studied than other shapes of NP (Tuttle, 2012; Delmaar *et al.*, 2015). As a result, the validity of conclusions generated from such studies is limited and cannot be generalized to other situations which are different from those studies in terms of types of NPs and / or species involved. In addition, the diversity of NPs studied, tested species and experimental procedures among different studies make it difficult to compare the outcomes of these studies in a consistent manner.

In contrast, our proposed generic dose calculation method can be used to model systematically differently shaped, differently sized and different metal-type NPs exposed to different species. In our study, we covered three kinds of metal-based nanoparticles, namely Cu NPs, ZnO NPs, and Ag NPs. The particle shapes included spheres, rods, sticks, and cubes. Data were obtained for nine species *in vivo* and for 6 types of mammalian cell lines *in vitro*. Hence, the conclusions derived from our method can be extrapolated across different NPs (including non-metallic NPs) and species and might even be applicable in the future to new generations of NPs not yet in production.

4.4.2 The adequate dose descriptor

In Figure 4.1, 21 out of the 24 endpoints of Cu NPs exposed to *Danio rerio*, and 11 out of the 12 endpoints of ZnO NPs, the slopes are around 3. This thus indicates that the volume (or mass) can be considered as an adequate dose descriptor when assessing the toxicity of ZnO NPs and Cu NPs to zebrafish embryos.

Using secondary data (Table 4.1), the S_{curve} are around 3 for all six species tested for ZnO NPs, and four species for Ag NPs. This suggests that volume (or mass) is generally a reliable dose descriptor when assessing the toxicity of ZnO NPs and Ag NPs to those test species (Table 4.1).

Our generic dose calculation results show that the majority of slopes are around 2 or 3 (Figures 4.1, 4.2). This indicates that the surface area is the best dose metric for some species and metal NPs, while for others types of species and metal NPs the volume (or mass) is the best dose metric. The best dose metric are different for different species and different metal NPs. This is in line with the study of Delmaar *et al.* (2015). This can explain why there is no consensus on the appropriate dose

metric from published papers.

4.4.3 Impact of metal ions released from NPs

The S_{curve} for most mammalian cells and *Oryzias latipes* are not close to either 0, 2 or 3. This indicates that among volume (or mass), surface area and number of NPs, none is an adequate dose descriptor when assessing the toxicity of ZnO NPs and Cu NPs to most mammalian cells and *Oryzias latipes*. One possible explanation is that the toxicity reported in the literature is due to the nanoparticle suspension ($NP_{(total)}$) which includes the particle form of NPs ($NP_{(particle)}$) and the released metal ions from NPs ($NP_{(ion)}$) (Hua *et al.*, 2014a, 2014b). The $NP_{(ion)}$ of metal-based NPs may have more severe effects on mammalian cells *in vitro* than on whole organisms *in vivo*. In our proposed method, the toxicity is assumed to be entirely due to the $NP_{(particle)}$ and the used properties (*e.g.* surface area, volume, diameter, number) in all the equations can be used to represent only $NP_{(particle)}$ rather than $NP_{(ion)}$. It is likely that ion release rates depend on both the shape of the NPs, and the experiment conditions. It is therefore unlikely that there is a relationship between ion release rates and a NP-related dose metrics, although surface area would on forehand the most appropriate dose descriptor for ion release. For metal-based NPs, the $NP_{(ion)}$ plays an important role in inducing acute or chronic toxicity of NPs to aquatic organisms (Nel *et al.*, 2013; Zhu *et al.*, 2013). Differently shaped and sized metal-based NPs release different concentrations of $NP_{(ion)}$ (Supplemental data 4.2) and thus the toxic contribution of $NP_{(ion)}$ to $NP_{(total)}$ will be different accordingly. If the toxicity of $NP_{(ion)}$ can be ruled out and we can only consider the toxicity of $NP_{(particle)}$, the S_{curve} are expected to change and subsequently the generic dose calculation method has the capability to find the appropriate dose metric. For instance, in our generic dose calculation results, the S_{curve} of $NP_{(particle)}$ are generally smaller than those of $NP_{(ion)}$ to hatching delay of zebrafish embryos when exposed to Cu and ZnO NPs (Figure 4.1, Supplemental data 4.7). Therefore, more studies should focus on the separation of the toxicity of $NP_{(total)}$ and report specifically the toxicity of $NP_{(particle)}$, which will facilitate more accurate modeling.

4.4.4 Impact of coating and experiments conditions

Another reason for the observation that S_{curve} do not converge to 0, 2 or 3 could be

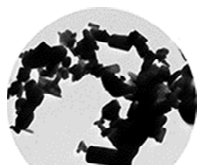

because the published studies were different in one or all of the following aspects: 1) tested NPs contain different coating *e.g.* PVP-coated, citrate-coated (Kashiwada *et al.*, 2012; Kennedy *et al.*, 2012; Yang *et al.*, 2012); 2) tested media are different, *e.g.* some studies used K^+ media (Yang *et al.*, 2012), while some others used standard media; 3) the different procedures in preparing the NPs suspensions (with or without dispersant, with or without sonicated, *etc*.). All these three factors, amongst various others, affect the experimental response results. For example, all three particles types considered in our study can undergo substantial dissolution/transformation reactions depending on the experimental conditions and the composition of the exposure media. Ag NPs will oxidize in the presence of free oxygen and subsequently Ag ions will be released into the experimental media (Xiu *et al.*, 2012). If Cl^- is present, then poorly soluble AgCl precipitates will immediately form, in turn mitigating the toxicity of the Ag NPs. However in the absence of Cl^-, Ag^+ will develop its full toxic potential, which will eventually be assigned to the Ag NPs (Xiu *et al.*, 2012).

Our studies were performed in the same system: 1) all NPs were uncoated; 2) egg water was used as the test medium in all cases; 3) the same procedure was used for preparation of all NPs suspensions. This could explain why most R^2-values of the equi-response curve are above 0.9 (Figure 4.1).

4.4.5 Impact of aggregate and agglomerates of NPs

For those slopes being between 2 and 3, other properties may also affect the toxic of NPs other than volume (or mass), surface area, and number. One of the properties may be the tendency of NPs to aggregate. The aggregated NPs could affect not only the toxicity of NPs but also change their effective total surface area (Buzea *et al.*, 2007; Zhu *et al.*, 2009). With respect to toxicity, aggregation of nanoparticles in water is an important factor, due to the more effective macrophage clearance for larger particles compared to smaller ones (Buzea *et al.*, 2007; Zhu *et al.*, 2009). In addition, the aggregation of NPs could change the total surface area in real experimental situations. For example, when two nanoparticles are aggregated, then the total surface area will be less than the sum of surface area of two single particles. Therefore, in the case of NPs with the same volume, NPs forming larger aggregates have a smaller total surface than NPs that form smaller aggregates. Moreover,

smaller aggregates of NPs have a larger contact area with the test species and therefore more toxic than larger aggregates of NPs. However, the total volume (the sum of the volume of all single pristine NPs) of aggregated NPs can be similar to that of non-aggregated NPs. Taken together, the aggregation will eventually change the SA/V value. It should be noted that the degree of aggregation is difficult to quantify and generally not reported in the literature, and thus the aggregation was not considered in our modeling method; the total surface area is simply computed as the number of particles multiplied with the surface area of all single pristine nanoparticles.

In the case of agglomerates of NPs, since their contact points are relatively small (Simko *et al.*, 2014), the total surface area and total volume can therefore be considered unchanged.

4.4.6 Impact of chemical composition of NPs

It is worth noting that all the S_{curve} of different NPs to *Danio rerio* are around 3 using both our experimental data (Figure 4.1) and other published data (Figure 4.2). This indicates that the volume (or mass) of the particles is the best dose metric for *Danio rerio* at least in the case of Ag, Cu and ZnO NPs. For A549 cells, our modeling results for Ag NPs (slopes are around 2) show that the surface area is best dose metric in this case. This is consistent with Rushton *et al.* (2010), who exposed TiO_2 to A549 cells and found that surface area is the best dose metric. However, our modeling results of ZnO NPs for A549 cells (slopes are close to 3) suggest that the best dose metric is volume (or mass). The difference in the identified best dose metric for the same A549 cells when exposed to different metal NPs indicates that the best dose metric is related to types of metal NPs. The possible reason may be due to the mode of action of different metal NPs, their interaction with released metal ions, and with other metal complexes in the aquatic medium. But the exact reasons are still unclear and should be investigated in future studies. Taken together, the best dose metric is species-dependent and, in some cases, metal-NPs dependent, and thus should be determined separately and specifically for a given studied species and metal NPs.

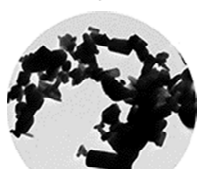

4.4.7 Limitation of database from literature survey

During our literature survey, we attempted to collect published data that related to the same test species, the same test duration and the same endpoint; we then merged the data. However, despite a huge number of studies investigating the toxicity of metal-based NPs, the above mentioned ideal attempt was not achieved. Note, the wider range of 95% CIs can be observed for cases with only three data points (Supplemental data 4.8). Therefore, a sufficient number (greater than 3) of data points is needed for a more accurate modeling. We found that endpoints and/or time durations reported in the separate published papers are often not consistent and incomparable for some cases. For example, some studies reported 28 h IC_{50} of Ag NPs to HepG2 cells (Kim *et al.*, 2009) and 4 h LC_{50} of ZnO NPs to *Caenorhabditis* elegans (Ma *et al.*, 2009), which were quite unique compared the common 24 h IC_{50} to HepG2 cells and 24 h LC_{50} to *Caenorhabditis elegans*. This inconsistency among papers makes their corresponding results incomparable, and it in turn is difficult to merge isolated results to form a large data group for generalization and modeling.

4.5 Conclusions

We developed a dose calculation method to assess the best dose metrics of metal-based NPs. We find that this method is suitable for NPs of a range of shapes and sizes, and also for analyzing the results of NP toxicity in a range of test species. The volume (or mass) of NPs is the appropriate dose metric for all six species for ZnO NPs, and for four out of 12 species for Ag NPs, especially for species of crustaceans, fish and nematode. For three out of 12 species for Ag NPs, the surface area is the best dose metric. Other properties than volume (or mass), surface area of NPs may also affect the toxic of NPs, such as released ions and aggregation. Taken together, the best generic dose metric is species-dependent and, in some cases, metal-NPs dependent.

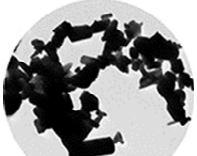

Supplemental data

Supplemental data 4.1 Nanoparticles properties and toxicity to zebrafish embryos

The Cu and ZnO nanoparticles data sets were obtained from our previous studies (Hua *et al.*, 2014a, 2014b). We also newly tested various Cu and ZnO nanoparticles in the same experimental system (Hua *et al.*, 2014a, 2014b).

In our previous studies, we assumed that the total NP suspensions ($NP_{(total)}$) were mixtures containing both the particle form of NPs ($NP_{(particle)}$) and metal ions released from the NPs ($NP_{(ion)}$). For that reason the toxicity was calculated using addition models to separate the $NP_{(particle)}$ effect from the effect of $NP_{(total)}$ (Hua *et al.*, 2014a, 2014b). The toxicity of $NP_{(particle)}$ and $NP_{(total)}$ to zebrafish embryos, the lethal concentration (LC_{20}, LC_{50}, and LC_{80}) values and the effect concentrations (EC_{20}, EC_{50}, and EC_{80}) of hatching inhibition are shown in the Supplementary data 2. The physicochemical properties of the particles and TEM images of NPs are presented in the Supplementary data 2 and 3, respectively. The parameters of the differently shaped NPs used in the calculations, are shown in Supplementary data 5. The mean primary diameter and the mean primary length of NPs are based on TEM measurements (only the clearly visible NPs shown in TEM images are considered).

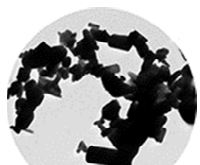

Supplemental data 4.2 Particles characterization and the 120 h LC_X values and EC_X of hatching inhibition of NPs to zebrafish embryos

Particle	Average size[a]	Shape using TEM	Size variation using TEM[b]	Concentration (mg/L)		LC_X of $NP_{(total)}$			LC_X of $NP_{(particle)}$			EC_X of $NP_{(total)}$			EC_X of $NP_{(particle)}$		
				$NP_{(total)}$	$NP_{(ion)}$	LC_{20}	LC_{50}	LC_{80}	LC_{20}	LC_{50}	LC_{80}	EC_{20}	EC_{50}	EC_{80}	EC_{20}	EC_{50}	EC_{80}
Cu25	25	spheres	26 nm (12-184 nm)	0.9	0.4	0.7	1.0	1.6	0.3	0.6	1.1	0.1	0.3	0.5	0.03	0.09	0.2
				7.4	0.8												
Cu50	50	spheres	53 nm (38-65 nm)	1.0	0.2	1.3	2.0	3.1	1.0	1.7	2.6	0.3	0.5	0.9	0.2	0.4	0.9
				7.6	0.6												
Cu78	78	rods	W: 29 nm (16-46 nm) L: 83 nm (56-128 nm)	1.0	0.3	0.8	2.5	7.4	0.6	2.6	10.7	0.01	0.07	0.4	0.01	0.06	0.4
				8.3	0.8												
Cu100	100	spheres	128 nm (84-363 nm)	0.9	0.2	1.8	2.3	3.1	1.4	1.9	2.6	0.1	0.3	1.0	0.08	0.3	1.0
				7.9	0.8												
Cu400	400	spheres	408 nm (167-849 nm)	0.4	0.1	0.4	0.6	0.8	0.3	0.4	0.5	0.1	0.2	0.2	0.2	0.2	0.2
				3.6	0.8												
ZnO18	18	spheres	21 nm (10-52 nm)	4.5	2.2	9.5	12.7	16.9	12.4	14.7	17.5	.3.1	6.5	13.8	10.3	19.0	35.0
				36.3	3.7												
ZnO43	43	spheres	27 nm (11-51 nm)	4.2	1.1	10.3	14.8	21.2	12.7	20.3	32.5	0.2	1.0	5.0	0.07	1.2	19.0
				33.2	3.5												
ZnO150	150	sticks	W: 32 nm (11-78 nm) L: 81 nm (27-157 nm)	3.6	1.2	6.5	8.9	12.2	6.3	10.5	17.4	0.00	0.05	0.9	0.00	0.07	1.5
				31.7	2.8												
ZnO200	200	cuboid	298 nm (52-1053 nm)	4.9	1.6	10.8	15.4	21.9	12.9	25.0	48.4	2.6	5.5	11.8	8.9	22.1	54.6
				39.3	3.8												
ZnO900	900	cuboid	202 nm (47-571 nm)	4.0	1.2	9.7	12.4	15.9	9.4	12.1	15.5	0.4	1.5	6.0	0.4	2.4	13.5
				30.6	1.8												

[a] According to the manufacturer information. [b] W: width; L:length. [c] Measured by AAS.

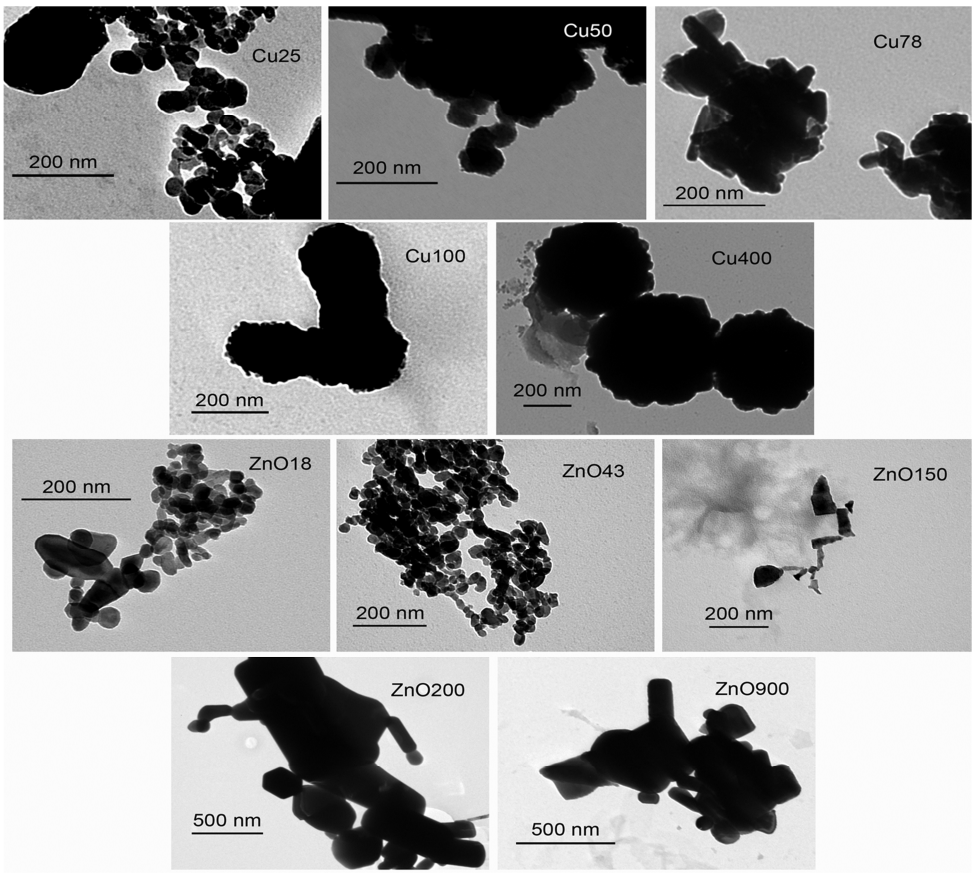

Supplemental data 4.3 The primary sizes and shapes were estimated by transmission electron microscopy (TEM). TEM images of Cu NPs and ZnO NPs in egg water at 1 h of incubation. Pictures were taken with a JEOL 1010 TEM at 70 kV.

Supplemental data 4.4 Modified dose-response curve modeling

A dose-response curve is an X-Y graph relating the magnitude of a stressor to the response of the receptor. The measured dose (usually in mass concentration) is generally plotted on the X axis and the response is plotted on the Y axis. Oberdörster *et al.* (2005) converted the mass concentration of NPs to surface area concentration of NPs on the X axis. The modified dose-response curve modeling method of Oberdörster *et al.* (2005) was applied and compared with our modeling method to evaluate the consistency of both modeling approaches. In our study,

different doses expressions (volume or mass concentration, surface area concentration, and number concentration of NPs) were plotted against the lethal concentration of zebrafish embryos. This is used to compare this approach with the outcome of the modeling methods mentioned in Section 4.2.2 in the text, enabling us to evaluate the consistency and robustness of both modeling approaches. $NP_{(particle)}$ was selected in our experimental dataset of zebrafish embryos to evaluate our proposed method. We thus ruled out the toxicity of $NP_{(ion)}$.

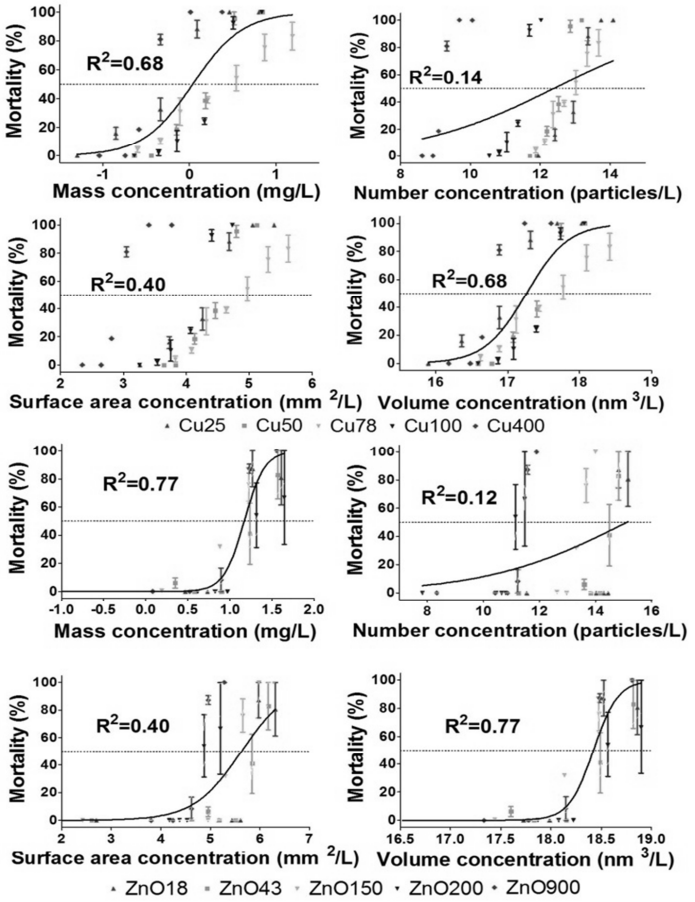

Figure S4.4 Mortality of zebrafish embryos exposed to 25, 50, 78, 100 and 400 nm Cu $NP_{(particle)}$ and 18, 43, 150, 200 and 900 nm ZnO $NP_{(particle)}$ plotted against different dose expressions (volume or mass concentration, surface area concentration, and number concentration of NPs) with the same dose response relationship.

The modified dose response curves of lethality of $NP_{(particle)}$ to zebrafish embryos are shown in Figure S4.4. The R^2-values in case of using the volume (or mass) dose metric are 0.68 and 0.77 for Cu NPs and ZnO NPs, respectively. The R^2-values of the other dose metrics are much lower, ranging from 0.12 to 0.40. Therefore, the particle volume (or mass) appears to be a more appropriate dose metric for comparing effects of different sized and shaped nano- and sub-micron particles to zebrafish embryos than surface area and number of NPs. Using the dose-response curve modeling method by Oberdörster *et al.* (2005) resulted in the same conclusion with that by our generic dose calculation method. Thus, this supports the validity of our proposed modeling method and our results of modeling.

Supplemental data 4.5 The parameters of differently shaped NPs used to calculating their mean primary particle surface area and mean primary particle volume.

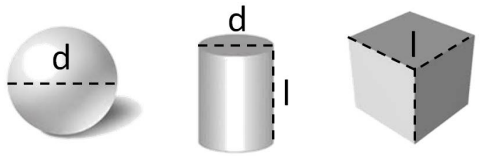

For easier calculation of the SA and V of differently shaped and sized NPs, we assumed that the shape and size are uniform with the same mean primary parameters in each type of NPs suspension. For nanospheres, we used the mean primary particle diameter (d) to calculate the SA and V; for nanosticks or nanorods, there are two parameters to calculate the SA and V: the mean primary particle diameter of the shorter aspect (d) and the mean primary particle length of the longer aspect (l); in the case of cuboidal particles the mean primary particle length (l) to calculate the SA and V. For nanospheres: $4*\pi*(d/2)^2$ is the surface area of NPs where d is the mean primary particle diameter measured by for instance TEM (Supplementary data 2 and 3), and $4/3*\pi*(d/2)^3$ is the volume of a uniform sphere, the SA/V is $6/d$; for nanosticks or nanorods: $2*\pi*(d/2)^2+\pi*d*l$ is surface area of NPs where d is the mean primary particle diameter measured by for instance TEM, l is the mean primary particle length measured by TEM (Supplementary data 2 and 3), $\pi*(d/2)^2*l$ is the volume of NPs, the SA/V is $4/d+2/l$; for cuboidal particles: $6*l^2$ is surface area of NPs where l is the mean primary particle length measured by TEM (Supplementary data 2 and 3), l^3 is the volume of particles, the SA/V is $6/l$.

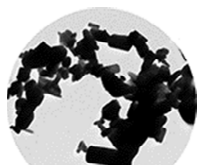

Supplemental data 4.6 Database from literature survey. A comprehensive dataset of diverse specifies and different nanoparticles have been constructed by collecting published data from literature.

NPs	Species	Shape	Diameter (nm)	Length (nm)	area (SA) (nm^2/parti	(V) (nm^3/parti	SA/V (nm^{-1})	Endpoint	L(E)C_{50} in literature	L(E)C_{50}(mg compound/L)	L(E)C_{50}number (particls/L)	Log SA/V	Log L(E)C_{50} number	Reference
Algae														
Ag	*Pseudokirchneriella subcapitata*	spheres	35		3848.45	22449.30	0.17	4.5h EC50	196.55uM	21.21	9.01E+13	-0.77	13.95	Wang *et al.*, 2012
Ag	*Pseudokirchneriella subcapitata*	spheres	80		20106.19	268082.57	0.08	4.5h EC50	37.14uM	4.01	1.43E+12	-1.12	12.15	Wang *et al.*, 2012
Ag	*Pseudokirchneriella subcapitata*	spheres	15		706.86	1767.15	0.40	4.5h EC50	8.31uM	0.9	4.86E+13	-0.40	13.69	Wang *et al.*, 2012
Ag	*Pseudokirchneriella subcapitata*	spheres	27		222.87	9854.70	0.23	96h LC50		0.19	1.84E+12	-0.65	12.26	Griffitt *et al.*, 2008
Ag	*Pseudokirchneriella subcapitata*	spheres	25		2026.83	8580.25	0.24	96h LC50		0.023	2.56E+11	-0.63	11.41	McLaughlin & Bonzongo, 2011
ZnO	*Pseudokirchneriella subcapitata*	spheres	60		11309.73	113097.34	0.10	72h IC50	0.042mg Zn/L	0.052	8.20E+10	-1.00	10.91	Aruoja *et al.*, 2009
ZnO	*Pseudokirchneriella subcapitata*	spheres	30		2827.43	14137.17	0.20	72h IC50	68 ug ZN/L	0.085	1.07E+12	-0.70	12.03	Franklin *et al.*, 2007
ZnO	*Pseudokirchneriella subcapitata*	spheres	30		2827.43	14137.17	0.20	72h IC50	49 ug Zn/L	0.061	7.70E+11	-0.70	11.89	Franklin *et al.*, 2007
Crustaceans														
Ag	*Daphnia magna*	spheres	124		48227.25	995892.68	0.05	48h LC50	28.7ug/L	0.029	2.78E+09	-1.31	9.44	Zhao & Wang, 2012
Ag	*Daphnia magna*	spheres	80		19955.68	265077.94	0.08	48h LC50	2.0ug/L	0.002	7.19E+08	-1.12	8.86	Zhao & Wang, 2012
Ag	*Daphnia magna*	spheres	65		13396.03	145793.50	0.09	48h LC50	1.1ug/L	0.011	7.19E+09	-1.04	9.86	Zhao & Wang, 2012
Ag	*Daphnia magna*	spheres	10		314.16	523.60	0.60	48h LC50	6.955ug/L	0.007	1.27E+12	-0.22	12.11	Hoheisel *et al.*, 2012
Ag	*Daphnia maena*	spheres	20		1256.64	4188.79	0.30	48h LC50	10.81ug/L	0.011	2.50E+11	-0.52	11.40	Hoheisel *et al.*. 2012
Ag	*Daphnia magna*	spheres	30		2827.43	14137.17	0.20	48h LC50	18ug/L	0.018	1.21E+11	-0.70	11.08	Hoheisel *et al.* 2012

NPs	Species	Shape	Diameter (nm)	Length (nm)	area (SA) (nm^2/parti	(V) (nm^3/parti	SA/V (nm^{-1})	Endpoint	L(E)C_{50} in literature	L(E)C_{50}(mg compound/L)	L(E)C_{50}number (particle/L)	Log SA/V	Log L(E)C_{50} number	Reference
Ag	*Daphnia magna*	spheres	50		7853.98	65449.85	0.12	48h LC50	27.43ug/L	0.027	3.93E+10	-0.92	10.59	Hoheisel *et al.*, 2012
Ag	*Daphnia magna*	spheres	36		4071.50	24429.02	0.17	48h LC50	4ug/L	0.004	1.56E+10	-0.78	10.19	Li *et al.*, 2010
Ag	*Daphnia magna*	spheres	52		8494.87	73622.18	0.12	48h LC50	6ug/L	0.006	7.77E+09	-0.94	9.89	Li *et al.*, 2010
Ag	*Daphnia magna*	spheres	66		13684.78	150532.55	0.09	48h LC50	10ug/L	0.01	6.33E+09	-1.04	9.80	Li *et al.*, 2010
Ag	*Daphnia magna*	spheres	5.5		95.03	87.11	1.09	48h LC50	2.75ug/L	0.003	3.28E+12	0.04	12.52	Das *et al.*, 2013
Ag	*Chydorus sphaericus*	spheres	35		3848.45	22449.30	0.17	48h EC50	0.28uM	0.03	1.27E+11	-0.77	11.11	Wang *et al.*, 2012
Ag	*Chydorus sphaericus*	spheres	80		20106.19	268082.57	0.08	48h EC50	0.12uM	0.013	4.62E+09	-1.12	9.66	Wang *et al.*, 2012
Ag	*Chydorus sphaericus*	spheres	15		706.86	1767.15	0.40	48h EC50	0.08uM	0.009	4.86E+11	-0.40	11.69	Wang *et al.*, 2012
Ag	*Ceriodaphnia dubia*	spheres	21		1385.44	4849.05	0.29	48h LC50	4.8ug/L	0.005	9.83E+10	-0.54	10.99	Kennedy *et al.*, 2012
Ag	*Ceriodaphnia dubia*	spheres	102		32685.13	555647.21	0.06	48h LC50	26.7ug/L	0.027	4.63E+09	-1.23	9.67	Kennedy *et al.*, 2012
Ag	*Ceriodaphnia dubia*	spheres	27		2222.87	9854.70	0.23	48h LC50		0.067	6.48E+11	-0.65	11.81	Griffitt *et al.*, 2008
ZnO	*Daphnia magna*		60		11309.73	113097.34	0.10	48h LC50		3.2	5.05E+12	-1.00	12.70	Heinlaan *et al.*, 2008
ZnO	*Daphnia magna*	strips	20	20	1884.96	6283.19	0.30	48h LC50		1.511	4.29E+13	-0.52	13.63	Zhu *et al.*, 2009
ZnO	*Daphnia magna*	spheres	358		402639.08	24024131.82	0.02	48h LC50		1.25	9.28E+09	-1.78	9.97	Zhu *et al.*, 2009
ZnO	*Daphnia magna*	spheres	48		7238.23	57905.84	0.13	48h LC50		1.48	4.56E+12	-0.90	12.66	Zhao *et al.*, 2012
ZnO	*Daphnia magna*		60		11309.73	113097.34	0.10	48h LC50		2.1	3.31E+12	-1.00	12.52	Naddafi *et al.* 2011
ZnO	*Daphnia magna*	spheres	30		2827.43	14137.17	0.20	48h LC50	1.02mg Zn/L	1.26	1.59E+13	-0.70	13.20	Lopes *et al.* 2014

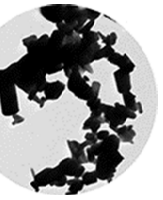

NPs	Species	Shape	Diameter (nm)	Length (nm)	area (SA) (nm^2/parti	(V) (nm^3/parti	SA/V (nm^{-1})	Endpoint	L(E)C_{50} in literature	L(E)C_{50}(mg compound/L)	L(E)C_{50}number (particls/L)	Log SA/V	Log L(E)C_{50} number	Reference
Fish														
Ag	*Danio rerio*	spheres	6		113.10	113.10	1.00	120h LC50	93.31uM	10.07	8.49E+15	0.00	15.93	Bar-Ilan *et al.*, 2009
Ag	*Danio rerio*	spheres	15		706.86	1767.15	0.40	120h LC50	125.66uM	13.56	7.31E+14	-0.40	14.86	Bar-Ilan *et al.*, 2009
Ag	*Danio rerio*	spheres	51		8171.28	69455.90	0.12	120h LC50	126.96uM	13.7	1.88E+13	-0.93	13.27	Bar-Ilan *et al.*, 2009
Ag	*Danio rerio*	spheres	109		37325.26	678075.60	0.06	120h LC50	137.26uM	14.81	2.08E+12	-1.26	12.32	Bar-Ilan *et al.*, 2009
Ag	*Oryzias latipes*	spheres	3.6		40.72	24.43	1.67	96h LC50		1.39	5.42E+15	0.22	15.73	Kashiwada *et al.*, 2012
Ag	*Oryzias latipes*	spheres	30		2808.62	13996.27	0.20	96h LC50		0.87	5.93E+12	-0.70	12.77	Wu & Zhou, 2013
Ag	*Oryzias latipes*	spheres	50		7728.82	63891.58	0.12	96h LC50		0.035	5.22E+10	-0.92	10.72	Chae *et al.*, 2009
Ag	*Pimephales spromelas*	spheres	10		314.16	523.60	0.60	96h LC50	89.4ug/L	0.089	1.62E+13	-0.22	13.21	Hoheisel *et al.*, 2012
Ag	*Pimephales spromelas*	spheres	35		3848.45	22449.30	0.17	96h LC50		9.4	3.99E+13	-0.77	13.60	Laban *et al.*, 2010
Ag	*Pimephales spromelas*	spheres	100		31415.93	523598.78	0.06	96h LC50		10.6	1.93E+12	-1.22	12.29	Laban *et al.*, 2010
ZnO	*Danio rerio*	strips	20	20	1884.96	6283.19	0.30	96h LC50		1.793	5.09E+13	-0.52	13.71	Zhu *et al.*, 2008
ZnO	*Danio rerio*	spheres	358		402639.08	24024131.82	0.02	96h LC50		1.55	1.15E+10	-1.78	10.06	Zhu *et al.*, 2008
ZnO	*Danio rerio*	spheres	80		20106.19	268082.57	0.08	96h LC50		3.969	2.64E+12	-1.12	12.42	Yu *et al.*, 2011
ZnO	*Danio rerio*	spheres	454		647532.51	48996626.69	0.01	96h LC50		2.525	9.19E+09	-1.88	9.96	Yu *et al.*, 2011
ZnO	*Danio rerio*	spheres	30		2827.43	14137.17	0.20	96h LC50		4.92	6.21E+13	-0.70	13.79	Xiong *et al.*, 2011
ZnO	*Danio rerio*	rods	100	300	109955.74	235619449	0.05	96h LC50		3.31	2.51E+11	-1.33	11.40	Xiong *et al.*, 2011

NPs	Species	Shape	Diameter (nm)	Length (nm)	area (SA) (nm^2/parti	(V) (nm^3/parti	SA/V (nm^{-1})	Endpoint	L(E)C_{50} in literature	L(E)C_{50}(mg compound/L)	L(E)C_{50}number (particls/L)	Log SA/V	Log L(E)C_{50} number	Reference
Nematode														
Ag	*Caenorhabditis elegans*	spheres	1		3.14	0.52	6.00	72h EC50		13.4	2.44E+18	0.78	18.39	Ellegaard-Jensen *et al.* 2012
Ag	*Caenorhabditis elegans*	spheres	28		2463.01	11494.04	0.21	72h EC50		2.8	2.32E+13	-0.67	13.37	Ellegaard-Jensen *et al.* 2012
Ag	*Caenorhabditis elegans*	spheres	51		8043.61	67834.43	0.12	72h EC50		55	7.73E+13	-0.93	13.89	Kim *et al.*, 2001
Ag	*Caenorhabditis elegans*	spheres	8		201.06	268.08	0.75	72h EC50	0.9 ppm	0.9	3.20E+14	-0.12	14.51	Yang *et al.*, 2012
Ag	*Caenorhabditis elegans*	spheres	38		4536.46	28730.91	0.16	72h EC50	0.4 pmm	0.4	1.33E+12	-0.80	12.12	Yang *et al.*, 2012
Ag	*Caenorhabditis elegans*	spheres	21		1385.44	4849.05	0.29	72h EC50	4.3 ppm	4.3	8.45E+13	-0.54	13.93	Yang *et al.*, 2012
Ag	*Caenorhabditis elegans*	spheres	75		17671.46	220893.23	0.08	72h EC50	11.7 ppm	11.7	5.05E+12	-1.10	12.70	Yang *et al.*, 2012
Ag	*Caenorhabditis elegans*	spheres	7		153.94	179.59	0.86	72h EC50	3.3 ppm	3.3	1.75E+15	-0.07	15.24	Yang *et al.*, 2012
Ag	*Caenorhabditis elegans*	spheres	5		78.54	65.45	1.20	72h EC50	0.09 ppm	0.09	1.31E+14	0.08	14.12	Yang *et al.*, 2012
Ag	*Caenorhabditis elegans*	spheres	22		1520.53	5575.28	0.27	72h EC50	0.3 ppm	0.3	5.13E+12	-0.56	12.71	Yang *et al.*, 2012
Ag	*Caenorhabditis elegans*	spheres	8		201.06	268.08	0.75	72h EC50	1.4 ppm	1.4	4.98E+14	-0.12	14.70	Yang *et al.*, 2012
Ag	*Caenorhabditis elegans*	spheres	38		4536.46	28730.91	0.16	72h EC50	1.8 ppm	1.8	5.97E+12	-0.80	12.78	Yang *et al.*, 2012
Ag	*Caenorhabditis elegans*	spheres	21		1385.44	4849.05	0.29	72h EC50	50 ppm	50	9.83E+14	-0.54	14.99	Yang *et al.*, 2012
Ag	*Caenorhabditis elegans*	spheres	75		17671.46	220893.23	0.08	72h EC50	45 ppm	45	1.94E+13	-1.10	13.29	Yang *et al.*, 2012
Ag	*Caenorhabditis elegans*	spheres	7		153.94	179.59	0.86	72h EC50	40 ppm	40	2.12E+16	-0.07	16.33	Yang *et al.*, 2012
Ag	*Caenorhabditis elegans*	spheres	5		78.54	65.45	1.20	72h EC50	0.9 ppm	0.9	1.31E+15	0.08	15.12	Yang *et al.*, 2012

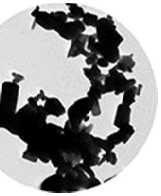

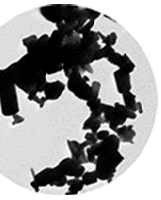

NPs	Species	Shape	Diameter (nm)	Length (nm)	area (SA) (nm^2/parti	(V) (nm^3/parti	SA/V (nm^{-1})	Endpoint	L(E)C_{50} in literature	L(E)C_{50}(mg compound/L)	L(E)C_{50}number (particls/L)	Log SA/V	Log L(E)C_{50} number	Reference
Ag	*Caenorhabditis elegans*	spheres	22		1520.53	5575.28	0.27	72h EC50	1.5 ppm	1.5	2.56E+13	-0.56	13.41	Yang *et al.*, 2012
ZnO	*Caenorhabditis elegans*	cuboids	550		1815000.00	166375000.00	0.01	24h LC50	38mg Zn/L	47	5.04E+10	-1.96	10.70	Ma *et al.*, 2011
ZnO	*Caenorhabditis elegans*	rods	40	100	15079.64	125663.71	0.12	24h LC50	17mg Zn/L	21	2.98E+13	-0.92	13.47	Ma *et al.*, 2011
ZnO	*Caenorhabditis elegans*	spheres	1.5		13.5	3.38	4.00	24h LC50	789mg Zn/L	982	5.19E+19	0.60	19.72	Ma *et al.*, 2011
ZnO	*Caenorhabditis elegans*	spheres	532		889146.12	788376 22.57	0.01	24h LC50		2.3	5.20E+09	-1.95	9.72	Wang *et al.*, 2009
ZnO	*Caenorhabditis elegans*	spheres	20		1256.64	4188.79	0.30	24h LC50		2.2	9.37E+13	-0.52	13.97	Wang *et al.*, 2009
ZnO	*Caenorhabditis elegans*	spheres	25		1963.50	8181.23	0.24	24h LC50		0.32	6.98E+12	-0.62	12.84	Khare *et al.*, 2011
ZnO	*Caenorhabditis elegans*	spheres	100		31415.93	523598.78	0.06	24h LC50		2	6.81E+11	-1.22	11.83	Khare *et al.*, 2011
Mammalian cells														
Ag	A549 cells	spheres	5		78.54	64.45	1.20	24h EC50	1.02ug/mL	1.02	1.49E+15	0.08	15.17	Liu *et al.*, 2010
Ag	A549 cells	spheres	20		1256.64	4188.79	0.30	24h EC50	9.96ug/mL	9.96	2.27E+14	-0.52	14.36	Liu *et al.*, 2010
Ag	A549 cells	spheres	50		7853.98	65449.85	0.12	24h EC50	14.31ug/mL	14.31	2.08E+13	-0.92	13.32	Liu *et al.*, 2010
Ag	A549 cells	spheres	69		14957.12	172006.91	0.09	24h EC50	7.50ug/mL	7.5	4.16E+12	-1.06	12.62	Foldbjerg *et al.*, 2011
Ag	HepG2 cells	spheres	10		314.16	523.60	0.60	24h IC50	2.9ug/mL	2.9	5.28E+14	-0.22	14.72	Nowrouzi *et al.* 2010
Ag	HepG2 cells	spheres	7.5		176.71	220.89	0.80	28h IC50	3.38ug/mL	3.38	1.46E+15	-0.10	15.16	Kim *et al.*, 2009
Ag	HepG2 cells	spheres	5		78.54	64.45	1.20	24h EC50	0.59ug/mL	0.59	8.59E+14	0.08	14.93	Liu *et al.*, 2010
Ag	HepG2 cells	spheres	20		1256.64	4188.79	0.30	24h EC50	25.35ug/mL	25.35	5.77E+14	-0.52	14.76	Liu *et al.*, 2010

NPs	Species	Shape	Diameter (nm)	Length (nm)	area (SA) (nm^2/parti	(V) (nm^3/parti	SA/V (nm^{-1})	Endpoint	L(E)C_{50} in literature	L(E)C_{50}(mg compound/L)	L(E)C_{50}number (particles/L)	Log SA/V	Log L(E)C_{50} number	Reference
Ag	HepG2 cells	spheres	50		7853.98	65449.85	0.12	24h EC50	33.57ug /mL	33.57	4.89E+13	-0.92	13.69	Liu *et al.*, 2010
Ag	THP-1 cells	spheres	20		1256.64	4188.79	0.30	24h IC50	110 ug/mL	110	2.50E+15	-0.52	15.40	Haase *et al.*, 2012
Ag	THP-1 cells	spheres	40		5026.55	33510.32	0.15	24h IC50	140 ug/mL	140	3.98E+14	-0.82	14.60	Haase *et al.*, 2012
Ag	THP-1 cells	spheres	69		14957.12	172006.91	0.09	24h IC50	2.44 ug/mL	2.44	1.35E+12	-1.06	12.13	Foldbjerg *et al.*, 2009
Ag	MCF-7 cells	spheres	5		78.54	65.45	1.20	24h EC50	0.51 ug/mL	0.51	7.43E+14	0.08	14.87	Liu *et al.*, 2010
Ag	MCF-7 cells	spheres	20		1256.64	4188.79	0.30	24h EC50	14.33 ug/mL	14.33	3.26E+14	-0.52	14.51	Liu *et al.*, 2010
Ag	MCF-7 cells	spheres	50		7853.98	65449.85	0.12	24h EC50	47.64 ug/mL	47.64	6.94E+13	-0.92	13.84	Liu *et al.*, 2010
Ag	SGC-7901 cells	spheres	5		78.54	65.45	1.20	24h EC50	0.92 ug/mL	0.92	1.34E+15	0.08	15.13	Liu *et al.*, 2010
Ag	SGC-7901 cells	spheres	20		1256.64	4188.79	0.30	24h EC50	50.94 ug/mL	50.94	1.16^{E}+15	-0.52	15.06	Liu *et al.*, 2010
Ag	SGC-7901 cells	spheres	50		7853.98	65449.85	0.12	24h EC50	112.03ug/mL	112.03	1.63E+14	-0.92	14.21	Liu *et al.*, 2010
ZnO	A549 cells	rods	70	70	23090.71	269391.57	0.09	24h IC50	13.6 ug/mL	13.6	9.01E+12	-1.07	12.95	Lin *et al.*, 2009
ZnO	A549 cells	rods	420	420	831265.42	58188579.13	0.01	24h IC50	14.2 ug/mL	14.2	4.36E+10	-1.85	10.64	Lin *et al.*, 2009
ZnO	A549 cells	spheres	50		7853.98	65449.85	0.12	24h IC50	55 ug/mL	55	1.50E+14	-0.92	14.18	Seiffert *et al.*, 2011
ZnO	Ana-1 cells	rods	342	173	369602.09	15892352.77	0.02	24h IC50	44.56 ug/mL	44.56	5.00E+11	-1.63	11.70	Song *et al.*, 2010
ZnO	Ana-1 cells	rods	108	60	38679.29	549653.05	0.07	24h IC50	43.94 ug/mL	43.94	1.43E+13	-1.15	13.15	Song *et al.*, 2010
ZnO	Ana-1 cells	rods	71	40	16840.51	158367.69	0.11	24h IC50	40.41	40.41	4.55E+13	-0.97	13.66	Song *et al.*, 2010
ZnO	Ana-1 cells	spheres	19		1134.11	3591.36	0.32	24h IC50	30.95	30.95	1.54E+15	-0.50	15.19	Song *et al.*, 2010

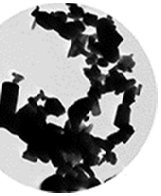

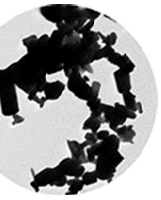

Supplementary data 4.7 The slope and intercept of the equi-response curve (mean ± 95% CI) of Cu NPs and ZnO NPs to zebrafish embryos from our own experiments

Particle		Cu NPs								ZnO NPs			
		Spherically shaped (n=4)				All shapes (n=5)				All shapes (n=5)			
		Slope	Intercept	R^2	P value	Slope	Intercept	R^2	P value	Slope	Intercept	R^2	P value
$NP_{(total)}$	LC_{20}	2.9±0.2	14.9±0.2	0.99	0.003	2.7±0.2	14.7±0.3	0.98	0.001	3.2±0.2	16.2±0.2	0.99	0.0006
	LC_{50}	2.9±0.1	15.1±0.2	0.99	0.003	2.9±0.1	15.0±0.2	0.99	0.0002	3.1±0.4	16.3±0.5	0.95	0.006
	LC_{80}	3.0±0.1	15.3±0.2	0.99	0.003	3.0±0.1	15.4±0.2	0.99	0.0002	3.2±0.2	16.5±0.3	0.99	0.0008
	EC_{20}	2.8±0.3	14.1±0.4	0.98	0.01	2.4±0.7	13.2±0.9	0.78	0.046	2.7±1.4	14.1±1.6	0.54	0.16
	EC_{50}	2.9±0.2	14.5±0.2	0.99	0.004	2.6±0.5	13.9±0.6	0.91	0.01	2.8±1.0	15.0±1.2	0.72	0.07
	EC_{80}	3.0±0.1	14.8±0.2	0.99	0.002	2.8±0.3	14.5±0.4	0.97	0.003	3.0±0.6	15.8±0.7	0.89	0.02
$NP_{(particle)}$	LC_{20}	2.8±0.3	14.6±0.4	0.98	0.009	2.7±0.3	14.5±0.3	0.98	0.002	3.2±0.3	16.3±0.3	0.98	0.001
	LC_{50}	2.9±0.2	14.9±0.3	0.99	0.007	2.9±0.2	15.0±0.2	0.99	0.0006	3.1±0.4	16.4±0.4	0.96	0.004
	LC_{80}	3.0±0.2	15.3±0.3	0.99	0.006	3.1±0.3	15.5±0.3	0.98	0.001	3.1±0.3	16.5±0.4	0.97	0.002
	EC_{20}	2.3±0.3	13.2±0.4	0.96	0.02	2.0±0.5	12.6±0.7	0.82	0.04	2.4±1.6	14.0±1.9	0.42	0.23
	EC_{50}	2.6±0.3	13.9±0.3	0.98	0.01	2.3±0.4	13.5±0.5	0.92	0.01	2.7±1.2	15.1±1.4	0.63	0.11
	EC_{80}	2.8±0.3	14.5±0.4	0.98	0.01	2.7±0.3	14.3±0.3	0.97	0.002	2.9±0.8	16.1±0.9	0.83	0.03

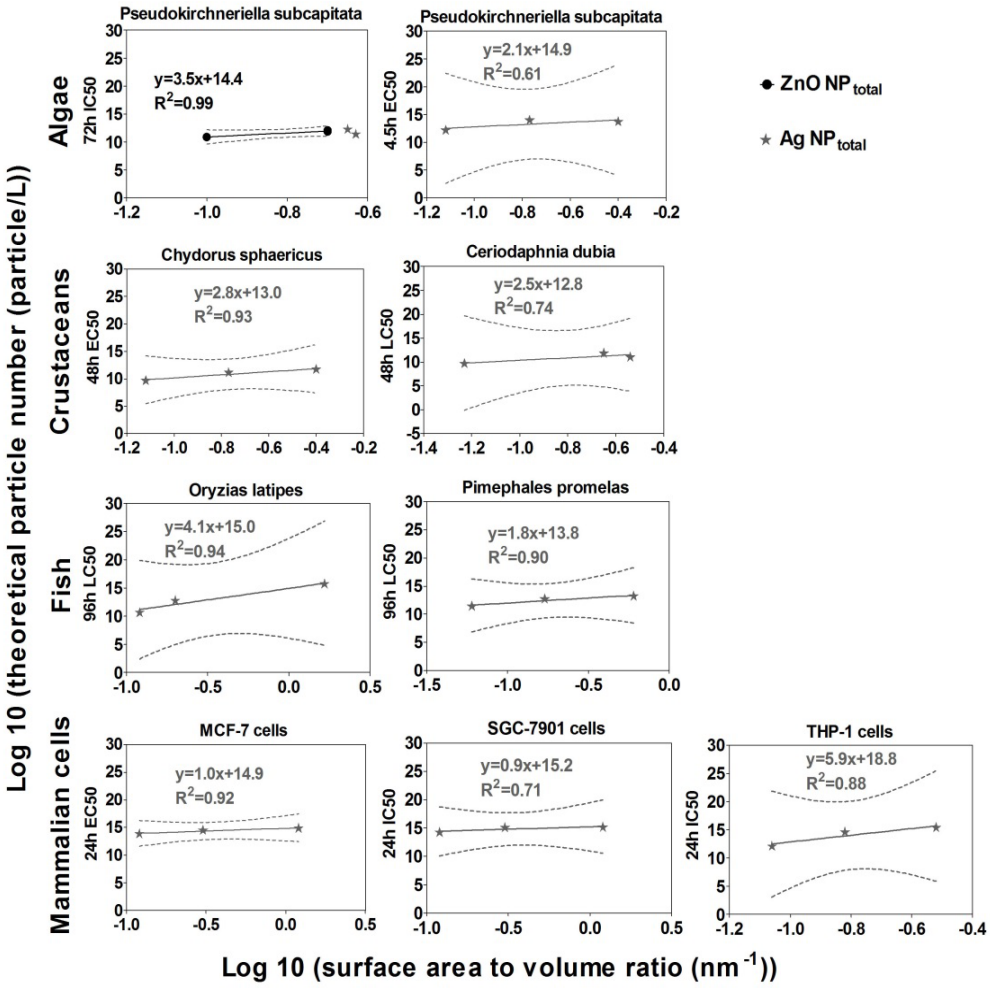

Supplemental data 4.8 Logarithm of $L(E)C_{50}$ values plotted against logarithm of SA/V for particle number of Ag NPs (star) and ZnO NPs (dot) (n = 3). The best-fit lines from linear regression analysis are displayed (solid lines) as well as their associated 95% CIs (dashed lines).

Sydney, Australia

Photo by Jing HUA

5

TiO_2 nanoparticles reduce the effects of ZnO nanoparticles and Zn ions on zebrafish embryos (*Danio rerio*)[4]

5.1 Introduction

The application of nanomaterials presents a scientific breakthrough in industry and in consumer products. Some of the most commonly applied nanoparticles (NPs) are metallic oxides NPs. Both zinc oxide nanoparticles (ZnO NPs) and titanium dioxide nanoparticles (TiO_2 NPs) are widely used in products such as pigments for paints and cosmetics, and also as a UV filter in sunscreens (Zallen and Moret, 2006; Xia *et al*., 2008). These NPs promise remarkable benefits, but they will inevitably be released into the aquatic and the terrestrial environment. More attention is therefore required with regard to their ecotoxicological effects.

Zn is an important essential metal to all cells in all known organisms (Hogstrand, 2011). However, Zn can cause adverse effects when present in excess and is regarded as an important pollutant for fish and other aquatic biota. ZnO NPs have been classified as "extremely toxic" (Kahru and Dubourguier, 2010), and can be absorbed by the intestine as well as the gills of fish (Hogstrand, 2011). TiO_2 on the other hand is generally considered to be an inert material. The acute toxicity of TiO_2 NPs to aquatic organisms is low (Griffitt *et al*., 2008). Besides their low direct

[4] Based on: Hua, J., Peijnenburg, W.J.G.M., and Vijver, M.G. (2015), TiO_2 nanoparticles reduce the effects of ZnO nanoparticles and Zn ions on zebrafish embryos (*Danio rerio*). Under revision.

toxic effects, the presence of TiO_2 NPs may cause indirect adverse effects, for example by adsorbing metals and subsequently influencing their toxicity and bioaccumulation in the aquatic environment (Hartmann *et al*., 2010a; Hartmann *et al*., 2010b). The uptake and retention of Zn to *Daphnia magna* may be enhanced when the zinc ions are adsorbed on TiO_2 NPs (Tan *et al*., 2012). In addition, Tang *et al*. (2013) found that low concentrations of TiO_2 NPs (<1.0 mg/L) significantly enhanced the toxicity of Zn^{2+}, whereas the toxicity of Zn^{2+} decreased with increasing TiO_2 NPs concentration (10 mg/L). They reported that the possible reason is the substantial adsorption of Zn^{2+} by TiO_2 NPs (Tang *et al*., 2013). TiO_2 NPs have a relatively large surface area, thereby providing a great potential for sorption of metal ions and environmental contaminants (Hartmann *et al*., 2010a; Hartmann *et al*., 2010b).

The toxicity of metal-based NPs has received considerable attention in recent years, especially with regard to effects induced by individual NPs. Mixtures of NPs or composite NPs are nevertheless very common in the environment, and also in the various NP-based products. Therefore, organisms are typically exposed to mixtures of various types of contaminants. Li *et al*. (2015a) investigated the toxic effect of a mixture of ZnO NPs and Cu NPs, and found that ZnO NPs at non-toxic concentrations enhance Cu NPs toxicity *in vitro*. However, to our knowledge there is no other existing publication on the toxicity of binary mixtures of metal-based NPs. Other studies were focused on the toxicity of mixtures of NPs with other metal components.

Although dissolved metal ions play an important role in inducing acute or chronic toxicity of metal-based NPs to aquatic organisms, it has been reported in various studies that the particulate form of metal-based NPs also contributes significantly to the toxic effects observed (Hua *et al*., 2014a; Hua *et al*., 2014b; Song *et al*., 2014; Xiao *et al*., 2015). The first aim of this study is the assessment of the fate of NPs suspensions and assessment of the interactive effect of the particulate form of NPs and metal ions. The second aim is to investigate the interaction of ZnO NPs and TiO_2 NPs with regard to the toxicity of these NPs to zebrafish embryos *in vivo*.

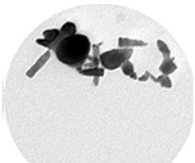

5.2 Materials and methods

5.2.1 Preparation of stock solutions and suspensions of nanoparticles

Stick-shaped ZnO NPs were purchased from IoLiTec GmbH (Heilbronn, Germany). The stick-shaped ZnO NPs were selected because they are more toxic than other shapes of ZnO NPs (Hua *et al*., 2014b). Moreover, they are visually easier to identify when mixed with spherical-shaped TiO_2 NPs. TiO_2 NPs (20 nm, anatase crystalline phase, 99.5% purity, according to manufacturer) were purchased from IoLiTec GmbH (Heilbronn, Germany), and their diameter was chosen to be similar to the width of the ZnO NPs tested. $Zn(NO_3)_2$ was purchased from Sigma Aldrich (Zwijndrecht, The Netherlands). $Zn(NO_3)_2$ and dry powder ZnO NPs were weighed and suspended in egg water (0.21 g 'Instant Ocean® salt in 1 L of Milli-Q water and 1µL of methylene blue, pH 6.5-7.0), which was shaken and sonicated for 10 min in an S 40 H Elmasonic water bath sonicator (Elma, Germany), and the suspension was then diluted with egg water to obtain the desired concentrations. To investigate the interaction of ZnO NPs and TiO_2 NPs, nominal concentrations (C_N) of ZnO NPs ranging from 0 to 32 mg Zn/L were applied alone or together with TiO_2 NPs (with C_N ranging from 0 to 24 mg Ti/L). C_N of $Zn(NO_3)_2$ ranging from 0 to 40 mg Zn/L were also applied alone or together with TiO_2 NPs to investigate the interaction of Zn^{2+} and TiO_2 NPs.

5.2.2 Physicochemical characterization of NPs

The particle size and shape of NPs present in the suspensions were characterized after around 1 h of incubation in egg water using transmission electron microscopy (TEM) (JEOL 1010, JEOL Ltd., Japan). The particle size distribution was analyzed using software Nano Measurer version 1.2 (Fudan University, China). Size distribution analysis was performed only on samples in which individual NPs could be defined. Dynamic light scattering (DLS) was measured on a Zetasizer Nano-ZS instrument (Malvern Instruments Ltd., UK) and was performed to detect the distribution of the hydrodynamic diameter of aggregated spherical NPs in egg water. We also used DLS for non-spherical particles to determine their hydrodynamic diameter. The actual total concentrations of metal (C_A) and the dissolved metal ions from NPs (C_I) in egg water (mg metal/L) were analyzed using inductively coupled plasma optical emission spectrometry (ICP-OES, iCAP 5100,

Thermo Scientific, Cambridge, UK) after 24 h of equilibration of the samples. To determine concentrations of C_I in egg water, 5 mL of the suspensions was sampled after 24 h of incubation and centrifuged at 13300 g for 20 min following Fernandez-Cruz *et al*. (2013). The centrifugation of the samples removed ZnO NPs, TiO_2 NPs and ions which might be sorbed to the TiO_2 NPs. The preparation of ZnO NPs digested samples is described in our previous study (Hua *et al*., 2014b). For TiO_2 NPs, liquid and suspended solid samples were acid digested using the HNO_3/H_2SO_4 digestion method for Ti as described by Standard Method 3030 G and 2540 D for water and wastewater analysis (APHA-AWWA-WEF, 2005). The digested samples were then analyzed by ICP-OES.

5.2.3 Toxicity tests

Zebrafish embryos were obtained from AB wild type zebrafish. Embryos were assessed and distributed into 96 well-plates with one embryo per well from 24 hours post-fertilization (hpf) to 120 hpf following the method previously described (Hua *et al*., 2014b). The embryos were exposed to 250 µL/well of ZnO NPs together with or without TiO_2 NPs in egg water. $Zn(NO_3)_2$ solutions were also applied with or without TiO_2 NPs to investigate the interaction of Zn^{2+} and TiO_2 NPs. Various concentrations were selected, namely, 0, 2, 4, 8, 16, 32 mg Zn/L for ZnO NPs, 0, 2.5, 5, 10, 20, 40 mg Zn/L for $Zn(NO_3)_2$ solutions and 0, 1.5, 3, 6, 12, 24 mg Ti/L for TiO_2 NPs. Throughout all procedures, the embryos and solutions were kept at 28.5 ± 0.5°C. Zebrafish embryos were exposed in triplicate to either a control or different concentrations of ZnO NPs, $Zn(NO_3)_2$, TiO_2 NPs, or binary combination of ZnO NPs with TiO_2 NPs, or $Zn(NO_3)_2$ with TiO_2 NPs, each replicate contained 16 embryos for each treatment (48 embryos in total). Mortality and hatching rate were assessed every 24 h. Embryos were scored as dead according to OECD guideline 157 (2011). In addition, we also investigated the impact of the particle-specific ZnO NPs on the toxicity of Zn ions ($Zn(NO_3)_2$) as a reference, the methods are shown in the Supplemental data 5.1.

The median lethal concentration (LC_{50}) and the median effect concentration (EC_{50}) of hatching inhibition of zebrafish caused by stock solutions of NPs were calculated using GraphPad Prism 5 (California, USA) according to the following equation to describe the dose-response curve:

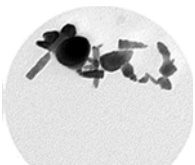

$$E = \frac{1}{1 + 10^{(LogEC_{50} - LogC_A)\rho}} \quad (5.1)$$

where E is the effect (mortality, hatching inhibition) on zebrafish embryos caused by stock solutions of NPs (scaled from 0 to 1). C_A describes the initial actual exposure concentration of NPs and ρ represents the slope of the curve.

5.2.4 Toxic contribution of the particulate and ionic form of ZnO NPs

As described in our previous study, we assumed that ZnO NPs suspensions contain both the particulate form of ZnO NPs and released ions from the ZnO NPs (Hua *et al*., 2014b). TiO_2 NPs suspensions are expected to be present solely in their solid phase not in ionic forms (Antignano and Manning, 2008). The combined effects of two compounds can be calculated by the response addition model (RA) (Altenburger *et al*., 2003). Based on our previous study, we found increased toxic effects by using concentration addition model (CA) than by using RA and therefore an increased relative contribution of the particle form of NPs. In addition, both results from CA and RA allowed us to conclude that the particle form of NPs was the main factor in inducing toxicity to zebrafish embryos for all NPs suspensions tested. Hence, the RA model was selected to explicitly account for the toxic impacts of the particulate form of ZnO NPs (ZnO $NP_{(particle)}$) and the ionic form shed from ZnO NPs ($ZnO_{(ion)}$) (Hua *et al*., 2014b). In the RA model, the toxic effects (mortality and hatching inhibition) of embryos induced by the ZnO $NP_{(particle)}$ ($E_{(particle)}$) can be computed as follows:

$$E_{(total)} = 1 - \left[\left(1 - E_{(ion)}\right)\left(1 - E_{(particle)}\right)\right] \quad (5.2)$$

where $E_{(total)}$ and $E_{(ion)}$ represent the effect of zebrafish embryos caused by ZnO $NP_{(total)}$ and ZnO $NP_{(ion)}$ (scaled from 0 to 1), respectively. This leaves $E_{(particle)}$ as the only unknown, allowing for direct calculation of the effect caused by the particles at any specific initial actual particle concentration.

The actual concentrations of ZnO $NP_{(total)}$ and of ZnO $NP_{(ion)}$ were measured by ICP-OES after 24 h of incubation in egg water. The actual concentrations of ZnO $NP_{(particle)}$ were calculated as the difference of the actual concentrations of ZnO $NP_{(total)}$ and the actual concentrations of ZnO $NP_{(ion)}$. The toxicity of ZnO $NP_{(ion)}$ was experimentally quantified on the basis of the concentration-response curve of $Zn(NO_3)_2$ alone or together with TiO_2 NPs. The total toxicity of ZnO $NP_{(total)}$ was

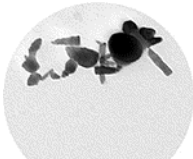

assessed experimentally. An example of the calculation of the relative contribution to toxicity of ZnO $NP_{(particle)}$ and ZnO $NP_{(ion)}$ at the LC_{50} value of suspensions is shown in Supplemental data 5.2.

5.2.5 Statistical analysis

The experiments were repeated three times independently (with 16 embryos per treatment group, giving in total 48 embryos). Data are presented as mean with 95% confidence intervals (95% CI) or standard error of the mean (SEM). Mortality data obtained at 120 hpf were used to calculate LC_{50} values. The LC_{50} values, EC_{50} values of hatching rate, and 95% confidence intervals were calculated (equation 5.1) using GraphPad Prism 5. The 95% confidence intervals of LC_{50} values and EC_{50} values were calculated based on three dose-response curves obtained in the three independent experiments. Statistical analyses were performed using one-way analysis of variance (ANOVA) with Tukey's multiple comparisons to compare ZnO NPs or $Zn(NO_3)_2$ alone and together with TiO_2 NPs. The homogeneity of variance was checked before one-way ANOVA. The significance level in all calculations was set at $p < 0.05$.

5.3 Results

5.3.1 Characterization of nanoparticles

The primary sizes and shapes of the particles were estimated from TEM images (Figure 5.1). We tested one type of ZnO nanosticks (width: 32 ± 20 nm; length: 81 ± 40 nm), and one type of TiO_2 nanospheres. The pristine TiO_2 NPs are of spherical shape, 19 ± 4 nm in size. Both metal-based NPs were present as aggregates in egg water. The original size of dry particles changed as soon as the particles were submerged in egg water. The hydrodynamic particle sizes of aggregates ZnO NPs, TiO_2 NPs, the mixtures of ZnO NPs and TiO_2 NPs, and the mixtures of TiO_2 NPs and $Zn(NO_3)_2$ measured by DLS after 24 h of submerging in egg water were 600 nm, >1300 nm, 900 nm and >1250 nm, respectively. It should be noted that DLS is not the most suited method for determining the hydrodynamic diameter for non-spherical NPs. The results of DLS measurements obtained for the ZnO NPs thus need to be considered as indicative values. Their zeta-potentials were -26 mV, -20 mV, -24 mV, and -19 mV, respectively. This means that the NPs suspensions

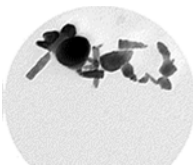

had relative low degrees of stability and the NPs eventually aggregated due to Van Der Waals inter-particle attractions.

5.3.2 Fate of nanoparticles

Results of ICP-OES measurements of the actual total concentration (C_A, including the particulate form and the ionic form of NPs) and ionic concentration (C_I) of zinc and titanium after 24 h of incubation are shown in Table 5.1. ZnO NPs were partially dissolved (<3.3 mg Zn/L) after 24 h of incubation in egg water. The C_I of zinc ions shed from ZnO NPs increased with the total zinc concentrations, and ranged from 0.01 to 3.3 mg Zn/L. The C_I of Ti ranged from 0.1 to 539 µg Ti/L (Table 5.1). The C_I of zinc ions shed from ZnO NPs in egg water slightly increased upon increase of the total concentrations of titanium (Table 5.1). The concentrations of Zn^{2+} in $Zn(NO_3)_2$ solutions with and without TiO_2 NPs ranged from 0.01 to 39.9 mg Zn/L.

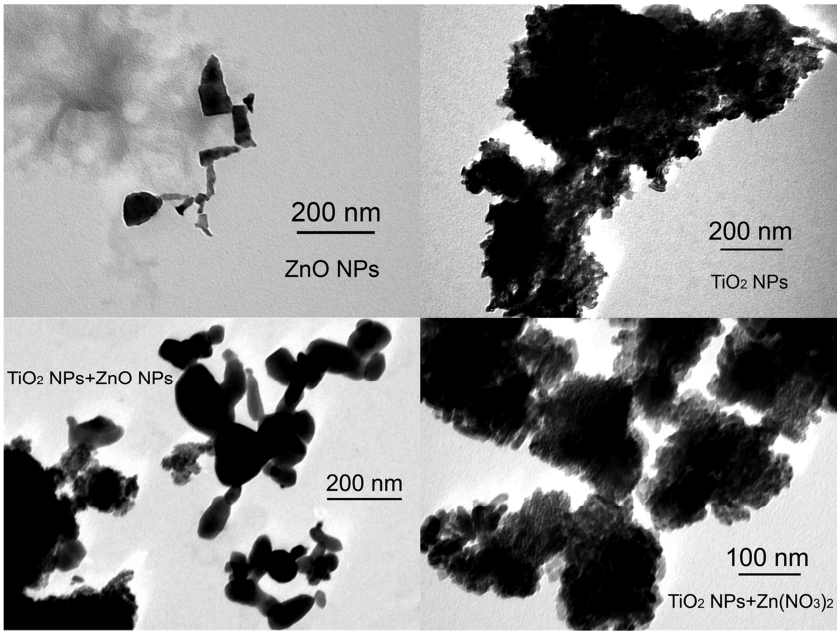

Figure 5.1 TEM images of nanoparticles in egg water after about 1 h of incubation. Pictures were taken with a JEOL 1010 TEM at 70 kV.

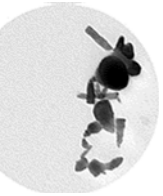

Table 5.1 The actual and ionic concentration of Zn^{2+} and Ti after centrifugation of suspensions obtained after 24 h of incubation in egg water.

		C_I of Zn^{2+} (unit: mg Zn/L)							C_I of TiO_2 (unit: µg Ti/L)				
C_N of Zn	C_A of Zn	C_N of TiO_2	0	1.5	3	6	12	24	0	1500	3000	6000	12000	24000
		C_A of TiO_2	0.01	1.4	2.7	5.4	10.8	21.6	0.1	1400	2700	5400	10800	21600
ZnO NPs														
0	0.01		0.01	0.01	0.01	0.01	0.01	0.01	**0.1**	**5**	**7**	**7**	**60**	**11**
2	2.0		1.6	1.0	1.0	1.0	0.9	0.9	0.1	1	1	32[b]	62	126[c]
4	4.0		1.8	1.4	1.5	1.5	1.5	1.5	0.1	1	2	29[a]	102	230[c]
8	7.9		2.1	1.9	1.9	2.0	2.1	2.1	0.1	1	5	25[a]	142[c]	333[c]
16	15.8		2.3	2.3	2.4	2.5	2.6	2.7[a]	0.1	1	9	22	181[c]	436[c]
32	31.7		2.5	2.7	2.9	3.0	3.2[a]	3.3[a]	0.1	1	10	18	221[c]	539[c]
$Zn(NO_3)_2$														
0	0.01		0.01	0.01	0.01	0.01	0.01	0.01	**40**	**41**	**41**	**41**	**41**	**41**
2.25	2.5		2.5	2.4	2.4	2.5	2.5	2.5	43	124[c]	134[c]	145[c]	155[c]	165[c]
4.5	4.9		4.9	4.8	4.9	4.9	5.0	5.0	33	93[c]	100[b]	107[c]	115[c]	122[c]
9	9.8		9.8	9.7	9.8	9.8	9.9	10.0	24	61	65	70[a]	75[a]	79[c]
18	19.6		19.6	19.3	19.5	19.7	19.8	20.0	14[a]	29	31	33	34	36
36	39.2		39.2	38.7	39.0	39.3	39.6	39.9	11[a]	23	24	25	27	28[a]

C_I: Actual metal ion concentrations of NPs after 24 h of incubation in egg water; C_N: Nominal total concentrations of NPs; C_A: Actual total concentrations of NPs. Significant differences are indicated with letters, a, b, c with respect to the C_I of metal. For Zn^{2+}, significant differences between ZnO NPs or $Zn(NO_3)_2$ applied with different C_N of TiO_2 NPs to ZnO NPs alone (in underline); For TiO_2, significant differences between TiO_2 NPs applied with different C_N of ZnO NPs or $Zn(NO_3)_2$ to TiO_2 NPs alone (in bold). [a]: $p< 0.05$, [b]: $p< 0.01$ and [c]: $p\leq 0.001$.

5.3.3 Lethality

The lethality of the ZnO NPs used in this study to zebrafish embryos has been reported in our previous study and the LC_{50} value is 7.1±0.3 mg/L (Hua *et al.*, 2014b).

None of the TiO_2 NPs caused toxicity to zebrafish embryos at any concentration tested, even at the highest concentration of 24 mg Ti/L in egg water.

To investigate the interaction between zinc ions and TiO_2 NPs, we added TiO_2 NPs to the $Zn(NO_3)_2$ solutions. We found that the addition of TiO_2 NPs to $Zn(NO_3)_2$ caused a considerable decrease in the toxicity of $Zn(NO_3)_2$ to zebrafish embryos at the concentrations of 10 and 20 mg Zn/L at 120 hpf (Figure 5.2A). At a concentration of 10 mg Zn/L $Zn(NO_3)_2$ with different concentrations of TiO_2 NPs, a clear dose-response curve was obtained. Upon addition of 1.5 mg Ti/L of TiO_2 NPs to a 10 mg Zn/L $Zn(NO_3)_2$ solution, the mortality decreased from 65% ($Zn(NO_3)_2$ alone) to 40%. When the concentration of TiO_2 NPs was 24 mg Ti/L, the mortality was only 6% (Figure 5.2A). The significant reduction in the toxicity of 9 mg Zn/L $Zn(NO_3)_2$ occurred with addition of 1.5 mg Ti/L and higher concentrations of TiO_2 NPs ($p<0.001$). The actual concentrations of Zn^{2+} and Ti^{2+} in suspensions and their toxic effects to zebrafish embryos will be discussed later.

We further investigated the interaction between the particulate form of ZnO NPs and TiO_2 NPs. For this purpose, different concentrations of TiO_2 NPs (0-24 mg Ti/L) were added to suspensions of ZnO NPs (0-32 mg Zn/L). As shown in Figure 5.2B, upon addition of 1.5 mg Ti/L of TiO_2 NPs into 4 mg Zn/L ZnO NPs suspensions, the mortality of embryos (21%) was significantly increased ($p<0.001$) as compared to the case in which no TiO_2 NPs were added (4%). However, the mortality of zebrafish embryos is shown to decrease significantly with addition of TiO_2 NPs (>3 mg Ti/L) to the suspension of ZnO NPs at concentrations of 8 mg Zn/L at 120 hpf ($p<0.05$). As shown in Table 5.1, the concentrations of C_1 of Zn^{2+} of ZnO NPs in egg water are significantly but nevertheless only slightly increased upon addition of TiO_2 NPs. Based on the increase of toxicity of Zn ions observed after exposure to $Zn(NO_3)_2$, the slight increase in the concentration of ZnO $NP_{(ion)}$ can only cause a slight increase in toxicity. However, it was actually found that the toxicity of ZnO $NP_{(total)}$ was decreased due to the addition of TiO_2 NPs. Therefore, it is to be

concluded that the TiO_2 NPs not only interact with ZnO $NP_{(ion)}$, but also with ZnO $NP_{(particle)}$.

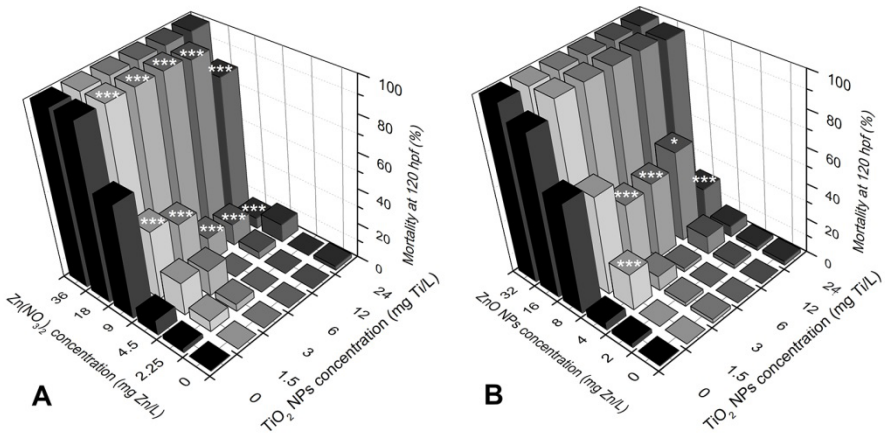

Figure 5.2 The mortality of zebrafish embryos exposed to ZnO NPs or $Zn(NO_3)_2$ with addition of TiO_2 NPs. The nominal concentrations of ZnO NPs, $Zn(NO_3)_2$, and TiO_2 NPs ranged from 0 to 32 mg Zn/L, 0 to 40 mg Zn/L and 0 to 24 mg Ti/L, respectively. The actual concentration of each component did not show much deviation to the nominal concentration, and the actual concentrations are given in Table 5.1. One-way ANOVA with Turkey's multiple comparisons was used to detect significant differences between different concentrations of TiO_2 NPs (from 1.5 to 24 mg/L) and samples without addition of TiO_2 NPs. Asterisks denote differences with respect to the mortality of the mixtures of different concentrations of (A) $Zn(NO_3)_2$, (B) ZnO NPs with TiO_2 NPs. * $p< 0.05$, ** $p< 0.01$ and *** $p\leq 0.001$.

5.3.4 Hatching rate

The inhibiting effect of ZnO NPs on hatching of zebrafish embryos has been reported in our previous study and the EC_{50} value is 1.3 ± 0.2 mg/L (Hua *et al*., 2014b). The TiO_2 NPs did not induce hatching inhibition to zebrafish embryos at any concentration up to the 24 mg/L tested (Figure 5.3). Upon addition of 20 mg Zn/L of $Zn(NO_3)_2$ with and without TiO_2 NPs, as well as of 16 mg Zn/L of ZnO NPs, none of the embryos hatched (Figure 5.3). Similar to the observations with regard to the mortality assessment of zebrafish, the addition of TiO_2 NPs to the ZnO NPs caused a clear increase in hatching rate to zebrafish embryos at concentrations of

2.5 to 10 mg/L of $Zn(NO_3)_2$ and 2 to 8 mg/L ZnO NPs (Figure 5.3). The adverse effects observed were therefore less in the case of addition of TiO_2 NPs as compared to the case in which TiO_2 NPs were absent. The results on hatching rate (Figure 5.3) show that the TiO_2 NPs interact with both Zn ions generated by the ZnO NPs and with the particulate form of ZnO NPs in case of the endpoint of hatching.

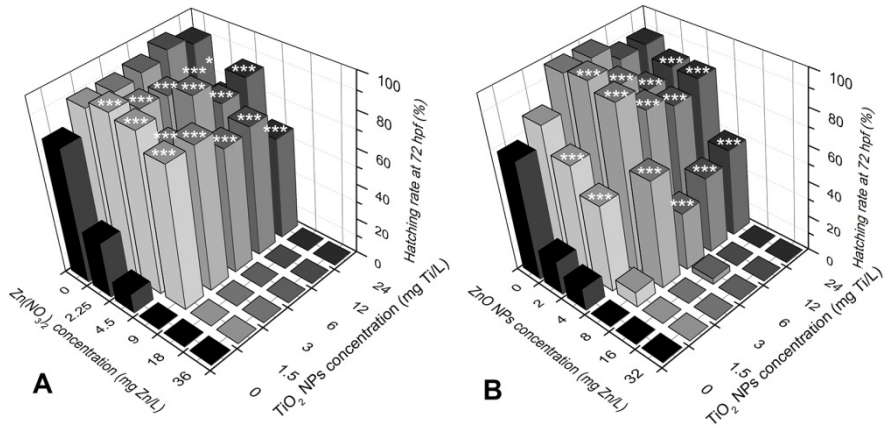

Figure 5.3 The hatching rate of zebrafish embryos exposed to ZnO NPs or $Zn(NO_3)_2$ with addition of TiO_2 NPs. The nominal concentrations of ZnO NPs, $Zn(NO_3)_2$, and TiO_2 NPs ranged from 0 to 32 mg Zn/L,0 to 40 mg Zn/L and 0 to 24 mg Ti/L, respectively. The actual concentration of each component did not show much deviation to the nominal concentration, and the actual concentrations are given in Table 5.1. One-way ANOVA with Turkey's multiple comparisons was used to detect significant differences between different concentrations of TiO_2 NPs (from 1.5 to 24 mg/L) and samples without addition of TiO_2 NPs. Asterisks denote differences with respect to the hatching rate of the mixtures of different concentrations of (A) $Zn(NO_3)_2$, (B) ZnO NPs with TiO_2 NPs. * $p< 0.05$, ** $p< 0.01$ and *** $p\leq 0.001$.

To investigate the interaction between the particulate form of ZnO NPs and $Zn(NO_3)_2$, embryos were exposed to binary mixtures at each EC_{50} and EC_{75} value of ZnO NPs (EC_{50} value: 1.4 mg/L, EC_{75} value: 1.9 mg/L) and $Zn(NO_3)_2$ (EC_{50} value: 1.7 mg/L, EC_{75} value: 2.5 mg/L). The mortality was in all cases less than 5%. However, in the case of hatching rate, only less than 20% of embryos hatched

(Supplemental data 5.1). The actual toxic effect of zebrafish embryos exposed to mixtures of ZnO NPs and $Zn(NO_3)_2$ were comparable to the effect calculated by RA (equation 5.2) in Supplemental data 5.3. These results show that the actual combined effect of ZnO NPs and $Zn(NO_3)_2$ was similar to the combined effect expected on the basis of response addition. It is thus unlikely that interactions occur between ZnO NPs and $Zn(NO_3)_2$ at low exposure concentrations.

Table 5.2 The $L(E)C_{50}$ values of the mixtures of different concentrations of TiO_2 NPs with ZnO NPs or with $Zn(NO_3)_2$ after exposure to zebrafish embryos at 120 hpf. Data are presented as $L(E)C_{50}$ with 95% CI.

C_N of TiO_2 NPs (unit: mg Zn/L)	0	1.5	3	6	12	24
LC_{50} values (95% CI)						
$Zn(NO_3)_2$+TiO_2 NPs	8.7 (7.9-9.6)	10.2 (9.2-11.3)	11.0** (9.9-12.2)	10.3* (10.0-10.8)	11.4** (9.9-13.0)	11.7*** (10.2-13.6)
ZnO NPs $NP_{(total)}$+TiO_2	7.1 (6.8-7.5)	6.8 (6.3-7.4)	8.4** (7.9-8.9)	8.2* (7.8-8.6)	7.6 (7.2-8.0)	9.5*** (8.8-10.3)
ZnO NPs $NP_{(particle)}$+TiO_2	8.0 (7.4-8.5)	6.8 (4.1-11.4)	9.0 very wide	6.7 very wide	8.8 very wide	12.7 very wide
EC_{50} values (95% CI)						
$Zn(NO_3)_2$+TiO_2 NPs	1.8 (1.6-2.1)	11.4*** (7.5-17.3)	11.7*** (7.5-18.4)	11.0*** (9.2-13.3)	11.4*** (9.1-14.3)	9.3*** (7.2-12.1)
ZnO NPs $NP_{(total)}$+TiO_2	1.3 (1.1-1.5)	3.2* (2.5-4.0)	8.5*** (8.1-8.9)	6.3*** (5.7-7.1)	6.3*** (5.1-7.6)	7.3*** (6.1-8.7)
ZnO NPs $NP_{(particle)}$+TiO_2	0.4 (0.2-0.9)	6.2* very wide	9.0** very wide	12.9* very wide	8.8** very wide	6.6* very wide

C_N: Nominal concentrations of TiO_2 NPs (mg Ti/L). Significant differences are indicated with asterisks in $L(E)C_{50}$ values of mixtures for the addition of different concentrations of TiO_2 NPs in ZnO NPs suspensions (Tukey's multiple comparisons, one-way ANOVA). * $p< 0.05$, ** $p< 0.01$ and *** $p\leq 0.001$.

5.3.5 Effect of TiO_2 NPs on the toxicity of ZnO NP suspensions

Dose response curves of mortality and hatching rate of zebrafish embryos exposed to $Zn(NO_3)_2$ or ZnO NPs alone or with addition of different concentrations of TiO_2 NPs are shown in Figures 5.4A-5.4D. The LC_{50} values, EC_{50} values and 95% CI of suspensions of ZnO NPs mixed with different concentrations of TiO_2 NPs are shown in Table 5.2. The LC_{50} value and the 95% CI of suspensions of ZnO NPs

was 7.1 (6.8-7.5) mg/L at 120 hpf. The LC_{50} values of ZnO NPs suspensions with the addition of 3, 6, and 24 mg/L TiO_2 NPs (8.4, 8.2, and 9.5 mg/L, respectively) were significantly different from the LC_{50} value without addition of TiO_2 NPs (p<0.05). The addition of higher concentrations of TiO_2 NPs (3 mg/L or higher) to solutions of $Zn(NO_3)_2$ induced significant differences of toxicity (LC_{50} values ranging from 10.3 mg/L to 11.7 mg/L) as compared to the case in which no TiO_2 NPs were added (LC_{50} value is 8.7 mg/L).

The EC_{50} values and 95% CI of suspensions of ZnO NPs and of $Zn(NO_3)_2$ were 1.3 (1.1-1.5) mg/L and 1.8 (1.3-2.5) mg/L at 72 hpf, respectively (Table 5.2). The EC_{50} values of ZnO NPs suspensions with the addition of TiO_2 NPs (EC_{50} values ranging from 3.2 to 8.5 mg/L, i.e. up till a factor of 6.3) were significantly higher compared to the EC_{50} value without addition of TiO_2 NPs (p<0.05).

5.3.6 Effect of TiO_2 NPs on the toxicity of the particulate form of ZnO NPs

Dose response curves of mortality and hatching rate of zebrafish embryos exposed to ZnO $NP_{(particle)}$ alone or with addition of different concentrations of TiO_2 NPs are shown in Figures 5.4E and 5.4F. The LC_{50} value and the 95% CI of ZnO $NP_{(particle)}$ was 8.0 (7.4-8.5) mg Zn/L at 120 hpf. The LC_{50} values of ZnO $NP_{(particle)}$ with the addition of 1.5 to 24 mg Ti/L TiO_2 NPs were 6.8, 9.0, 6.6, 8.8, and 12.7 mg Zn/L, respectively. The 95% CI of the LC_{50} values of ZnO $NP_{(particle)}$ were very wide (reported by GraphPad Prism 5) as calculated by the RA model, and hence, there were no values for 95% CI values given in Table 5.2. Due to the large variation of the slope of dose-response curves and very wide 95% CI of the LC_{50} values, the LC_{50} value of ZnO $NP_{(particle)}$ was not statistically significantly different from the LC_{50} value obtained after addition of TiO_2 NPs. The EC_{50} value and 95% CI for the effect of ZnO $NP_{(particle)}$ on hatching was 0.4 (0.2-0.9) mg Zn/L at 72 hpf (Table 5.2). The EC_{50} values of ZnO $NP_{(particle)}$ with the addition of 1.5 to 24 mg/L TiO_2 NPs were 6.2, 9.0, 12.9, 8.8, and 6.6 mg Zn/L. The EC_{50} value of ZnO $NP_{(particle)}$ was thus found to be significantly different from the EC_{50} value obtained after addition of TiO_2 NPs.

5.3.7 Contribution of the particulate form and the ionic form of ZnO NPs to toxicity

The relative contribution to toxicity of ZnO $NP_{(particle)}$ and ZnO $NP_{(ion)}$ with addition of TiO_2 NPs to zebrafish embryos using the response addition model (equation 5.2) is given in Table 5.3. At the LC_{50} of the suspensions of ZnO NPs with different concentrations of TiO_2 NPs, the contributions of the particulate form of ZnO NPs to the lethal effects observed after exposure to suspensions of ZnO NPs alone or with different concentrations of TiO_2 NPs ranging from 0 to 24 mg Ti/L was 65%, 69%, 66%, 66%, 64%, and 62%, respectively. In the case of the 50% hatching inhibition concentration of ZnO NPs with different concentrations of TiO_2 NPs, the particle contribution to hatching inhibition of suspensions of ZnO NPs alone or with different concentrations of TiO_2 NPs (0 to 24 mg Ti/L) was 82%, 74%, 66%, 67%, 65% and 64%, respectively. The particulate form of ZnO NPs was thus found to be the dominant factor affecting lethality and inhibition of hatching of zebrafish embryos after exposure to TiO_2 NPs applied with suspensions of ZnO NPs.

Table 5.3 Relative contribution to toxicity of ZnO $NP_{(particle)}$ and ZnO $NP_{(ion)}$ at the LC_{50}-value of the suspensions and at the EC_{50}-value of the suspensions for hatching inhibition with addition of different concentrations of TiO_2 NPs.

C_N of TiO_2 NPs	0	1.5	3	6	12	24
LC_{50} values (mg Zn/L)	7.1	6.8	8.4	8.2	7.6	9.5
relative contribution to toxicity of $NP_{(ion)}$	35	31	34	34	36	38
relative contribution to toxicity of $NP_{(particle)}$	65	69	66	66	64	62
EC_{50} values (mg Zn/L)	1.3	3.2	8.5	6.3	6.3	7.3
relative contribution to toxicity of $NP_{(ion)}$	18	26	34	33	35	36
relative contribution to toxicity of $NP_{(particle)}$	82	74	66	67	65	64

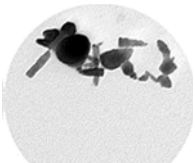

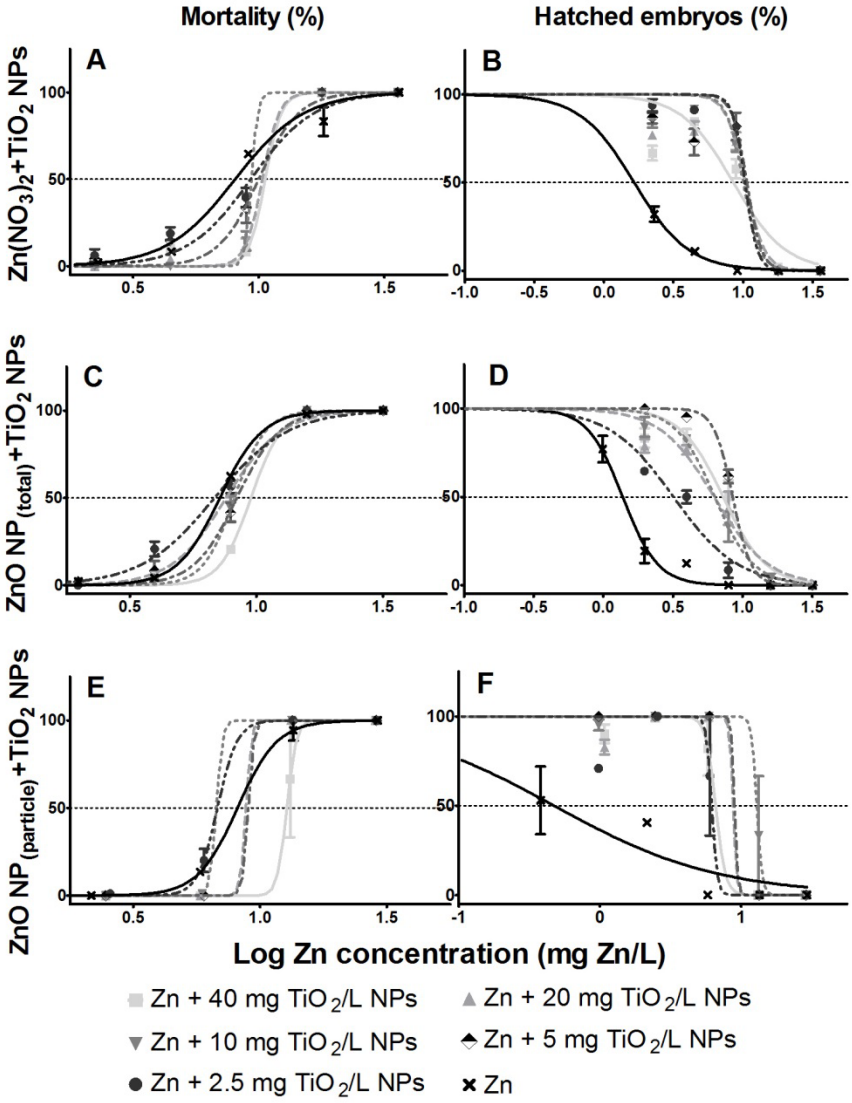

Figure 5.4 Dose response curves of mortality of zebrafish embryos exposed to (A) $Zn(NO_3)_2$, (C) ZnO NPs suspensions, and (E) the particulate form of ZnO NPs at 120 hpf, dose response curves of hatching of zebrafish embryos exposed to (B) $Zn(NO_3)_2$ and (D) ZnO NPs suspensions, and (F) the particulate form of ZnO NPs at 72 hpf, following exposure to $Zn(NO_3)_2$ or ZnO NPs alone or with addition of different concentrations of TiO_2 NPs. Actual log-transformed Zn concentrations (mg Zn/L) are plotted on the X-axis. Data are presented as mean of three independent replicates ± SEM.

5.4 Discussion

5.4.1 Characterization and fate of nanoparticles

The ZnO NPs, TiO_2 NPs and their mixtures were aggregated to a high extend after submersion in egg water. The tendency of these NPs to aggregate may be attributed to the high concentrations of various cations in egg water (Atkinson and Bingman, 1998; French *et al*., 2009). Previous studies have reported that the aggregation of nanoparticles in exposure medium is an important factor in assessing their toxicity. Aggregates of nanoparticles with a diameter that is less than 0.5-0.7 μm can easily penetrate into the perivitelline space of embryos *via* the chorion pore canals (Lee *et al*., 2007). Moreover, after uptake, macrophage clearance was found to be more effective for larger particles compared to smaller ones (Buzea *et al*., 2007; Zhu *et al*., 2009a).

TiO_2 NPs have a strong adsorption capacity and retention for various metals (*e.g.* Zn, Cd) (Zhang *et al*., 2007; Pettibone *et al*., 2008; Hartmann *et al*., 2010a; Hartmann *et al*., 2010b; Tan *et al*., 2012; Tang *et al*., 2013). The adsorption capacity of TiO_2 NPs is due to their large surface area (Cho *et al*., 2010). The interactions of Zn^{2+} with TiO_2 NPs were determined by examining the sorption equilibrium within 10 h (Tang *et al*., 2013). Tang *et al*. found monolayer sorption of Zn^{2+} on TiO_2 NPs and a correlation between the amount of Zn^{2+} sorbed on the TiO_2 NPs and the non-sorbed Zn^{2+} concentration in the culture medium. In our previous study it was observed for ZnO NPs of various shapes and sizes that the time to reach pseudo-dissolution equilibrium is about 1 h, as the concentrations of zinc ions in egg water did not change significantly after this time period (Hua *et al*., 2014b). This finding was confirmed in the current study, as the concentrations of zinc ions of at 1 and 24 h were similar. Thereupon, dissolved zinc concentrations remained low (3.3 mg Zn/L), even at the highest actual concentration of ZnO NPs (31.7 mg Zn/L) applied with the highest actual concentration of TiO_2 NPs (21.6 mg Ti/L). Taken together, the particulate form of ZnO NPs and the Zn ions released from the ZnO NPs that were either sorbed on the TiO_2 NPs or present in solution, reached a pseudo-dissolution-sorption equilibrium in egg water in the early stages of exposure of the embryos. Hence, the dissolved concentrations of zinc ions (C_I) did not change significantly upon addition of low concentrations of TiO_2 NPs

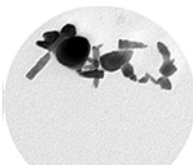

(Table 5.1). The measured concentrations of Ti in our experiments ranged from 0.1 to 539 µg Ti/L in the binary mixtures of ZnO NPs and TiO_2 NPs. The concentrations of Ti in egg water in general slightly increased upon increase of the total concentrations of TiO_2 NPs and of the total zinc concentrations of ZnO NPs (Table 5.1). The possible reason would be that after centrifugation there were still some quite smaller sized ZnO NPs and TiO_2 NPs present in the supernatant, although their concentrations are quite low. The concentrations of released Zn ions ranged from 0.9 to 3.3 mg Zn/L in our study. We are not expecting any large deviation of the release measurements of Zn ions (in mg/L scale) because we observed very low concentration of ZnO NPs (in µg/L scale) in the supernatant. However, in the case of the TiO_2 NPs, the dissolution of Ti can be considered negligible (concentration quite low, in µg/L scale), it appears that the concentration of Ti in the supernatants was affected by the concentrations of ZnO NPs. However, in the case of binary mixtures of $Zn(NO_3)_2$ and TiO_2 NPs, the soluble Ti concentrations decreased upon increase of the total concentrations of Zn and of Ti.

5.4.2 Effects of TiO_2 NPs on the toxicity of ZnO NP suspensions

The addition of higher concentrations of TiO_2 NPs into $Zn(NO_3)_2$ solutions or into ZnO NPs suspensions markedly decreased the toxicity of $Zn(NO_3)_2$ or ZnO NPs to zebrafish embryos (Figure 5.2). The reduction effect by TiO_2 NPs was also observed in studies in which algae when exposed to 300 nm TiO_2 particles and cadmium (Hartmann *et al*., 2010b), and toxicity of Zn to *Anabaena sp*. was reduced by the addition of TiO_2 NPs (Tang *et al*., 2013). From Figure 5.2B, it can be seen that 1.5 mg/L of TiO_2 NPs addition to 4 mg/L ZnO NPs significantly increased the mortality by a factor of 5 compared to the mortality observed in the suspension of 4 mg/L ZnO NPs without TiO_2 NPs added. Similar results were reported by another study (Tang *et al*., 2013); these authors reported that the presence of lower concentrations of TiO_2 NPs (< 1.0 mg/L) enhanced the toxicity of Zn^{2+} while the toxicity of Zn^{2+} decreased with higher concentrations of TiO_2 NPs (10 mg/L) applied. Tang *et al*. (2013) claimed that TiO_2 NPs reduced the soluble Zn^{2+} concentration by adsorbing Zn^{2+} on the TiO_2 NPs. Subsequently, the proposed mechanism was that adsorbed Zn^{2+} on the TiO_2 NPs had direct contact with the algae; while with TiO_2 NPs at high concentrations, the toxicity was reduced because the TiO_2 NPs settled down and the soluble Zn^{2+} concentration in the

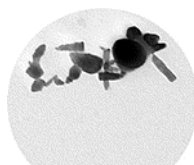

medium surrounding the organisms was low.

Various studies found that Zn ions released from ZnO NPs play an important role in inducing acute or chronic toxicity of ZnO NPs to aquatic organisms (Xia *et al*., 2008; Bai *et al*., 2010b; Xia *et al*., 2011; Adam *et al*., 2014). Zinc ions were found to induce various adverse cellular outcomes, such as reactive oxidative species production, lysosome damage, mitochondrial perturbation, and excitation of proinflammatory cytokine and chemokine production (Xia *et al*., 2008; Nel *et al*., 2009; Zhu *et al*., 2009b; George *et al*., 2010; George *et al*., 2011b). Dissolved Zn ions were also found to interfere in the functioning of zebrafish hatching enzymes (Lin *et al*., 2013b).

Although the mechanism of toxicity of NPs is still not clear, one of the reasons why TiO_2 NPs decrease the toxicity of ZnO NP suspensions, is that TiO_2 NPs formed larger aggregates with ZnO NPs (900 nm), which exceed the typical size of aggregates of ZnO NPs (600 nm). The TiO_2 NPs and $Zn(NO_3)_2$ or ZnO NPs aggregates might block the pore canals of the chorion, and either less Zn^{2+} or less of the particulate form of ZnO NPs would be able to enter into the embryo chorion (Zhu *et al*., 2009a). This means the NPs cannot pass through the chorion and affect the embryos before they hatched. As can be seen from particularly the left-bottom part of the image depicted in Figure 5.1, TEM measurements verified the larger size of aggregated stick-shaped ZnO NPs together with spherically shaped TiO_2 NPs. In addition, it was observed by microscopy that aggregates of TiO_2 NPs in the presence and absence of $Zn(NO_3)_2$ as well as aggregates of TiO_2 NPs and ZnO NPs attached to the chorion of the embryos (Supplemental data 5.4). Opposed to the larger sized mixed aggregates of TiO_2 NPs and ZnO NPs, aggregates of only ZnO NPs have the potential to penetrate into embryos *via* the chorion pore canals with a size of in between 0.5-0.7 μm (Lee *et al*., 2007).

5.4.3 Effect of TiO_2 NPs on the toxicity of the particulate form of ZnO NPs

In our previous study using stick-shaped ZnO NPs individually, we reported that the toxicity of zebrafish embryos cannot be explained only by the Zn ions released from ZnO NPs (<3.3 mg Zn/L). Despite the relative high intrinsic lethality of Zn^{2+}, the ZnO $NP_{(particle)}$ was the dominant factor inducing lethality to zebrafish embryos

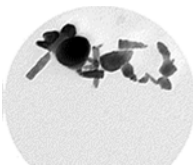

(Hua *et al*., 2014b). Similar findings were reported for various other metal-based NPs (Griffitt *et al*., 2008; Asharani *et al*., 2011; Wang *et al*., 2012; Fernandez-Cruz *et al*., 2013; Song *et al*., 2104; Xiao *et al*., 2015). Hence, the interaction of NPs with embryos is the predominant factor inducing toxicity of NPs. Li *et al*. (2015a) found that metal-based NPs could penetrate into and accumulate in cells, thereby altering cellular membranes and increasing the cytotoxicity of NPs. In addition, Li *et al*. corroborated the presence of NPs in HepG2 cells using TEM analysis as well as energy dispersive X-ray analysis.

The reason for the reduction of toxicity of ZnO NPs by TiO_2 NPs as observed in our study may be due to the different shapes of NPs, which could impact the mechanisms of uptake of NPs. In one of our previous studies, stick-shaped ZnO NPs were found to be more toxic than cuboidal-shaped and spherically shaped ZnO NPs (Hua *et al*., 2014b). Although Agarwal *et al*. (2013) also have shown that rod-shaped NPs with a relatively larger volume displayed higher uptake rates in different cell lines compared to their smaller counterparts, this has not been previously reported for zebrafish embryos. These findings may be explained by the fact that when the longitudinal axis of the sticks interacts with embryos, stick-shaped NPs have a larger direct contact area with embryos than spherical NPs (Huang *et al*., 2010b). Moreover, the uptake of rod-shaped NPs in mammalian cells (which are similar to stick-shaped NPs in this study) was found to depend mainly on the width of the NPs (Chithrani and Chan, 2007). It was suggested that nanoparticle endocytosis is mainly manifested through three parameters related to their shape and size: the surface contact area to the cell membrane, the strain energy for membrane deformation, and the sedimentation or local particle concentration at the cell membrane (Agarwal *et al*., 2013). In our study, the smaller sized, spherically shaped TiO_2 NPs could attach to larger sized, stick-shaped ZnO NPs, thereby changing the direct surface contact area of ZnO NPs to embryos. TiO_2 NPs formed larger aggregates with ZnO NPs, which could modify sedimentation of ZnO NPs. Therefore, the addition of TiO_2 NPs may modify at least two of the above mentioned three parameters related to shape and size, thereby impacting the uptake of ZnO NPs, and further decreasing the toxicity of ZnO NPs to zebrafish embryos.

5.4.4 Relative contribution of ions and particles

The response addition model was used to estimate the combined effects of the particles versus the ions within the metal-based NPs mixtures. This simplified way of determining the relative distribution has been done earlier using the RA model (Hua *et al*., 2014a; Hua *et al*., 2014b; Song *et al*., 2014; Xiao *et al*., 2015). At the 50% mortality concentration of suspensions of ZnO NPs with addition of different concentrations of TiO_2 NPs, the relative contribution to toxicity of ZnO $NP_{(particle)}$ (more than 60%) was higher than that of the ZnO $NP_{(ion)}$ (Table 5.3). The concentrations of the ionic form of ZnO NPs in the ZnO NPs suspensions from 0-3.3 mg/L (Table 5.1) are included in the range between 0-4.5 mg/L in Figures 5.2A and 5.3A. As can be seen from Figures 5.2A and 5.3A, such low concentrations were insufficient to exert considerable toxic effects in suspensions of ZnO NPs. Therefore, the Zn ions did not induce any toxic effect to embryos in these concentration ranges. Consequently, the contribution of ZnO $NP_{(ion)}$ was lower than the contribution of ZnO $NP_{(particle)}$. We can corroborate that, despite the relative high toxicity of Zn^{2+}, the particulate form of ZnO NPs was found to be the main factor causing lethality and inhibition of hatching of zebrafish embryos after exposure to TiO_2 NPs applied with suspensions of ZnO NPs.

5.4.5 Societal implications

Studies on safety and environmental impact of NPs are of extreme importance to support sustainable development of nanotechnology. Our results showed that mixtures of metallic NPs interact with each other. With addition of TiO_2 NPs, the toxicity of both zinc ions and ZnO NPs was diminished. Generating more mechanistic knowledge on these findings could add a mixture-for-safety purpose within the production of nanomaterials, and mechanistic studies might thus have direct implications for the manufacturing of safer-by-design products.

5.5 Conclusions

A decrease in toxicity of both $Zn(NO_3)_2$ and ZnO NPs to zebrafish embryos occurred with addition of TiO_2 NPs. The ZnO NPs formed larger aggregates with addition of TiO_2 NPs and thus decreased the toxicity of metal-based NPs. The contribution to toxicity of ZnO $NP_{(particle)}$ was dominant over the contribution of

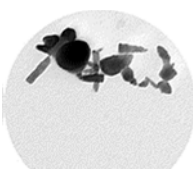

$ZnO\ NP_{(ion)}$ when explaining toxicity of ZnO NPs in the absence and presence of TiO_2 NPs for zebrafish embryos. TiO_2 NPs interact with both the particulate form and the ionic form of ZnO NPs.

Supplemental data

Supplemental data 5.1 The mortality at 120 hpf and hatching rate at 72 hpf of zebrafish embryos exposed to mixtures of ZnO NPs suspensions and $Zn(NO_3)_2$ solutions. Zebrafish embryos were exposed to binary mixture of ZnO NPs suspensions and $Zn(NO_3)_2$ solutions. The EC_{50} values and EC_{75} values of ZnO NPs and $Zn(NO_3)_2$ are shown in parentheses. Due to the quite low concentrations, the mortality of embryos was in general very low. However, in the case of hatching rate, only less than 20% of embryos were hatched. Data are presented as mean of three independent replicates ± SEM.

Treatments	Mortality (%)	Hatching rate (%)
EC_{75} ZnO NPs (1.9 mg/L) + EC_{75} $Zn(NO_3)_2$ (2.5 mg/L)	4.17 ± 2.08	10.8 ± 2.1
EC_{75} ZnO NPs (1.9 mg/L) + EC_{50} $Zn(NO_3)_2$ (1.7 mg/L)	2.08 ± 2.08	14.8 ± 2.0
EC_{50} ZnO NPs (1.4 mg/L) + EC_{75} $Zn(NO_3)_2$ (2.5 mg/L)	2.08 ± 2.08	10.7 ± 2.2
EC_{50} ZnO NPs (1.4 mg/L) + EC_{50} $Zn(NO_3)_2$ (1.7 mg/L)	2.08 ± 2.08	19.0 ± 3.4

Supplemental data 5.2 An example of the calculation of the relative contribution to toxicity of $ZnO\ NP_{(particle)}$ and $ZnO\ NP_{(ion)}$ at the LC_{50} value of suspensions.

As shown in Table 5.1 in the text, the actual total zinc concentrations (C_A) of ZnO NPs were from 0.01 to 31.7 mg Zn/L, and dissolved zinc ions concentrations (C_I) of ZnO NPs were from 0.01 to 2.5 mg Zn/L. The non-linear regression of CI of Zn is shown in the following Figure.

The concentrations of $ZnO\ NP_{(particle)}$ are calculated according to the non-linear regression $y = 0.31ln(x) + 1.4219$. For the case that, the LC_{50} value of ZnO NPs suspension is 7.1 mg Zn/L, the C_I of Zn was 2 mg Zn/L at LC_{50} value of ZnO NPs

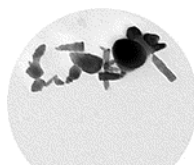

suspension, and then the concentration of the particulate form of ZnO NPs can be calculated to be 5.1 mg Zn/L

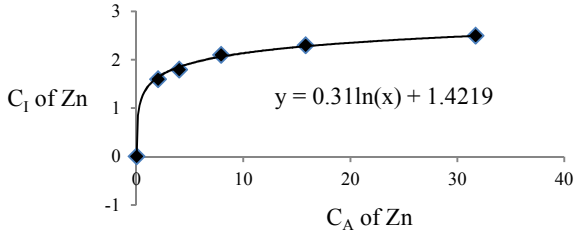

Then, according to the dose-response curve (equation 5.1) of $Zn(NO_3)_2$ and ZnO $NP_{(particle)}$ shown in Figure 5.4 using GraphPad Prism 5. The mortality of embryos at 2 mg Zn/L of $Zn(NO_3)_2$ was 53% (0.53 in scale 0-1). The mortality of embryos at 5.1 mg Zn/L of ZnO $NP_{(particle)}$ was 99% (0.99 in scale 0-1). Finally, the relative contribution can be calculated as following:

The relative toxic contribution of ZnO $NP_{(particle)}$=0.99/(0.52+0.99)*100% = 65%;
The relative toxic contribution of ZnO $NP_{(particle)}$=0.52/(0.52+0.99)*100% = 35%.

Supplemental data 5.3 The toxic effect of zebrafish embryos exposed to mixtures of ZnO NPs suspensions and $Zn(NO_3)_2$ solutions. The actual effect of the EC_{75} value of ZnO NPs applied with the EC_{75} value of $Zn(NO_3)_2$ or applied with EC_{50} value of $Zn(NO_3)_2$ were less than calculated effect. In the case of the EC_{50} value of ZnO NPs together with the EC_{75} value of $Zn(NO_3)_2$ or together with EC_{50} value of $Zn(NO_3)_2$, the actual effect are slightly more than the calculated effect. The EC_{50} values and EC_{75} values of ZnO NPs and $Zn(NO_3)_2$ are shown in parentheses.

Treatments	Actual effect (scale 0-1)	Calculated effect* (scale 0-1)
EC_{75} ZnO NPs (1.9 mg/L) + EC_{75} $Zn(NO_3)_2$ (2.5 mg/L)	89%	94%
EC_{75} ZnO NPs (1.9 mg/L) + EC_{50} $Zn(NO_3)_2$ (1.7 mg/L)	85%	87.5%
EC_{50} ZnO NPs (1.4 mg/L) + EC_{75} $Zn(NO_3)_2$ (2.5 mg/L)	89%	87.5%
EC_{50} ZnO NPs (1.4 mg/L) + EC_{50} $Zn(NO_3)_2$ (1.7 mg/L)	81%	75%

* Calculated effect was computed by the response addition model (equation 5.2 in the body text).

Supplemental data 5.4 Aggregates of TiO_2 NPs and ZnO NPs attached to the chorion of the embryos at higher concentrations.

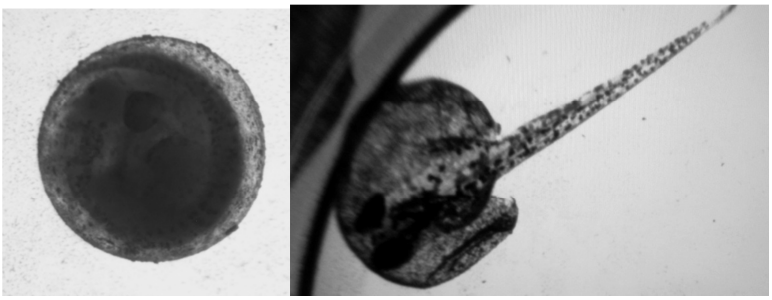

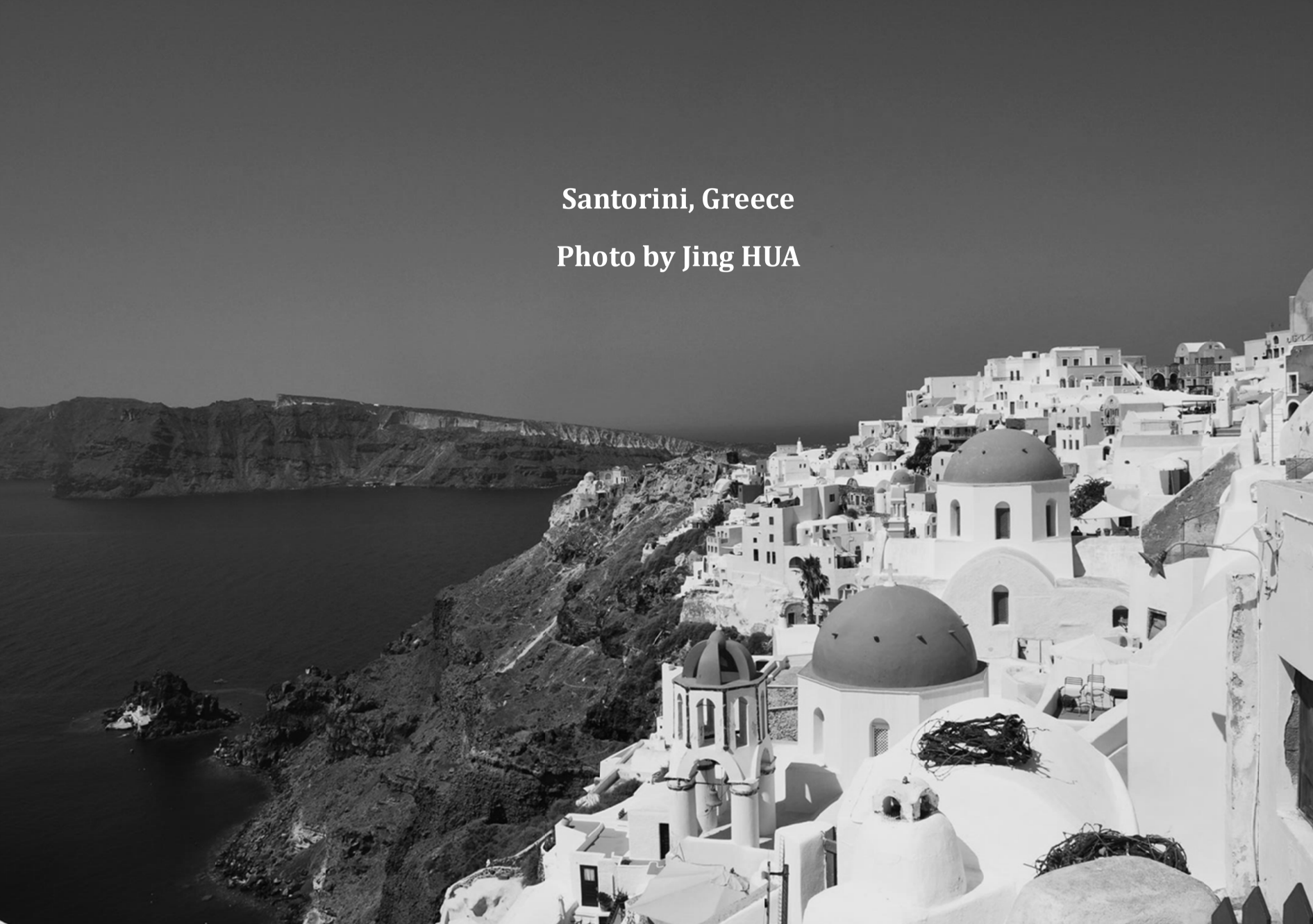

Santorini, Greece

Photo by Jing HUA

6

Discussion

In almost all cases, the dose of chemicals inducing an effect (whether adverse or not) is commonly expressed in mass units (g), either as a dose per mass body weight (g/kg), soil or sediment (g/kg) or per volume of water or air (g/L or g/m^3). So far, the dose of mass was also used to describe exposure to particulates. However, with the more recent development of particulates in the nano-range it has become clear that mass as a dose metric is not always suitable to express responses induced by NPs. This thesis has the aim to unravel dose metrices expressing the responses of metal-based NPs to zebrafish embryos. Assessment of the 'best' metrics to express the effective or adverse dose of NPs is further clouded by the fact that following their exposure, particles are subject to a number of distribution and complexation processes (most notoriously agglomeration/ aggregation, surface coating by proteins, lipids, and humic materials), which may affect their biological behavior (*i.e.* transport across biological barriers). This not only determines the fate of NPs in the biotic (humans, animals and plants) and the abiotic environment (air, water and soil), but also determines which and how many NPs reach the sites of toxic action.

This chapter provides a synthesis of the main findings of the preceding four separate chapters. In this thesis, we investigated the toxic effects of differently sized and shaped NPs (Cu NPs, ZnO NPs), with a special focus on zebrafish embryos (*Danio rerio*). The overall aim of this PhD thesis is, therefore, to assess the physicochemical dependent toxicity of nanoparticles and shift from toxicity testing in animal models to computational modeling, thus assessing the proper dose metrics of metal-based nanoparticles. To address the overall aim, three specific objectives were set as the basis of this thesis:

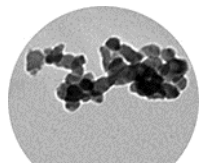

(1) To determine how physicochemical properties (size, shape, and ion release) of metal-based nanoparticles affect the toxicity of the nanoparticles to zebrafish embryos;
(2) To develop a generic dose calculation method and determine which property or properties are the most appropriate as a dose metric when assessing dose-response relationships of different metal-based nanoparticles.
(3) To assess the toxicity of mixtures of metal-based nanoparticles at different component ratios and concentration levels.

A generic approach to find the most appropriate dose metrics for NPs is required to enable scientists, industries and manufacturers, and policy makers to prepare the best fitting dose-response curves. Those curves subsequently ensure to determine safe levels and perform risk assessments.

Four main research questions were formulated for this PhD study. The answers to these questions are given in the preceding four chapters:

(1) Is the toxicity of metal-based NPs to zebrafish embryos related to NPs' size or shape? What properties of NPs should also be considered when assessing the toxicity of NPs? (Chapter 2, 3 and 4)
(2) Are the ions released from nanoparticles or the particle itself the main factor causing toxicity? How to make a quantitative assessment of the relative contribution to toxicity of ions and particles? (Chapter 2, 3 and 5)
(3) Which physicochemical property of nanoparticles (such as surface area, volume, or number) is an appropriate dose metric of NPs? (Chapter 4)
(4) How does a mixture of metal-based nanoparticles (ZnO NPs and TiO_2 NPs) impact the overall toxicity as compared to the toxicity of the individual particles? (Chapter 5)

6.1 Answers to research questions

(1) Is the toxicity of metal-based NPs to zebrafish embryos related to NPs' size or shape? What properties of NPs should also be considered when assessing the toxicity of NPs?

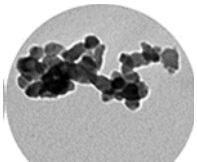

Both size and shape of NPs are important physicochemical factors when assessing the toxicity of NPs. Although the toxicity of nanoparticles is not size dependent for all metal-based NPs, the toxicity of Cu NPs and ZnO NPs to zebrafish embryos was found to be size dependent in our studies. Smaller Cu NPs were more toxic than larger Cu NPs to zebrafish, while submicron-sized particle and Cu ions were found to be more toxic to zebrafish embryos than the Cu NPs (Chapter 2). In particular, the 25 nm Cu NPs with LC_{50} of 1 mg/L was one time more toxic than the 50 nm Cu NPs with LC_{50} of 2 mg/L. This is also the case for the LC_{50} values of 21 nm and 27 nm ZnO NPs (Chapter 4), as the 78% smaller sized ZnO NPs induced 86% less toxicity to zebrafish embryos.

The stick-shaped ZnO NPs exerted more toxicity than spherical-shaped and cuboidal-shaped NPs (Chapter 3), the LC_{50} value differed by up to a maximum of a factor of 1.7. However, Cu nanorods induced less toxicity compared to any of the other spherical-shaped NPs no matter what size of Cu NPs (Chapter 4). Shape of NPs was found to be the predominant modifier of the toxicity of NPs. The relative contact surface area to organisms was considered the main factor to affect the uptake and toxicity of NPs (Chapter 2, 3 and 4). In addition, the parameters related to shape (*e.g.* the aspect ratio, *etc*) also should be taken into account as factors in the toxicity of NPs.

Besides the size and morphology of NPs, the chemical composition, the aggregation state, dissolution and ion release, and suspension stability also have an influence on its biological behavior and toxicity (Chapter 2, 3 and 4).

(2) Are the ions released from nanoparticles or the particle itself the main factor causing toxicity? How to make a quantitative assessment of the relative contribution to toxicity of ions and particles?

Dissolution of metal-based NPs and the subsequent ion toxicity have been considered as a main factor to express the toxicity of NPs. However, based on our studies using mixture toxicity modeling, released ions from NPs were not the primary cause of NPs toxicity to zebrafish embryos. The main contribution to the toxicity was in general from the particulate form of the NPs rather than from the ionic form of NPs (Chapter 2, 3 and 5). The relative contributions to toxicity of

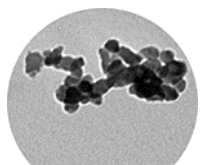

$NP_{(particle)}$ and $NP_{(ion)}$ are shown in Table 6.1.

Conceptual models were used to explicitly account for the toxic impacts of the particle-specific NPs in this thesis. The commonly used response addition (RA) model (Chapter 2, 3 and 5) and concentration addition (CA) model (Chapter 3) were used to calculate the toxic effects of the particulate form of NPs and the toxic effects of the released ions from NPs. At the LC_{50} of the suspensions of NPs, $NP_{(particle)}$ was mostly responsible for the effects observed rather than $NP_{(ion)}$ (Table 6.1). The CA results generally showed an even higher contribution of the particles to the total toxicity than in the alternative case of RA. Both results from the response addition model and the concentration addition model allowed us to conclude that the particle-specific contribution of NPs was the main factor in inducing toxicity of suspensions of nanoparticles for all particle tested.

Table 6.1 Relative contribution to toxicity of $NP_{(particle)}$ and $NP_{(ion)}$ at the LC_{50} value of the suspensions using the response addition model

	Relative contribution to toxicity (%)	
Particle	$NP_{(particle)}$	$NP_{(ion)}$
Cu NPs	> 71%	< 29%
ZnO NPs	> 52%	< 48%

(3) Which physicochemical property of nanoparticles (such as surface area, volume, or number) is an appropriate dose metric of NPs?

A generic dose calculation method was proposed, and can be used to model systematically the toxicity of differently shaped, differently sized and different metal-type NPs exposed to different species. For the majority of the responses of biological species (algae, crustaceans, fish, nematode, and mammalian cells), volume (or mass) of ZnO NPs and Ag NPs is the appropriate dose metric. For three species (*Pseudokirchneriella* and *Pimephales promelas in vivo, A549 cells in vitro*) exposed to Ag NPs, the surface area is the best dose metric. So in general, volume is a very workable and appropriate dose expression for some species and nanoparticle types, this should be determined separately.

In addition, according to the proposed generic dose calculation method, the value

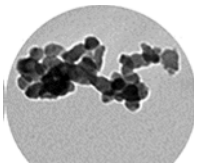

of the intercept can reflect the toxicity of NPs exposure to the same species at the same endpoint. A small value of the intercept indicates a higher intrinsic toxicity of the NPs. When the surface area to volume ratio of NPs are similar, Cu NPs are more toxic than ZnO NPs to *Danio rerio* while ZnO NPs are less toxic than Ag NPs to *Daphnia magna* and A549 cells.

(4) How does a mixture of metal-based nanoparticles (ZnO NPs and TiO_2 NPs) impact the overall toxicity as compared to the toxicity of the individual particles?

Titanium dioxide NPs have an antagonistic effect on the toxicity of ZnO NPs to zebrafish embryos when the embryos are exposed to a binary mixture of these NPs. By adding TiO_2 NPs in $Zn(NO_3)_2$ solutions, the same tendency of lowered toxicity of Zn^{2+} for zebrafish embryos was found. The reason for the reduction of toxicity of ZnO NPs by TiO_2 NPs may be due to the fact that different shapes of NPs could impact the mechanisms of uptake of NPs.

6.2 Implications

6.2.1 Implications for society

The book 'Silent Spring' cataloged the environmental effects of dichloro diphenyl trichloroethane (DDT) and questioned the logic of releasing potentially dangerous chemicals into the environment without an adequate understanding of their impacts on environment and human beings (Carson, 1962). Nowadays, we have a new revolution on chemicals produced. More and more new nanomaterials are produced without having knowledge on their exact risks. Different from the last decades, we now have outstanding analytical equipment and lots of knowledge on chemicals and their fate and potential effects and we are now ahead from the environmental disasters in nature that are not yet visible.

Nanotechnology has remarkable economic and technological benefits. Hence, it is of utmost importance to make nanotechnology a green, sustainable technology. However, very little is known of their possible hazard potential. Recently, scientists all over the world started toxicity testing of products during and before production at a large scale. Nel *et al.* (2006) stressed that the public should

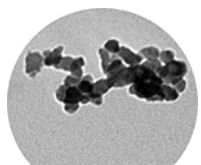

consider nanotechnology as a noteworthy hazard, and we should establish the principles and procedures to ensure the safety of nanotechnology during the process of being produced, used and disposed. On the one hand, we know that nanotechnologies can have a beneficial impact on human health, can improve a safer future, may reduce the depletion of resources, and so on. On the other hand, we need to keep up with our knowledge in the assessment of possible risks and more attention should be given to assessment of the toxicity of nanomaterials.

6.2.2 Implications for environmental risk assessment

In "Nanosafety in Europe 2015-2025: Towards Safe and Sustainable Nanomaterials and Nanotechnology Innovations" (Strategic Research Agenda; SRA), the key demands for the next several years of research on nanomaterials are defined as nanomaterial identification and classification, nanomaterial exposure and transformation, assessment of the mechanisms of toxicity related to effects on human health and the environment, and on tools for the predictive risk assessment and management (Savolainen *et al.*, 2013). Within this thesis the toxicity of differently sized and shaped nanoparticles was investigated and the best dose metrics of nanoparticles to express responses was assessed. These issues address two of the demands mentioned in the SRA.

In order to design more safe and less toxic NPs, more systematic toxicity studies are required by testing the toxicity of NPs with different properties (Savolainen *et al.*, 2013). The thesis addresses this issue, and based on the results of the toxicity testing, we found how properties of NPs (*e.g.* size, shape, *etc.*) impact their toxicity to specific species. Compared to their bulk forms, nanomaterials have specific characteristics (*e.g.* small size, high surface-to-volume ratio) that may endow them with specific mechanisms of toxicity that differ from the mechanisms of toxicity of non-particulate synthetic chemicals (Aillon *et al.*, 2009). This can modify the physicochemical properties of the material as well as create the opportunity to increase uptake and interaction with biological tissues.

Figure 6.1 shows a schematic representation of the scope of this thesis regarding the toxicity testing performed:

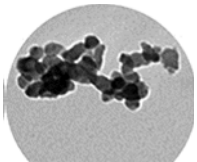

1. Various metal-based NPs with different size, shape and other different properties were selected to be exposed to the test organisms, such as Cu, ZnO, and TiO_2 (Chapters 2, 3, and 5). The toxicity of only the particulate form of metal-based NPs was calculated after ruling out the toxicity induced by the released ions form metal-based NPs using conceptual models (cross in Figure 6.1).

2. The model organisms tested so far include bacteria, fungi, algae, crustaceans, fish (more specific the zebrafish embryos were key organisms for the experiments performed in this thesis) and nematodes, as well as mammalian cells. They have been used in recent years for toxicological assessment of NPs (Chithrani *et al.*, 2006; Handy *et al.*, 2008; Heinlaan *et al.*, 2008; Navarro *et al.*, 2008; Farré *et al.*, 2009; Wang *et al.*, 2009). These tested organisms represent many different organisms of a variety of different biological levels and all play an important ecological role.

3. When producing specific functions of NPs (such as bactericides), they are supposed to have lethal effects on the target organisms (*e.g.* bacteria, yeast, fungi, and algae, *etc.*). For the above purposes, we can modify their physical properties until they are toxic to target organisms and stimulate the specific target oriented toxicity. When NPs are used as coatings, personal care products, electronic, and environmental technologies, they are supposed to have no or less impact to non-target organisms (Bondarenko *et al.*, 2013). The physical properties of NPs should also be modified for safety by design in products causing less unwanted side-effects to non-target organisms. By doing this, we can facilitate new product development.

4. After large amounts of toxicity testing of potentially dangerous NPs, it is essential for risk assessment of NPs to find a proper dose metrics of NPs for all species. A generic dose metric approach applicable across several aquatic species was developed in Chapter 4. The approach is required for safety evaluations of NPs. This will mean that new NPs will be safe-by-design, even safe-before-design, and this concept will be beneficial not only for Europe but for the whole world.

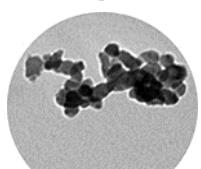

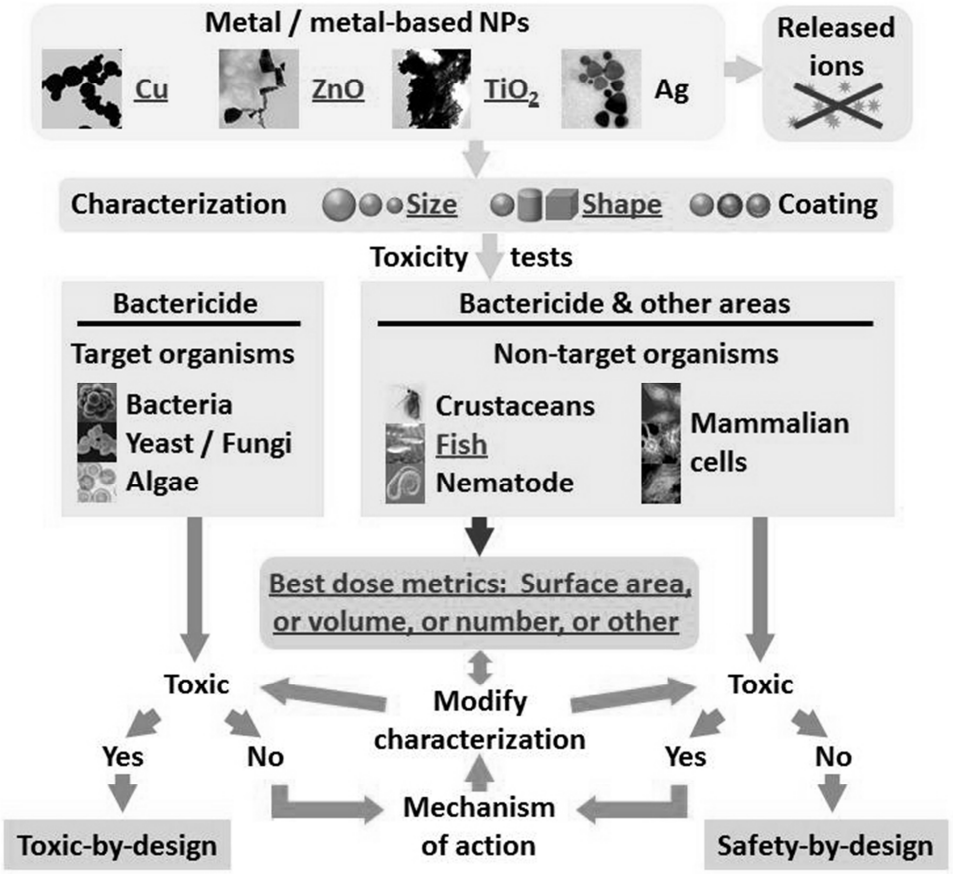

Figure 6.1 Schematic representation of the scope of the thesis. Contents underlined are directly related to previous chapters. The Figure was adapted from Bondarenko *et al.* (2013) (substantially modified). Firstly, large amounts of toxicity testing were performed for various metal-based NPs with different properties expose to tested organisms; the toxic effects caused by ions released from NPs should be eliminated (cross). Then, the toxicity analysis of different properties of NPs to specific species must follow; the mechanism of action should also be addressed. Finally, according to the toxicity testing, a generic dose calculation method for NPs to all species needs to be developed to find the appropriate dose metrics of NPs, *i.e.* surface area, volume, number or other properties of NPs.

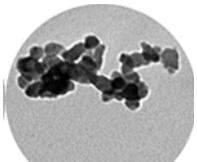

6.2.3 Justified alternative (non-animal) methods

In the past decade, risk assessments of NPs have primarily focused on risks to human health, especially to the inhalation system. However, increasing attention has been paid to the ecological implications of large amounts of potentially dangerous NPs into the environment. It is essential for risk assessment of NPs to find an appropriate dose metrics of NPs for all species, including organisms *in vivo* and mammalian cells *in vitro*.

Although toxic testing in this study was performed specifically with zebrafish embryos, a generic dose metric approach was developed in Chapter 4. This generic dose metric approach was validated by using experimental data collected within the ecotoxicology group at Leiden University (Chapter 2 and 3) and by using literature data across different species. It was found that the developed approach is applicable across several aquatic species, including algae, crustaceans, fish, and terrestrial species exposed predominantly via pore water such as nematodes, and cell lines: mammalian and piscine cells.

An issue of concern in developing new testing strategies is that due to the animal protection and financial costs of reproductive toxicity testing, there has been a great impetus to find alternative (non-animal) methods to testing that are capable of lowering the number of animals required for testing (van Leeuwen and Vermeire, 2007). This need is also strongly supported by the Registration, Evaluation, Authorisation and Restriction of Chemicals (REACH) regulation. For this purpose, the generic dose metric method developed in Chapter 4 could help us to find the suitable dose metrics for NPs (Figure 6.1), thereby producing specific functions of NPs (*e.g.* bactericides, other areas) as mentioned above.

6.2.4 Implications for mixture effects of NPs

In the natural environment, organisms are typically exposed to mixtures of various types of NPs. Commonly used nanomaterials in various products are listed in Table 1.1. For example, Ag NPs, Si (SiO_2) NPs, Au NPs, and Carbon-based NPs (including C_{60} and C_{70}) are widely used in cosmetics and personal care products; nano-sized Ag, TiO_2, and ZnO are used as antibacterial; Cu (CuO) and Au at the nano-scale are used in catalysts. Therefore, the potential risks of NPs

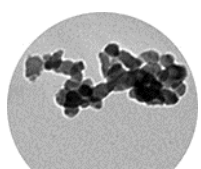

mixtures should be investigated. In Chapter 5, the interaction between ZnO NPs and TiO_2 NPs was investigated. ZnO NPs as well as TiO_2 NPs are widely used in painting, cosmetics, and sunscreens. Hence, their potential routes of release are similar during their life stages of production, use and disposal. The addition of TiO_2 NPs to suspensions of ZnO NPs markedly reduced the toxicity of ZnO NPs to zebrafish embryos. Antagonistic effects of these NPs may thus be expected during their entire life cycle, thereby reducing the toxicity of the mixtures of NPs in the environment.

In addition, it is difficult to distinguish the toxicity induced by released ions from the metal-based NPs from the toxicity induced by the particulate form of metal-based NPs. Especially the quantification of their relative contributions is difficult. In this thesis, suspensions of metal-based NPs were also treated as being a toxic mixture of the particulate form of metal-based NPs and released ions from the metal-based NPs. The conceptual models (non-interaction) were also used to calculate the toxic contributions of the particulate form of metal-based NPs and of the released ions from the metal-based NPs in the metal-based NPs suspensions.

6.3 Future research

Although toxicity assessment of NPs has been performed extensively in recent years, the understanding of the mechanisms of actions of these NPs is still far from sufficient. Various studies reported that toxicity of metal-based NPs suspensions to aquatic organisms is mainly dependent on particle dissolution and shedding of metal ions. The reported mechanism of actions of metal ions include: induction of higher levels of ROS, damage of DNA, lipid peroxidation, and disruption of homeostatic mechanisms (Zhu *et al.*, 2008; Chang *et al.*, 2012; Ivask *et al.*, 2014a). The results of our studies demonstrate that the particulate form of NPs plays a key role in nanomaterials toxicity. Some reported possible mechanistic pathways are membrane damage, mitochondrial damage, hypoxia (Bai *et al.*, 2010b; Ivask *et al.*, 2014a). However, the knowledge is still limited based on current results about the mechanism leading to toxicity by the particulate form of NPs. More studies should investigate the mechanism of actions of the particulate form of NPs. Such better understanding will help in the safe-by-design of new NPs.

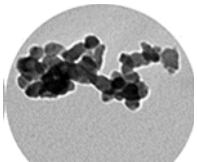

More attention should be paid to nanomaterial identification and classification. The key parameters representing the properties of NPs as well as biological interactions should be taken into account with regard to proper identification and classification of NPs. In addition, the exposure and fate of NPs should also be addressed. For instance, our studies investigated the contribution to toxicity of the particulate form of NPs and the ionic form of NPs using the response addition model and the concentration addition model. However, both of these models ignore interactions between mixture components. Therefore, we recommend that future studies should pay more attention to the interactions between the particulate form of NPs and the ionic form of NPs.

During the collection of toxicity data from previous studies, we found that test methods of different species are often not consistent, and endpoints and/or time durations reported in separately published papers are incomparable for many cases. Such differences and inconsistencies among different publications make it difficult to merge isolated results to construct a larger and more comprehensive data set for generalization and modeling purposes. Therefore, further standard test methods and guidance need to be developed, such as standard testing media and standard procedures for preparation of NPs suspensions. Such standardization would facilitate the generation of comprehensive datasets form isolated publications, thereby gaining better understanding of the toxicity of NPs.

More studies on green, safe and environmental friendly NPs mixtures are of the utmost importance to support sustainable development of nanotechnology. Our studies showed that metal-based NPs present in mixtures interact with each other. Further, assessment of the interactions of more binary and ternary mixtures should be performed. In addition, a broad range of concentration combinations needs to be investigated. If we want to generate safe NPs products, more mechanistic knowledge should be investigated on the interaction between mixtures of metal-based NPs. The more scenarios are exposed, the more direct implications would be gained for the manufacturing of mixture-for-safety products.

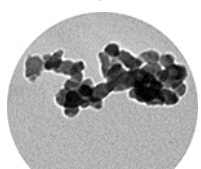

Lucerne, Switzerland

Photo by Jing HUA

References

Adam N, Schmitt C, Galceran J, Companys E, Vakurov A, Wallace R, Knapen D, Blust R. 2014. The chronic toxicity of ZnO nanoparticles and ZnCl to Daphnia magna and the use of different methods to assess nanoparticle aggregation and dissolution. *Nanotoxicology* 8:709-717.

Agarwal R, Singh V, Jurney P, Shi L, Sreenivasan SV, Roy K. 2013. Mammalian cells preferentially internalize hydrogel nanodiscs over nanorods and use shape-specific uptake mechanisms. *Proc Natl Acad Sci USA* 110:17247-17252.

Aillon KL, Xie YM, El-Gendy N, Berkland CJ, Forrest ML. 2009. Effects of nanomaterial physicochemical properties on in vivo toxicity. *Adv Drug Deliver Rev* 61:457-466.

Albanese A, Chan WCW. 2011. Effect of gold nanoparticle aggregation on cell uptake and toxicity. *ACS Nano* 5:5478-5489.

Ali S, Champagne DL, Alia A, Richardson MK. 2011a. Large-scale analysis of acute ethanol exposure in zebrafish development: A critical time window and resilience. *PLoS One* 6:e20037.

Ali S, Champagne DL, Spaink HP, Richardson MK. 2011b. Zebrafish embryos and larvae: A new generation of disease models and drug screens. *Birth Defects Res* 93:115-133.

Ali S, van Mil HGJ, Richardson MK. 2011c. Large-scale assessment of the zebrafish embryo as a possible predictive model in toxicity testing. *PLoS One* 6:e21076.

Alivisatos AP, Johnsson KP, Peng XG, Wilson TE, Loweth CJ, Bruchez MP Jr, Schultz PG. 1996. Organization of 'nanocrystal molecules' using DNA. *Nature* 382:609-611.

Altenburger R, Nendza M, Schuurmann G. 2003. Mixture toxicity and its modeling by quantitative structure-activity relationships. *Environ Toxicol Chem* 22:1900-1915.

Antignano A, Manning CE. 2008. Rutile solubility in H_2O, H_2O-SiO_2, and H_2O-$NaAlSi_3O_8$ fluids at 0.7-2.0 GPa and 700-1000 degrees C: Implications for mobility of nominally insoluble elements. *Chem Geol* 255:283-293.

APHA-AWWA-WEF. 2005. Standard methods for the examination of water and wastewater. Washington, D.C.

Aruoja V, Dubourguier HC, Kasemets K, Kahru A. 2009. Toxicity of nanoparticles of CuO, ZnO and TiO_2 to microalgae Pseudokirchneriella subcapitata. *Sci Total Environ* 407:1461-1468.

Asharani PV, Wu YL, Gong ZY, Valiyaveettil S. 2008. Toxicity of silver nanoparticles in zebrafish models. *Nanotechnology* 19:255102.

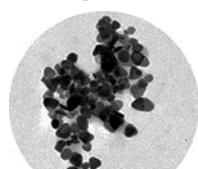

Asharani PV, Yi L, Gong Z, Valiyaveettil S. 2011. Comparison of the toxicity of silver, gold and platinum nanoparticles in developing zebrafish embryos. *Nanotoxicology* 5:43-54.

Atkinson MJ, Bingman C. 1998. Elemental composition of commercial seasalts. *J Aquariculture Aquatic Sci* 8:39-43.

Backhaus T, Scholze M, Grimme LH. 2000. The single substance and mixture toxicity of quinolones to the bioluminescent bacterium Vibrio fischeri. *Aquat Toxicol* 49:49-61.

Bai W, Tian W, Zhang Z, He X, Ma Y, Liu N, Chai Z. 2010a. Effects of copper nanoparticles on the development of zebrafish embryos. *J Nanosci Nanotechnol* 10:8670-8676.

Bai W, Zhang ZY, Tian WJ, He X, Ma YH, Zhao YL, Chai ZF. 2010b. Toxicity of zinc oxide nanoparticles to zebrafish embryo: A physicochemical study of toxicity mechanism. *J Nanopart Res* 12:1645-1654.

Bar-Ilan O, Albrecht RM, Fako VE, Furgeson DY. 2009. Toxicity assessments of multisized gold and silver nanoparticles in zebrafish embryos. *Small* 5:1897-1910.

Basu S, Sachidanandan C. 2013. Zebrafish: A multifaceted tool for chemical biologists. *Chem Rev* 113:7952-7980.

Batley GE, Kirby JK, McLaughlin M J. 2013. Fate and risks of nanomaterials in aquatic and terrestrial environments. *Acc Chem Res* 46:854-862.

Bervoets L, Blust R. 2000. Effects of pH on cadmium and zinc uptake by the midge larvae Chironomus riparius. *Aquat Toxicol* 49:145-157.

Bliss CI. 1939. The toxicity of poisons applied jointly. *Ann Appl Biol* 26:585-615.

Boyle D, Al-Bairuty GA, Ramsden CS, Sloman KA, Henry TB, Handy RD. 2013. Subtle alterations in swimming speed distributions of rainbow trout exposed to titanium dioxide nanoparticles are associated with gill rather than brain injury. *Aquat Toxicol* 126:116-127.

Brayner R, Ferrari-Iliou R, Brivois N, Djediat S, Benedetti MF, Fievet F. 2006. Toxicological impact studies based on Escherichia coli bacteria in ultrafine ZnO nanoparticles colloidal medium. *Nano Lett* 6:866-870.

Brunner TJ, Wick P, Manser P, Spohn P, Grass RN, Limbach LK, Bruinink A, Stark WJ. 2006. In vitro cytotoxicity of oxide nanoparticles: Comparison to asbestos, silica, and the effect of particle solubility. *Environ Sci Technol* 40:4374-4381.

Burgess HA, Granato M. 2007. Modulation of locomotor activity in larval zebrafish during light adaptation. *J Exp Biol* 210:2526-2539.

Buzea C, Pacheco II, Robbie K. 2007. Nanomaterials and nanoparticles: Sources and toxicity. *Biointerphases* 2:MR17-MR71.

Campbell HA, Handy RD, Sims DW. 2002. Increased metabolic cost of swimming and

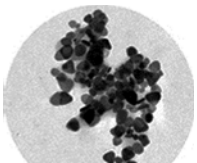

consequent alterations to circadian activity in rainbow trout (*Oncorhynchus mykiss*) exposed to dietary copper. *Can J Fish Aquat Sci* 59:768-777.

Carlson C, Hussain SM, Schrand AM, Braydich-Stolle LK, Hess KL, Jones RL, Schlager JJ. 2008. Unique cellular interaction of silver nanoparticles: size-dependent generation of reactive oxygen species. *J Phys Chem B* 112:13608-13619.

Carson R. 1962. Silent Spring. Houghton Mifflin.

Chae YJ, Pham CH, Lee J, Bae E, Yi J, Gu MB. 2009. Evaluation of the toxic impact of silver nanoparticles on Japanese medaka (Oryzias latipes). *Aquat Toxicol* 94:320-327.

Chang YN, Zhang MY, Xia L, Zhang J, Xing GM. 2012. The toxic effects and mechanisms of CuO and ZnO nanoparticles. *Materials* 5:2850-2871.

Chen TH, Lin CC, Meng PJ. 2014. Zinc oxide nanoparticles alter hatching and larval locomotor activity in zebrafish (*Danio rerio*). *J Hazard Mater* 277:134-140.

Chen Z, Meng HA, Xing GM, Chen CY, Zhao YL, Jia GA, Wang TC, Yuan H, Ye C, Zhao F, Chai ZF, Zhu CF, Fang XH, Ma BC, Wan LJ. 2006. Acute toxicological effects of copper nanoparticles in vivo. *Toxicol Lett* 163:109-120.

Chithrani BD, Ghazani AA, Chan WC. 2006. Determining the size and shape dependence of gold nanoparticle uptake into mammalian cells. *Nano lett* 6:662-668.

Chithrani BD, Chan WC. 2007. Elucidating the mechanism of cellular uptake and removal of protein-coated gold nanoparticles of different sizes and shapes. *Nano Lett* 7:1542-1550.

Cho HH, Wepasnick K, Smith BA, Bangash FK, Fairbrother DH, Ball WP. 2010. Sorption of aqueous Zn[II] and Cd[II] by multiwall carbon nanotubes: The relative roles of oxygen-containing functional groups and graphenic carbon. *Langmuir* 26:967-981.

Cho WS, Duffin R, Thielbeer F, Bradley M, Megson IL, Macnee W, Poland CA, Tran CL, Donaldson K. 2012. Zeta potential and solubility to toxic ions as mechanisms of lung inflammation caused by metal/metal oxide nanoparticles. *Toxicol Sci* 126:469-477.

Cioffi N, Ditaranto N, Torsi L, Picca RA, De Giglio E, Sabbatini L, Novello L, Tantillo G, Bleve-Zacheo T, Zambonin PG. 2005. Synthesis, analytical characterization and bioactivity of Ag and Cu nanoparticles embedded in poly-vinyl-methyl-ketone films. *Anal Bioanal Chem* 382:1912-1918.

Das P, Xenopoulos MA, Metcalfe CD. 2013. Toxicity of silver and titanium dioxide nanoparticle suspensions to the aquatic invertebrate, Daphnia magna. *B Environ Contam Tox* 91:76-82.

Delmaar CJ, Peijnenburg WJ, Oomen AG, Chen J, de Jong WH, Sips AJ, Wang Z, Park MV. A practical approach to determine dose metrics for nanomaterials. *Environ Toxicol*

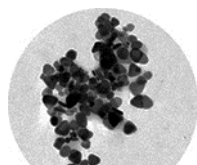

Chem 34:1015-1022.

Dobrovolskaia MA, Mcneil SE. 2007. Immunological properties of engineered nanomaterials. *Nat Nanotechnol* 2:469-478.

Donaldson K, Stone V, Gilmour PS, Brown DM, MacNee W. 2000. Ultrafine particles: Mechanisms of lung injury. *Philos Trans R Soc A* 358:2741-2748.

Ellegaard-Jensen L, Jensen KA, Johansen A. 2012. Nano-silver induces dose-response effects on the nematode Caenorhabditis elegans. *Ecotoxicol Environ Saf* 80:216-223.

Farré M, Gajda-Schrantz K, Kantiani L, Carceló D. 2009. Ecotoxicity and analysis of nanomaterials in the aquatic environment. *Anal Bioanal Chem* 393:81-95.

Faust M, Altenburger R, Backhaus T, Blanck H, Boedeker W, Gramatica P, Hamer V, Scholze M, Vighi M, Grimme LH. 2003. Joint algal toxicity of 16 dissimilarly acting chemicals is predictable by the concept of independent action. *Aquat Toxicol* 63:43-63.

Ferin J, Oberdorster G, Penney DP. 1992. Pulmonary retention of ultrafine and fine particles in rats. *Am J Resp Cell Mol* 6:535-542.

Fernández-Cruz ML, Lammel T, Connolly M, Conde E, Barrado AI, Derick S, Perez Y, Fernandez M, Furger C, Navas JM. 2013. Comparative cytotoxicity induced by bulk and nanoparticulated ZnO in the fish and human hepatoma cell lines PLHC-1 and Hep G2. *Nanotoxicology* 7:935-952.

Fischer HC, Chan WCW. 2007. Nanotoxicity: The growing need for in vivo study. *Curr Opin Biotech* 18:565-571.

Foldbjerg R, Olesen P, Hougaard M, Dang DA, Hoffmann HJ, Autrup H. 2009. PVP-coated silver nanoparticles and silver ions induce reactive oxygen species, apoptosis and necrosis in THP-1 monocytes. *Toxicol Lett* 190:156-162.

Foldbjerg R, Dang DA, Autrup H. 2011. Cytotoxicity and genotoxicity of silver nanoparticles in the human lung cancer cell line, A549. *Arch Toxicol* 85:743-750.

Franklin NM, Rogers NJ, Apte SC, Batley GE, Gadd GE, Casey PS. 2007. Comparative toxicity of nanoparticulate ZnO, bulk ZnO, and $ZnCl_2$ to a freshwater microalga (Pseudokirchneriella subcapitata): The importance of particle solubility. *Environ Sci Technol* 41:8484-8490.

French RA, Jacobson AR, Kim B, Isley SL, Penn RL, Baveye PC. 2009. Influence of ionic strength, pH, and cation valence on aggregation kinetics of titanium dioxide nanoparticles. *Environ Sci Technol* 43:1354-1359.

Garner KL, Keller AA. 2014. Emerging patterns for engineered nanomaterials in the environment: A review of fate and toxicity studies. *J Nanopart Res* 16:2503.

George S, Pokhrel S, Xia T, Gilbert B, Ji ZX, Schowalter M, Rosenauer A, Damoiseaux R,

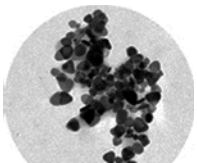

Bradley KA, Madler L, Nel AE. 2010. Use of a rapid cytotoxicity screening approach to engineer a safer zinc oxide nanoparticle through iron doping. *ACS Nano* 4:15-29.

George S, Pokhrel S, Ji ZX, Henderson BL, Xia T, Li LJ, Zink JI, Nel AE, Madler L. 2011a. Role of Fe doping in tuning the band gap of TiO_2 for the photo-oxidation-induced cytotoxicity paradigm. *J Am Chem Soc* 133:11270-11278.

George S, Xia TA, Rallo R, Zhao Y, Ji ZX, Lin SJ, Wang X, Zhang HY, France B, Schoenfeld D, Damoiseaux R, Liu R, Lin S, Bradley KA, Cohen Y, Nel AE. 2011b. Use of a high-throughput screening approach coupled with in vivo zebrafish embryo screening to develop hazard ranking for engineered nanomaterials. *ACS Nano* 5:1805-1817.

George S, Lin SJ, Ji ZX, Thomas CR, Li L, Mecklenburg M, Meng H, Wang X, Zhang H, Xia T, Hohman JN, Lin S, Zink JI, Weiss PS, Nel AE. 2012. Surface defects on plate-shaped silver nanoparticles contribute to its hazard potential in a fish gill cell line and zebrafish embryos. *ACS Nano* 6:3745-3759.

Gilbert B, Ono RK, Ching KA, Kim CS. 2009. The effects of nanoparticle aggregation processes on aggregate structure and metal uptake. *J Colloid Interf Sci* 339:285-295.

Griffitt RJ, Weil R, Hyndman KA, Denslow ND, Powers K, Taylor D, Barber DS. 2007. Exposure to copper nanoparticles causes gill injury and acute lethality in zebrafish (*Danio rerio*). *Environ Sci Technol* 41:8178-8186.

Griffitt RJ, Luo J, Gao J, Bonzongo JC, Barber DS. 2008. Effects of particle composition and species on toxicity of metallic nanomaterials in aquatic organisms. *Environ Toxicol Chem* 27:1972-1978.

Gurr JR, Wang ASS, Chen CH, Jan KY. 2005. Ultrafine titanium dioxide particles in the absence of photoactivation can induce oxidative damage to human bronchial Epithelial cells. *Toxicology* 213:66-73.

Gutleb AC, Cambier S, Fernandes T, Georgantzopoulou A, Kuhlbusch T, Lynch I, Macken AL, Mehennaoui K, Moeller R, Nickel C, Peijnenburg W, Serchi T. 2015. Environmental fate and effects of nanomaterials in aquatic freshwater environments. In preperation

Haase A, Mantion A, Graf P, Plendl J, Thuenemann AF, Meier W, Taubert A, Luch A. 2012. A novel type of silver nanoparticles and their advantages in toxicity testing in cell culture systems. *Arch Toxicol* 86:1089-1098.

Handy RD, Sims DW, Giles A, Campbell HA, Musonda MM. 1999. Metabolic trade-off between locomotion and detoxification for maintenance of blood chemistry and growth parameters by rainbow trout (*Oncorhynchus mykiss*) during chronic dietary

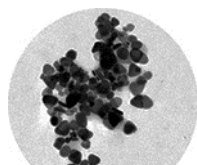

exposure to copper. *Aquat Toxicol* 47:23-41.

Handy RD, Henry TB, Scown TM, Johnston BD, Tyler CR. 2008. Manufactured nanoparticles: Their uptake and effects on fish-a mechanistic analysis. *Ecotoxicology* 17:396-409.

Hartmann NB, Baun A. 2010a. The nano cocktail: Ecotoxicological effects of engineered nanoparticles in chemical mixtures. *Integr Environ Assess Manag* 6:311-313.

Hartmann NB, Von der Kammer F, Hofmann T, Baalousha M, Ottofuelling S, Baun A. 2010b. Algal testing of titanium dioxide nanoparticles-testing considerations, inhibitory effects and modification of cadmium bioavailability. *Toxicology* 269:190-197.

Heinlaan M, Ivask A, Blinova I, Dubourguier HC, Kahru A. 2008. Toxicity of nanosized and bulk ZnO, CuO and TiO_2 to bacteria Vibrio fischeri and crustaceans Daphnia magna and Thamnocephalus platyurus. *Chemosphere* 71:1308-1316.

Hogstrand C, Verbost PM, Bonga SEW, Wood CM. 1996. Mechanisms of zinc uptake in gills of freshwater rainbow trout: Interplay with calcium transport. *Am J Physiol Regul Integr Comp Physiol* 270:R1141-R1147.

Hogstrand C. 2011. Fish physiology. Academic Press. 31:135-200.

Hoheisel SM, Diamond S, Mount D. 2012. Comparison of nanosilver and ionic silver toxicity in Daphnia magna and Pimephales promelas. *Environ Toxicol Chem* 31:2557-2563.

Hua J, Vijver MG, Ahmad F, Richardson MK, Peijnenburg WJ. 2014a. Toxicity of different-sized copper nano- and submicron particles and their shed copper ions to zebrafish embryos. *Environ Toxicol Chem* 33:1774-1782.

Hua J, Vijver MG, Richardson MK, Ahmad F, Peijnenburg WJ. 2014b. Particle-specific toxic effects of differently shaped ZnO nanoparticles to zebrafish embryos (*Danio rerio*). *Environ Toxicol Chem* 33:2859-2868.

Huang CC, Aronstam RS, Chen DR, Huang YW. 2010a. Oxidative stress, calcium homeostasis, and altered gene expression in human lung Epithelial cells exposed to ZnO nanoparticles. *Toxicol In Vitro* 24:45-55.

Huang XL, Teng X, Chen D, Tang FQ, He JQ. 2010b. The effect of the shape of mesoporous silica nanoparticles on cellular uptake and cell function. *Biomaterials* 31:438-448.

Huang XL, Li LL, Liu TL, Hao NJ, Liu HY, Chen D, Tang FQ. 2011. The shape effect of mesoporous silica nanoparticles on biodistribution, clearance, and biocompatibility in vivo. *ACS Nano* 5:5390-5399.

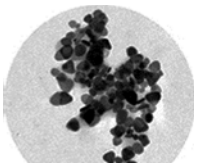

Hussain SM, Hess KL, Gearhart JM, Geiss KT, Schlager JJ. 2005. In vitro toxicity of nanoparticles in BRL 3A rat liver cells. *Toxicol In Vitro* 19:975-983.

Hussain SM, Javorina AK, Schrand AM, Duhart HM, Ali SF, Schlager JJ. 2006. The interaction of manganese nanoparticles with PC-12 cells induces dopamine depletion. *Toxicol Sci* 92:456-463.

Hwang ET, Lee JH, Chae YJ, Kim YS, Kim BC, Sang BI, Gu MB. 2008. Analysis of the toxic mode of action of silver nanoparticles using stress-specific bioluminescent bacteria. *Small* 4:746-750.

II, GWS. 2006. Ecological risk assessment, second edition.

Ispas C, Andreescu D, Patel A, Goia DV, Andreescu S, Wallace KN. 2009. Toxicity and developmental defects of different sizes and shape nickel nanoparticles in zebrafish. *Environ Sci Technol* 43:6349-6356.

Ivask A, Juganson K, Bondarenko O, Mortimer M, Aruoja V, Kasemets K, Blinova I, Heinlaan M, Slaveykova V, Kahru A. 2014a. Mechanisms of toxic action of Ag, ZnO and CuO nanoparticles to selected ecotoxicological test organisms and mammalian cells in vitro: A comparative review. *Nanotoxicology* 8:57-71.

Ivask A, Kurvet I, Kasemets K, Blinova I, Aruoja V, Suppi S, Vija H, Kakinen A, Titma T, Heinlaan M, Visnapuu M, Koller D, Kisand V, Kahru A. 2014b. Size-dependent toxicity of silver nanoparticles to bacteria, yeast, algae, crustaceans and mammalian cells in vitro. *PLoS One* 9:e102108.

Jiang J, Oberdorster G, Elder A, Gelein R, Mercer P, Biswas P. 2008a. Does nanoparticle activity depend upon size and crystal phase? *Nanotoxicology* 2:33-42.

Jiang W, Kim BYS, Rutka JT, Chan WCW. 2008b. Nanoparticle-mediated cellular response is size-dependent. *Nat Nanotechnol* 3:145-150.

Kahru A, Dubourguier HC. 2010. From ecotoxicology to nanoecotoxicology. *Toxicology* 269:105-119.

Karlsson HL, Cronholm P, Gustafsson J, Moller L. 2008. Copper oxide nanoparticles are highly toxic: A comparison between metal oxide nanoparticles and carbon nanotubes. *Chem Res Toxicol* 21:1726-1732.

Kashiwada S, Ariza ME, Kawaguchi T, Nakagame Y, Jayasinghe BS, Gärtner K, Nakamura H, Kagami Y, Sabo-Attwood T, Ferguson PL, Chandler GT. 2012. Silver nanocolloids disrupt medaka embryogenesis through vital gene expressions. *Environ Sci Technol* 46:6278-6287.

Kennedy AJ, Chappell MA, Bednar AJ, Ryan AC, Laird JG, Stanley JK, Steevens JA. 2012. Impact of organic carbon on the stability and toxicity of fresh and stored silver

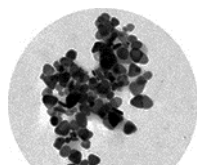

nanoparticles. *Environ Sci Technol* 46:10772-10780.

Khare P, Sonane M, Pandey R, Ali S, Gupta KC, Satish A. 2011. Adverse effects of TiO_2 and ZnO nanoparticles in soil nematode, Caenorhabditis elegans. *J Biomed Nanotechnol* 7:116-117.

Kim SK, Lund J, Kiraly M, Duke K, Jiang M, Stuart JM, Eizinger A, Wylie BN, Davidson GS. 2001. A gene expression map for Caenorhabditis elegans. *Science* 293:2087-2092.

Kim S, Choi JE, Choi J, Chung KH, Park K, Yi J, Ryu DY. 2009. Oxidative stress-dependent toxicity of silver nanoparticles in human hepatoma cells. *Toxicol In Vitro* 23:1076-1084.

Kim KT, Klaine SJ, Lin SJ, Ke PC, Kim SD. 2010. Acute toxicity of a mixture of copper and single-walled carbon nanotubes to Daphnia magna. *Environ Toxicol Chem* 29:122-126.

Kimmel CB, Ballard WW, Kimmel SR, Ullmann B, Schilling TF. 1995. Stages of embryonic development of the zebrafish. *Dev Dyn* 203:253-310.

Klaine SJ, Alvarez PJJ, Batley GE, Fernandes TF, Handy RD, Lyon DY, Mahendra S, McLaughlin M J, Lead JR. 2008. Nanomaterials in the environment: Behavior, fate, bioavailability, and effects. *Environ Toxicol Chem* 27:1825-1851.

Laban G, Nies LF, Turco RF, Bickham JW, Sepulveda MS. 2010. The effects of silver nanoparticles on fathead minnow (Pimephales promelas) embryos. *Ecotoxicology* 19:185-195.

Lansdown AB. 2007. Critical observations on the neurotoxicity of silver. *Crit Rev Toxicol* 37:237-250.

Lee KJ, Nallathamby PD, Browning LM, Osgood CJ, Xu XH. 2007. In vivo imaging of transport and biocompatibility of single silver nanoparticles in early development of zebrafish embryos. *ACS Nano* 1:133-143.

Lee KJ, Browning LM, Nallathamby PD, Desai T, Cherukuri PK, Xu XH. 2012. In vivo quantitative study of sized-dependent transport and toxicity of single silver nanoparticles using zebrafish embryos. *Chem Res Toxico* 25:1029-1046.

Lee Y, Choi JR, Lee KJ, Stott NE, Kim D. 2008. Large-scale synthesis of copper nanoparticles by chemically controlled reduction for applications of inkjet-printed electronics. *Nanotechnology* 19:415604.

Lee JH, Ju JE, Kim BI, Pak PJ, Choi EK, Lee HS, Chung N. 2014. Rod-shaped iron oxide nanoparticles are more toxic than sphere-shaped nanoparticles to murine macrophage cells. *Environ Toxicol Chem* 33:2759-2766.

Li Y, Yang RT, Liu CJ, Wang Z. 2007. Hydrogen storage on carbon doped with platinum

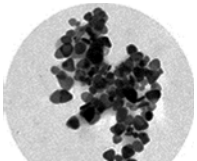

nanoparticles using plasma reduction. *Ind Eng Chem Res* 46:8277-8281.

Li T, Albee B, Alemayehu M, Diaz R, Ingham L, Kamal S, Rodriguez M, Bishnoi SW. 2010. Comparative toxicity study of Ag, Au, and Ag-Au bimetallic nanoparticles on Daphnia magna. *Anal Bioanal Chem* 398:689-700.

Li L, Fernández-Cruz ML, Connolly M, Conde E, Fernández M, Schuster M, Navas JM. 2015a. The potentiation effect makes the difference: Non-toxic concentrations of ZnO nanoparticles enhance Cu nanoparticle toxicity in vitro. *Sci Total Environ* 505:253-260.

Li L, Wu H, Peijnenburg WJGM, van Gestel CA. 2015b. Both released silver ions and particulate Ag contribute to the toxicity of AgNPs to earthworm Eisenia fetida. *Nanotoxicology* 11:1-10.

Lin DH, Xing BS. 2007. Phytotoxicity of nanoparticles: Inhibition of seed germination and root growth. *Environ Pollut* 150:243-250.

Lin WS, Xu Y, Huang CC, Ma YF, Shannon KB, Chen DR, Huang YW. 2009. Toxicity of nano- and micro-sized ZnO particles in human lung epithelial cells. *J Nanopart Res* 11:25-39.

Lin DH, Tian XL, Wu FC, Xing BS. 2010. Fate and transport of engineered nanomaterials in the environment. *J Environ Qual* 39:1896-1908.

Lin SJ, Zhao Y, Xia T, Meng H, Ji ZX, Liu R, George S, Xiong SJ, Wang X, Zhang HY, Pokhrel S, Madler L, Damoiseaux R, Lin S, Nel AE. 2011. High content screening in zebrafish speeds up hazard ranking of transition metal oxide nanoparticles. *ACS Nano* 5:7284-7295.

Lin SJ, Zhao Y, Nel AE, Lin S. 2013a. Zebrafish: An in vivo model for nano EHS studies. *Small* 9:1608-1618.

Lin SJ, Zhao Y, Ji ZX, Ear J, Chang CH, Zhang HY, Low-Kam C, Yamada K, Meng H, Wang X, Liu R, Pokhrel S, Madler L, Damoiseaux R, Xia T, Godwin HA, Lin S, Nel AE. 2013b. Zebrafish high-throughput screening to study the impact of dissolvable metal oxide nanoparticles on the hatching enzyme, ZHE1. *Small* 9:1776-1785.

Liu W, Wu YA, Wang C, Li HC, Wang T, Liao CY, Cui L, Zhou QF, Yan B, Jiang GB. 2010. Impact of silver nanoparticles on human cells: Effect of particle size. *Nanotoxicology* 4:319-330.

Loewe S, Muischnek H. 1926. Effect of combinations: Mathematical basis of the problem. *Arch Exp Pathol Pharmakol* 114:313-326.

Lopes S, Ribeiro F, Wojnarowicz J, Lojkowski W, Jurkschat K, Crossley A, Soares AM, Loureiro S. 2014. Zinc oxide nanoparticles toxicity to Daphnia magna: Size-dependent

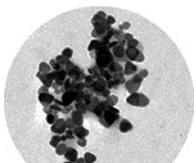

effects and dissolution. *Environ Toxicol Chem* 33:190-198.

Lubick N. 2007. Copper nanoparticles harm zebrafish. *Environ Sci Technol* 41:7958-7959.

Ma HB, Bertsch PM, Glenn TC, Kabengi NJ, Williams PL. 2009. Toxicity of manufactured zinc oxide nanoparticles in the nematode Caenorhabditis elegans. *Environ Toxicol Chem* 28:1324-1330.

Ma H, Kabengi NJ, Bertsch PM, Unrine JM, Glenn TC, Williams PL. 2011. Comparative phototoxicity of nanoparticulate and bulk ZnO to a free-living nematode Caenorhabditis elegans: The importance of illumination mode and primary particle size. *Environ Pollut* 159:1473-1480.

Manusadzianas L, Caillet C, Fachetti L, Gylyte B, Grigutyte R, Jurkoniene S, Karitonas R, Sadauskas K, Thomas F, Vitkus R, Ferard JF. 2012. Toxicity of copper oxide nanoparticle suspensions to aquatic biota. *Environ Toxicol Chem* 31:108-114.

Maynard AD, Aitken RJ, Butz T, Colvin V, Donaldson K, Oberdorster G, Philbert MA, Ryan J, Seaton A, Stone V, Tinkle SS, Tran L, Walker NJ, Warheit DB. 2006. Safe handling of nanotechnology. *Nature* 444:267-269.

McGrath P, Li CQ. 2008. Zebrafish: A predictive model for assessing drug-induced toxicity. *Drug Discov Today* 13:394-401.

McLaughlin J, Bonzongo JC. 2012. Effects of natural water chemistry on nanosilver behavior and toxicity to Ceriodaphnia dubia and Pseudokirchneriella subcapitata. *Environ Toxicol Chem* 31:168-175.

Meng H, Chen Z, Xing GM, Yuan H, Chen CY, Zhao F, Zhang CC, Zhao YL. 2007. Ultrahigh reactivity provokes nanotoxicity: Explanation of oral toxicity of nano-copper particles. *Toxicol Lett* 175:102-110.

Monteiro-Riviere NA, Tran CL. 2007. Nanotoxicology: Characterization, dosing and health effects, New York: Informa Healthcare.

Naddafi K, Zare MR, Nazmara S. 2011. Investigating potential toxicity of phenanthrene adsorbed to nano-ZnO using Daphnia magna. *Toxicol Environ Chem* 93:729-737.

Navarro E, Baun A, Behra R, Hartmann NB, Filser J, Miao A, Quigg A, Santschi P H, Sigg L. 2008. Environmental behavior and ecotoxicity of engineered nanoparticles to algae, plants, and fungi. *Ecotoxicology* 17:372-386.

Nel A, Xia T, Madler L, Li N. 2006. Toxic potential of materials at the nanolevel. *Science* 311:622-627.

Nel A, Madler L, Velegol D, Xia T, Hoek EMV, Somasundaran P, Klaessig F, Castranova V, Thompson M. 2009. Understanding biophysicochemical interactions at the nano-bio interface. *Nat Mater* 8:543-557.

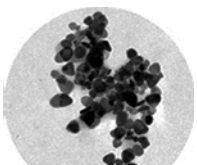

Nel A, Xia T, Meng H, Wang X, Lin S, Ji Z, Zhang H. 2013. Nanomaterial toxicity testing in the 21st century: Use of a predictive toxicological approach and high-throughput screening. *Acc Chem Res* 46:607-621.

Ngô C, Voorde MVd. 2014. Nanotechnology in a nutshell-from simple to complex.

Nordberg GF, Fowler BA, Nordberg M. 2014. Handbook on the toxicology of metals, 4th Edition. Vol. Volume I: General considerations.

Nowrouzi A, Meghrazi K, Golmohammadi T, Golestani A, Ahmadian S, Shafiezadeh M, Shajary Z, Khaghani S, Amiri AN. 2010. Cytotoxicity of subtoxic AgNP in human hepatoma cell line (HepG2) after long-term exposure. *Iran Biomed J* 14:23-32.

Oberdorster G. 1996. Significance of particle parameters in the evaluation of exposure-dose-response relationships of inhaled particles. *Inhalation Toxicol* 8 Suppl:73-89.

Oberdorster G. 2000. Toxicology of ultrafine particles: In vivo studies. *Philos Trans R Soc A* 358:2719-2739.

Oberdorster G, Maynard A, Donaldson K, Castranova V, Fitzpatrick J, Ausman K, Carter J, Karn B, Kreyling W, Lai D, Olin S, Monteiro-Riviere N, Warheit D, Yang H. 2005. Principles for characterizing the potential human health effects from exposure to nanomaterials: Elements of a screening strategy. *Part Fibre Toxicol* 2:8.

Oberdorster G, Oberdorster E, Oberdorster J. 2007. Concepts of nanoparticle dose metric and response metric. *Environ Health Perspect* 115:A290-A290.

OECD. 2011. validation report (phase 1) for the zebrafish embryo toxicity test, series on testing and assessment, No. 157. http://www.oecd.org/env/ehs/testing/48572244.pdf.

OECD. 2012. validation report (phase 2) for the zebrafish embryo toxicity test, series on testing and assessment, No. 179. http://www.oecd.org/officialdocuments/publicdisplaydocumentpdf/?cote=env/jm/mono(2012)25&doclanguage=en.

OECD. 2012. Fish embryo acute aquatic toxicity (FET) test, guideline for the testing of chemicals http://www.wecd.wrg/env/ehs/testing/draft_fet_tg_v9_draft%2011%20dec%202012_clean.pdf.

Oh WK, Kim S, Choi M, Kim C, Jeong YS, Cho BR, Hahn JS, Jang J. 2010. Cellular uptake, cytotoxicity, and innate immune response of silica-titania hollow nanoparticles based on size and surface functionality. *ACS Nano* 4:5301-5313.

Pal S, Tak YK, Song JM. 2007. Does the antibacterial activity of silver nanoparticles depend on the shape of the nanoparticle? A study of the gram-negative bacterium Escherichia coli. *Appl Environ Microb* 73:1712-1720.

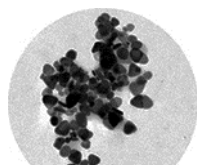

Pettibone JM, Cwiertny DM, Scherer M, Grassian VH. 2008. Adsorption of organic acids on TiO_2 nanoparticles: Effects of pH, nanoparticle size, and nanoparticle aggregation. *Langmuir* 24:6659-6667.

Pfaff G, Reynders P. 1999. Angle-dependent optical effects deriving from submicron structures of films and pigments. *Chem Rev* 99:1963-1981.

Prabhu BM, Ali SF, Murdock RC, Hussain SM, Srivatsan M. 2010. Copper nanoparticles exert size and concentration dependent toxicity on somatosensory neurons of rat. *Nanotoxicology* 4:150-160.

Radi A, Pradhan D, Sohn Y, Leung KT. 2010. Nanoscale shape and size control of cubic, cuboctahedral, and octahedral Cu-Cu_2O core-shell nanoparticles on Si(100) by one-step, templateless, capping-agent-free electrodeposition. *ACS Nano* 4:1553-1560.

Rihel J, Prober DA, Arvanites A, Lam K, Zimmerman S, Jang S, Haggarty SJ, Kokel D, Rubin LL, Peterson RT, Schier AF. 2010. Zebrafish behavioral profiling links drugs to biological targets and rest/wake regulation. *Science* 327:348-351.

Rubinstein AL. 2006. Zebrafish assays for drug toxicity screening. *Expert Opin Drug Metab Toxicol* 2:231-240.

Rushton EK, Jiang J, Leonard SS, Eberly S, Castranova V, Biswas P, Elder A, Han X, Gelein R, Finkelstein J, Oberdörster G. 2010. Concept of assessing nanoparticle hazards considering nanoparticle dosemetric and chemical/ biological response metrics. *J Toxicol Environ Health A* 73:445-461.

Salvador A, Pascual-Marti MC, Adell JR, Requeni A, March JG. 2000. Analytical methodologies for atomic spectrometric determination of metallic oxides in UV sunscreen creams. *J Pharmaceut Biomed* 22:301-306.

Savolainen K, Backman U, Brouwer D, Fadeel B, Fernandes T, Kuhlbusch T, Landsiedel R, Lynch I, Pylkkänen L. 2013. Nanosafety in Europe 2015-2025: Towards safe and sustainable nanomaterials and nanotechnology innovations. Finnish Institute of Occupational Health, Helsinki.

Sayes CM, Reed KL, Warheit DB. 2007. Assessing toxicity of fine and nanoparticles: Comparing in vitro measurements to in vivo pulmonary toxicity profiles. *Toxicol Sci* 97:163-180.

Schneider T, Jensen KA. 2009. Relevance of aerosol dynamics and dustiness for personal exposure to manufactured nanoparticles. *J Nanopart Res* 11:1637-1650.

Scholz S, Fischer S, Gundel U, Kuster E, Luckenbach T, Voelker D. 2008. The zebrafish embryo model in environmental risk assessment-Applications beyond acute toxicity testing. *Environ Sci Pollut R* 15:394-404.

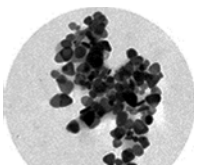

Seiffert JM, Baradez MO, Nischwitz V, Lekishvili T, Goenaga-Infante H, Marshall D. 2012. Dynamic monitoring of metal oxide nanoparticle toxicity by label free impedance sensing. *Chem Res Toxicol* 25:140-152.

Shaw BJ, Handy RD. 2011. Physiological effects of nanoparticles on fish: A comparison of nanometals versus metal ions. *Environ Int* 37:1083-1097.

Shaw BJ, Al-Bairuty G, Handy RD. 2012. Effects of waterborne copper nanoparticles and copper sulphate on rainbow trout (*Oncorhynchus mykiss*): Physiology and accumulation. *Aquat Toxicol* 116:90-101.

Simko M, Nosske D, Kreyling WG. 2014. Metrics, dose, and dose concept: The need for a proper dose concept in the risk assessment of nanoparticles. *Int J Environ Res Public Health* 11:4026-4048.

Simon-Deckers A, Gouget B, Mayne-L'Hermite M, Herlin-Boime N, Reynaud C, Carriere M. 2008. In vitro investigation of oxide nanoparticle and carbon nanotube toxicity and intracellular accumulation in A549 human pneumocytes. *Toxicology* 253:137-146.

Song WH, Zhang JY, Guo J, Zhang JH, Ding F, Li LY, Sun ZT. 2010. Role of the dissolved zinc ion and reactive oxygen species in cytotoxicity of ZnO nanoparticles. *Toxicol Lett* 199:389-397.

Song L, Vijver MG, Peijnenburg WJGM, De Snoo GR. 2011. Smart nanotoxicity testing for biodiversity conservation. *Environ Sci Technol* 45:6229-6230.

Song L, Connolly M, Fernandez-Cruz ML, Vijver MG, Fernandez M, Conde E, de Snoo GR, Peijnenburg WJGM, Navas JM. 2014. Species-specific toxicity of copper nanoparticles among mammalian and piscine cell lines. *Nanotoxicology* 8:383-393.

Stahlmecke B, Wagener S, Asbach C, Kaminski H, Fissan H, Kuhlbusch TAJ. 2009. Investigation of airborne nanopowder agglomerate stability in an orifice under various differential pressure conditions. *J Nanopart Res* 11:1625-1635.

Stoeger T, Reinhard C, Takenaka S, Schroeppel A, Karg E, Ritter B, Heyder J, Schulz H. 2006. Instillation of six different ultrafine carbon particles indicates a surface area threshold dose for acute lung inflammation in mice. *Environ Health Perspect* 114:328-333.

Stoehr LC, Gonzalez E, Stampfl A, Casals E, Duschl A, Puntes V, Oostingh GJ. 2011. Shape matters: Effects of silver nanospheres and wires on human alveolar Epithelial cells. *Part Fibre Toxicol* 8:36.

Tan C, Fan WH, Wang WX. 2012. Role of titanium dioxide nanoparticles in the elevated uptake and retention of cadmium and zinc in Daphnia magna. *Environ Sci Technol* 46:469-476.

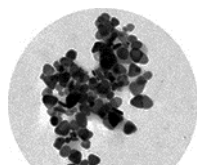

Tang YL, Li SY, Qiao JL, Wang HT, Li L. 2013. Synergistic effects of nano-sized titanium dioxide and zinc on the photosynthetic capacity and survival of Anabaena sp. *Int J Mol Sci* 14:14395-14407.

Tenzer S, Docter D, Rosfa S, Wlodarski A, Kuharev J, Rekik A, Knauer SK, Bantz C, Nawroth T, Bier C, Sirirattanapan J, Mann W, Treuel L, Zellner R, Maskos M, Schild H, Stauber RH. 2011. Nanoparticle size is a critical physicochemical determinant of the human blood plasma corona: A comprehensive quantitative proteomic analysis. *ACS Nano* 5:7155-7167.

Thomas CR, George S, Horst AM, Ji ZX, Miller RJ, Peralta-Videa JR, Xia TA, Pokhrel S, Madler L, Gardea-Torresdey JL, Holden PA, Keller AA, Lenihan HS, Nel AE, Zink JI. 2011. Nanomaterials in the environment: From materials to high-throughput screening to organisms. *ACS Nano* 5:13-20.

Tsoli M, Kuhn H, Brandau W, Esche H, Schmid G. 2005. Cellular uptake and toxicity of Au55 clusters. *Small* 1:841-844.

Tuttle GR. 2012. Size and surface area dependent toxicity of silver nanoparticles in zebrafish embryos (*Danio rerio*). Master thesis, Oregon State University.

van Leeuwen CJ, Vermeire TG. 2007. Risk assessment of chemicals: An introduction

van Ravenzwaay B, Landsiedel R, Fabian E, Burkhardt S, Strauss V, Ma-Hock L. 2009. Comparing fate and effects of three particles of different surface properties: Nano-TiO_2, pigmentary TiO_2 and quartz. *Toxicol Lett* 186:152-159.

Wang B, Feng WY, Wang TC, Guang J, Wang M, Shi JW, Zhang F, Zhao YL, Chai ZF. 2006. Acute toxicity of nano- and micro-scale zinc powder in healthy adult mice. *Toxicol Lett* 161:115-123.

Wang B, Feng WY, Wang M, Wang TC, Gu YQ, Zhu MT, Ouyang H, Shi JW, Zhang F, Zhao YL, Chai ZF, Wang HF, Wang J. 2008. Acute toxicological impact of nano- and submicro-scaled zinc oxide powder on healthy adult mice. *J Nanopart Res* 10:263-276.

Wang HH, Wick RL, Xing BS. 2009. Toxicity of nanoparticulate and bulk ZnO, Al_2O_3 and TiO_2 to the nematode Caenorhabditis elegans. *Environ Pollut* 157:1171-1177.

Wang Z, Chen J, Li X, Shao J, Peijnenburg WJGM. 2012. Aquatic toxicity of nanosilver colloids to different trophic organisms: Contributions of particles and free silver ion. *Environ Toxicol Chem* 31:2408-2413.

Wautelet P, Le Moigne J, Videva V, Turek P. 2003. Spin exchange interaction through phenylene-ethynylene bridge in diradicals based on iminonitroxide and nitronylnitroxide radical derivatives. 1. Experimental investigation of the

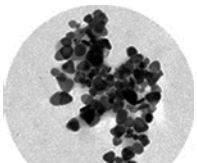

through-bond spin exchange coupling. *J Org Chem* 68:8025-8036.

Wittmaack K. 2007a. In search of the most relevant parameter for quantifying lung inflammatory response to nanoparticle exposure: Particle number, surface area, or what? *Environ Health Persp* 115:187-194.

Wittmaack K. 2007b. Dose and response metrics in nanotoxicology: Wittmaack responds to Oberdorster et al. and Stoeger et al. *Environ Health Perspect* 115:A291-A292.

Wu Y, Zhou QF. 2013. Silver nanoparticles cause oxidative damage and histological changes in medaka (Oryzias latipes) after 14 days of exposure. *Environ Toxicol Chem* 32:165-173.

Xia T, Kovochich M, Liong M, Madler L, Gilbert B, Shi HB, Yeh JI, Zink JI, Nel AE. 2008. Comparison of the mechanism of toxicity of zinc oxide and cerium oxide nanoparticles based on dissolution and oxidative stress properties. *ACS Nano* 2:2121-2134.

Xia T, Zhao Y, Sager T, George S, Pokhrel S, Li N, Schoenfeld D, Meng H, Lin S, Wang X, Wang M, Ji Z, Zink JI, Madler L, Castranova V, Nel AE. 2011. Decreased dissolution of ZnO by iron doping yields nanoparticles with reduced toxicity in the rodent lung and zebrafish embryos. *ACS Nano* 5:1223-1235.

Xiao Y, Vijver MG, Chen G, Peijnenburg WJGM. 2015. Toxicity and accumulation of Cu and ZnO nanoparticles in Daphnia magna. *Environ Sci Technol* 7:4657-4664.

Xiong DW, Fang T, Yu LP, Sima XF, Zhu WT. 2011. Effects of nano-scale TiO_2, ZnO and their bulk counterparts on zebrafish: Acute toxicity, oxidative stress and oxidative damage. *Sci Total Environ* 409:1444-1452.

Xiu Z, Zhang Q, Puppala HL, Colvin VL, Alvarez PJ. 2012. Negligible particle-specific antibacterial activity of silver nanoparticles. *Nano Lett*. 12:4271-4275.

Yang L, Kuang H, Zhang W, Aguilar ZP, Xiong Y, Lai W, Xu H, Wei H. 2015. Size dependent biodistribution and toxicokinetics of iron oxide magnetic nanoparticles in mice. *Nanoscale* 7:625-636.

Yang XY, Gondikas AP, Marinakos SM, Auffan M, Liu J, Hsu-Kim H, Meyer JN. 2012. Mechanism of silver nanoparticle toxicity is dependent on dissolved silver and surface coating in Caenorhabditis elegans. *Environ Sci Technol.* 46:1119-1127.

Yin M, Wu CK, Lou YB, Burda C, Koberstein JT, Zhu YM, O'Brien S. 2005. Copper oxide nanocrystals. *J Am Chem Soc* 127:9506-9511.

Yokohira M, Kuno T, Yamakawa K, Hosokawa K, Matsuda Y, Hashimoto N, Suzuki S, Saoo K, Imaida K. 2008. Lung toxicity of 16 fine particles on intratracheal instillation in a bioassay model using f344 male rats. *Toxicol Pathol* 36:620-631.

Yu LP, Fang T, Xiong DW, Zhu WT, Sima XF. 2011. Comparative toxicity of nano-ZnO and

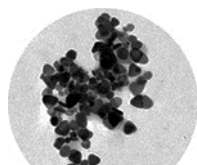

bulk ZnO suspensions to zebrafish and the effects of sedimentation, (OH)-O-center dot production and particle dissolution in distilled water. *J Environ Monit* 13:1975-1982.

Zallen R, Moret MP. 2006. The optical absorption edge of brookite TiO_2. *Solid State Commun* 137:154-157.

Zeng F, Hou C, Wu SZ, Liu XX, Tong Z, Yu SN. 2007. Silver nanoparticles directly formed on natural macroporous matrix and their anti-microbial activities. *Nanotechnology* 18:055605.

Zhang X, Sun H, Zhang Z, Niu Q, Chen Y, Crittenden JC. 2007. Enhanced bioaccumulation of cadmium in carp in the presence of titanium dioxide nanoparticles. *Chemosphere* 67:160-166.

Zhao CM, Wang WX. 2012. Importance of surface coatings and soluble silver in silver nanoparticles toxicity to Daphnia magna. *Nanotoxicology* 6:361-370.

Zhao HZ, Lu GH, Xia J, Jin SG. 2012. Toxicity of nanoscale CuO and ZnO to Daphnia magna. *Chem Res Chinese U* 28:209-213.

Zhu MT, Nie GJ, Meng H, Xia T, Nel AE, Zhao YL. 2013. Physicochemical properties determine nanomaterial cellular uptake, transport, and fate. *Acc Chem Res* 46:622-631.

Zhu XS, Zhu L, Duan ZH, Qi RQ, Li Y, Lang YP. 2008. Comparative toxicity of several metal oxide nanoparticle aqueous suspensions to Zebrafish (Danio rerio) early developmental stage. *J Environ Sci Health Part A Tox Hazard Subst Environ Eng* 43:278-284.

Zhu XS, Wang JX, Zhang XZ, Chang Y, Chen YS. 2009. The impact of ZnO nanoparticle aggregates on the embryonic development of zebrafish (Danio rerio). *Nanotechnology* 20:195103.

Zhu XS, Zhu L, Chen YS, Tian SY. 2009. Acute toxicities of six manufactured nanomaterial suspensions to Daphnia magna. *J Nanopart Res* 11:67-75.

Zhu X, Zhou J, Cai Z. 2011. TiO_2 nanoparticles in the marine environment: Impact on the toxicity of tributyltin to abalone (Haliotis diversicolor supertexta) embryos. *Environ Sci Technol* 45:3753-3758.

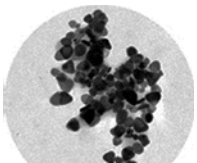

Acknowledgements

First of all, I would like to express my heartfelt gratitude to my supervisors Prof. Willie Peijnenburg and Dr. Martina Vijver for their excellent and warm guidance, advice, and encouragement during my PhD journey. I have gained a lot from you in professional and personal aspects. Your creative thoughts and great discussion have always inspired me. I appreciate your prompt responses to my concern and papers, which enables me to finalize my thesis on time.

The China Scholarship Council provided financial support for my four-year PhD study. Most of my experiments were performed in the Department of Integrative Zoology, IBL, Leiden University. I would like to thank Prof. Michael Richardson, Farooq Ahmad, Muhammad Ibrahim, Merijn de Bakker, Peter Snelderwaard for providing help in laboratory work and zebrafish facilities. Part of my work was performed in the Molecular Cell Biology, IBL, Leiden University. Many thanks go to Prof. Herman Spaink and Wouter Veneman. Kind thanks also go to Gerda Lamers and Eric van Genderen for their help with the TEM.

I am also grateful to the committee members Prof. dr. Bart Koelmans, Prof. dr. Herman Spaink, Dr. Eric Bleeker for reviewing my PhD thesis and giving their approval on the thesis.

I would like to thank Susanna van den Oever, Jory Sjardijn, Esther Philips, Maarten van 't Zelfde, and Paul de Hoog for taking care of all administrative and technical matters in our department. I would like to thank my colleagues in CML: Ellard Hunting, Anja Verschoor, Hao Qiu, Lan Song, Oleksandra Ieromina, Yang Liu, Guangchao Chen, Yinlong Xiao, Marinda van Pomeren, Tineke Kampen, Chimere Ohajinwa, Mingming Hu, Wenjie Liao, Jiali Rui, Kai Fang, Laura Bertola, Jeroen Admiraal, Benjamin Sprecher, Coen van der Giesen, Stefano Cucurachi, Patrik Henriksson, Angelica Mendoza Beltran, David Font Vivanco and all others. It was very joyful to meet my other friends (Yihao Li, Yan Yan, Yaqing Shu, Erkai He, Xiaofei Zhang and many others) in the Netherlands. I still remember the pleasant days that we spent together in preparing Chinese food, playing board games, discussing skills in traveling experiences and photography.

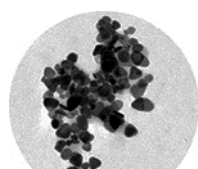

I would also like to thank my previous supervisor and colleagues during my Master study with whom I always have good discussions. Prof. Zhengyi Hu, thanks for your help, support and advice on my Master study and further professional career development. Thanks go to Peng Bao, Yuxin Ba, Chunyou Zhu, Lijuan Huang, Yichao Shi, Xiaoning Liu, Jinzhi Wang, Guoqi Wen, Jia Lu, and Xianchao Meng for creating a pleasant and friendly atmosphere in our team. I really enjoyed the memories that we conducted experiments together and arranged parties and other activities in Beijing.

Finally, I am deeply grateful to my family for their never-ending support and love. We always share the happy news in our family and my progress through the regular weekend skype, which enables me to feel like not being so far away from you. 感谢家人的养育之恩和无私的关爱，你们的支持是我不断前进的动力! My wholehearted thanks go to my beloved husband, Zheng Duan, for immense patience, love, support, encouragement, and cheerfulness when I encountered difficulties in study and life. I believe that we will definitely move forward together towards a bright future!

Jing Hua
Leiden, May 2015

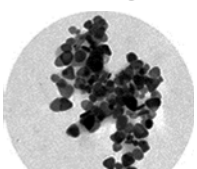

Curriculum Vitae

Jing Hua was born in Hohhot, Inner Mongolia Autonomous Region, China in November 1985. In her spare time, she likes travelling, drawing, photography and playing PC games. She studied in the Hohhot No. 2 High School, Inner Mongolian Autonomous Region, from 2001 to 2004.

In July 2008, she completed the B.Sc. in Environmental Science from the College of Environment and Planning, Henan University, Kaifeng, China.

In July 2011, she received the M.Sc. degree in Environmental Engineering from the College of Resources and Environment, University of Chinese Academy of Sciences (UCAS), Beijing, China. During her Master studies, she was deeply involved in the 'Dechlorination of organochlorine pesticides by sulfur in soil' project founded by the National Science Foundation of China, with the supervisions of Prof. Zhengyi Hu in UCAS and Prof. Yongguan Zhu in the Sino-Australian Joint Lab of Soil Environmental Science, Research Center for Eco-environmental Sciences, Chinese Academy of Sciences. Her master thesis topic was dechlorination process and mechanism of DDTs in waterlogged soils by dithionite.

In September 2011, she started her Ph.D. research at the Institute of Environmental Sciences (CML), Leiden University, the Netherlands. Her research was performed within the framework of the RIVM sponsored project IRAN, the NATO sponsored project SFPP·984401, and NWO-VIDI grant number 864.13.010 under the supervision of Prof. Willie Peijnenburg and Dr. Martina Vijver. Her research focused on determining the most appropriate dose metric for evaluating dose-response relationships of metal-based nanoparticles to zebrafish

embryos. This thesis is the outcome of her Ph.D. journey. During this journey, she conducted various academic activities. She attended the 2nd Summer School of the Marie Curie Initial Training Network "ChemOinformatics" given by Radboud University Nijmegen and Leiden University. Jing presented her research work on SETAC Europe 24th Annual Meeting, at Basel, Switzerland.

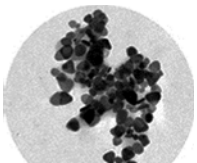

List of publications

Journal articles

Hua, J., Peijnenburg, W. J.G.M., and Vijver, M. G. (2015), TiO_2 nanoparticles reduce the effects of ZnO nanoparticles and Zn ions on zebrafish embryos (Danio rerio). Under revision.

Hua, J., Vijver, M. G., Chen, G., Richardson, M. K., and Peijnenburg, W. J.G.M. (2015), Dose metrics assessment for differently shaped and sized metal-based nanoparticles. Submitted.

Hua, J., Vijver, M. G., Richardson, M. K., Ahmad, F. and Peijnenburg, W. J.G.M. (2014), Particle-specific toxic effects of differently shaped zinc oxide nanoparticles to zebrafish embryos (Danio rerio). *Environmental Toxicology and Chemistry*, 33: 2859–2868. doi: 10.1002/etc.2758

Hua, J., Vijver, M. G., Ahmad, F., Richardson, M. K. and Peijnenburg, W. J.G.M. (2014), Toxicity of different-sized copper nano- and submicron particles and their shed copper ions to zebrafish embryos. *Environmental Toxicology and Chemistry*, 33: 1774–1782. doi: 10.1002/etc.2615

Hua, J., Hu, Z. Y., Bao, P., Ba, Y. X., and Wu, C. Y. (2012), Dechlorination process and mechanism of *p,p′*-DDT in waterlogged soils by dithionite. *Journal of Graduate University of Chinese Academy of Sciences*, 29: 206–211. (In Chinese)

Zhu, C. Y., Bao, P., Ba, Y. X., **Hua, J**., Liu, X. N., Hou, G. H., Liu, C. Z., Hu, Z. Y. (2013), Remediation of dicofol type DDTs-contaminated sediments by ferrous activated sodium persulfate oxidation. *Environment and Pollution*, 2: 30-39. doi: 10.5539/ep.v2n3p30

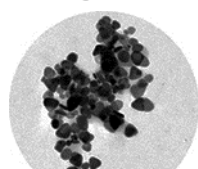

Bao, P., Hu, Z. Y., Wang, X. J., Chen, J., Ba, Y. X., **Hua, J**., Zhu, C. Y., Zhong, M., and Wu, C. Y. (2012), Dechlorination of *p,p'*-DDTs coupled with sulfate reduction by novel sulfate-reducing bacterium Clostridium sp. BXM. *Environmental Pollution*, 162: 303-310. doi: 10.1016/j.envpol.2011.11.037

Bao, P., Hu, Z. Y., Qiao, M., Ba, Y. X., Wu, C. Y., Zhu, C. Y., **Hua, J**., and Wu, J. Z. (2011), Dechlorination of DDT and DDE by dithionite in dicofol type DDTs-contaminated soil. *Journal of Chemical and Engineering Data*, 5: 917-928.

Ba, Y. X., Hu, Z. Y., Bao, P., Qiao, M., **Hua, J**., Wu, C. Y., and Wu, J. Z. (2011), Ferrous ions accelerate sulfide-induced abiotic dechlorination of DDT in waterlogged paddy soil and in soil solution. *Journal of Soils and Sediments*, 11: 1209-1220. doi: 10.1007/s11368-011-0396-6

Conference proceeding

Hua, J., Vijver, M. G., and Peijnenburg, W. J.G.M. (2014), Toxicity of different sized and shaped nanoparticles in zebrafish embryos. *SETAC Europe 24th Annual Meeting*, Basel, Switzerland